PROCEEDINGS
OF THE
NATIONAL ACADEMY OF SCIENCES
Volume 23 February 15, 1937 Number 2

REPRODUCTIVE BEHAVIOR AND HAPLOID PARTHENOGENESIS IN THE GRASS MITE, PEDICULOPSIS GRAMINUM (REUT.) (ACARINA, TARSONEMIDAE)

By Kenneth W. Cooper

Department of Zoölogy, Columbia University, New York

Communicated January 13, 1937

Despite a relatively large list of suspected forms, parthenogenesis has been indisputably established in but two species of mites,[1] namely *Tetranychus telarius* L.,[2] and *Pediculoides ventricosus* (Newp.).[3] In view of these facts additional cases are of particular importance. An investigation of *Pediculopsis graminum* (Reut.) seemed of especial interest, for in this species Reuter described the process of "merokinesis,"[4] which has found no parallel in any other organism. The results of a reinvestigation of merokinesis and a study of sex determination in this mite will be published elsewhere.

Specimens of *Pediculopsis graminum* (Reut.) were collected from heads of Herd's grass (*Agrostis alba* L.) at Flushing, Long Island, during the summer of 1936. From these collections were established the laboratory stocks upon which the present study is based. Not only do these mites possess the characters published as peculiar to the species *Pediculopsis graminum* (Reut.), but Enzio Reuter has determined and recorded[5] specimens from New York State as identical with the species he described from Finnish grasses. For these reasons it is believed that the mite under consideration is the same species as that which formed the basis of Reuter's classical investigation of merokinesis.

Following attachment to the source of food, the hysterosoma of the female swells with fluid from one- to five-hundred times the original body volume of the mite. Within this taut sac the eggs are formed and develop through larval and nymphal stages to adult mites. Mass birth, marked by the breakdown of the hysterosoma and consequent release of the sexually mature adult mites, is the rule. Occasionally an early larva or nymph may be extruded from the mother before such a breakdown; males, especially, may gain exit before the mass birth of the brood. It was early

found that the unborn mites normally hatch from their embryonic envelopes before the maternal hysterosoma has burst.

The entire brood dissected from 17 pregnant females totaled 1643 individuals. Of these, 74 or 4.50% were males. Similarly 11,446 offspring were obtained from 72 pregnant females. Here 511 or 4.46% were determined to be males. This confirms Reuter's observation that the males constitute about 5% of the normal brood.[6] It is interesting to note here that every brood contains at least one male. In each of 93 pregnant females, no one of which bore more than 10 offspring, there was found to be one male while the remainder were females. Nineteen of these mothers contained but one embryo, and in each case that one embryo was male.

To test the mite's capacity for parthenogenesis, unborn but hatched females were dissected from the hysterosomae of a number of mites and

FIGURE 1

a, Metaphase of the primary oöcyte division (4410×). *b*, Somatic metaphase plate in cleavage stage of haploid embryo (7050×). *c*, Late prophase of somatic mitosis from limb-bud of advanced embryo (7050×). *d*, Somatic metaphase plate in cleavage stage of diploid embryo (7050×).

placed in isolation culture. Such isolated females produced young in large numbers, a fact which would seem to indicate parthenogenesis. The broods of these mites, however, were found to be mixed, the sex ratio being close to that observed in broods from non-isolated females. A total of 4385 offspring was dissected from 30 of these isolated females. Of these, 226 or 5.15% were determined to be males. Each of the isolated and dissected females had contributed at least one male to this total.

The explanation of these findings was found in the mating habits of the animals. Reuter has described the copulation of these mites as taking place on the host plant.[6] Bradbury states that mating often occurs on the mother's abdomen,[7] as has been described for *Pediculoides ventricosus* (Newp.).[8] In the Flushing stocks of *Pediculopsis graminum* (Reut.), however, copulation may be seen to take place while the mites are still

within their mother's body. The adult mites may easily be observed, through the transparent walls of the hysterosoma, to be scrambling about and copulating a short time prior to their birth. If females in late stages of pregnancy are plunged into boiling water, a pair of offspring fixed *in copulo* may occasionally be dissected from among those massed within the hysterosomae. The copulatory position is similar to that figured by Brucker for *Pediculoides ventricosus* (Newp.).[8]

Duration of copulation has been observed to vary from 5 to 35 seconds. Females have been seen to mate with a number of males, while a male has been noted to mate with the same female twice in succession. In only four instances has copulation been observed in these cultures outside the maternal body, in spite of the fact that males and females are often to be found wandering over the abdomen of the pregnant female. In three of these four cases, copulation took place within the drop of fluid exuded from the collapsed hysterosoma. It has been noted that the mother is generally dead when her young are born. It is quite probable that the destruction of the tissues of the mother by her active offspring is the cause both of her death and of rupture of the hysterosoma.

Obviously copulation within the mother's body had prevented isolation of virgin females in the first experiment. Accordingly a second series of isolation experiments was performed. This time unborn females which were still within unruptured embryonic envelopes were isolated. Many of these females hatched within the isolation dishes. As Monterosso has shown for *Pediculoides ventricosus* (Newp.), initiation of the swelling (fisogastra) of the posterior abdomen is apparently a process of extreme difficulty for the virgin female.[9] In these isolations the females which hatched in the culture were very weak, and swelling was achieved by only two of them. These two produced a large number of eggs, and all of their 612 determinable offspring were males. Contrary to Reuter's negative findings,[6] it is concluded from these data that *Pediculopsis graminum* (Reut.) is facultatively parthenogenetic. Virgin females give rise only to males.

Reuter, basing his observations on studies of the egg cleavages as well as later somatic divisions, states that the diploid chromosome number is four.[4] The primary oöcytes in the stocks under investigation, however, show three tetrads at diakinesis, while the karyokinesis of the primary oöcyte is invariably characterized by the division of three tetrads (Fig. 1, *a*). Early cleavages of the fertilized egg and somatic mitoses of the advanced embryo present complements of six chromosomes (Fig. 1, *d*, *c*). Either Reuter erred in his determination of the diploid chromosome number of *Pediculopsis graminum* (Reut.), or, contrary to his opinion, the North American form here under investigation actually represents a different species with a greater chromosome number. If the latter suggestion

actually be the case, then the name *Pediculopsis dianthophilus* (Wolcott) should be applied to the American species.

It has been pointed out above that males represent approximately 5% of the normal brood. A count of the chromosome numbers of 180 embryos chosen at random showed 9, or 5%, of these to have haploid sets of three chromosomes (Fig. 1, *b*). Furthermore, a female containing but a single embryo was fixed. This embryo was in an early cleavage stage, and its sex was not determinable from its gross appearance. Microscopic investigation showed this embryo to possess the haploid complement of three chromosomes. It has been demonstrated above for cases in which females bear but one offspring that the unique offspring are male. From this statistical correspondence of the cytological data with those of the sex ratio, it seems highly probable that the males are haploid, and that *Pediculopsis graminum* (Reut.) is arrhenotokous.

This investigation has been carried on in the laboratory of Professor Franz Schrader, to whom I make grateful acknowledgment.

[1] *Cheyletus eruditus* Schr. and *Amblyomma dissimile* Koch are quite generally believed to be firmly established as parthenogenetic. However, the possibility that these species may be self-fertilizing hermaphrodites seems neither to have been ruled out nor considered.

[2] Schrader, F., *Arch. Mikr. Anat.*, **97,** 610 (1923).

[3] Patau, K., *Naturwiss.* **22,** 648 (1934); *Zool. Jahrb.* **56,** 277 (1936).

[4] Reuter, E., *Acta Soc. Sci. Fenn.*, **37,** 3 (1909).

[5] Reuter, E., *Acta Soc. Sci. Fenn.*, **36,** 1 (1909). See also, Stewart, F. G., and H. E. Hodgkiss, *N. Y. Agr. Exp. Sta., Tech. Bull.*, **7,** 83 (1908).

[6] Reuter. E., *Acta Soc. Sci. Fenn.*, **36,** 1 (1909).

[7] Bradbury, O. C., *Jour. Elisha Mitchell Sci. Soc.*, **42,** 94 (1926).

[8] Brucker, C. A., *Bull. Sci. France et Belg.*, **35,** 365 (1901).

[9] Monterosso, B., *Riv. Biol.*, **16,** 80 (1934).

THE GENERA OF THE ARTICULATED CORALLINES

By Artemio Valderrama Manza

Department of Botany, University of California

Communicated December 21, 1936

In 1904, Dr. Anna Weber-van Bosse (Siboga Exp., Monogr. 61, pp. 78–110) made certain revisions of the generic limits of the Articulated Corallines which direct the way toward a more consistent coördination of both the vegetative and the reproductive characters from microscopic as well as macroscopic viewpoints. In connection with certain work on the Articulated Corallines collected from the Pacific Coast of North America, it has been found necessary to extend the Weber-van Bosse

system and to make even more clear the lines of demarcation between the different genera recognized. This has been accomplished by instituting certain additional combinations of characters both macroscopic and microscopic, such as modes of branching, shapes of the segments, positions of the conceptacles, positions of the conceptacular pores and the varying microscopic structure in both the genicula and the intergenicula. In consequence, the following tentative outline is set forth:

A. Fronds with conceptacles all lateral,
  I. Conceptacles scattered over the intergenicula,
    a. Genicula unizonal or multizonal; intergenicular medullary filaments straight, with cells in long and short transverse zones,

1. *Amphiroa* Lamx. (emend. Weber-van Bosse).

Lamouroux, Nouv. Bull. des Sci. par la Soc. Philomat., 3, p. 186, 1812; Hist. Polyp. Flex., pp. 294–302, 1816; Weber-van Bosse, Siboga Exp., Monogr. 61, pp. 86–101, 1904.

Type of the genus: *Amphiroa fragilissima* (L.) Lamouroux, Hist. Polyp. Flex., p. 298, 1816.

Type locality: "O. Americano."

b. Genicula multizonal; intergenicular medullary filaments straight, with cells in transverse zones of uniform length,

2. *Metagoniolithon* Weber-van Bosse, Siboga Exp., Monogr. 61, pp. 86, 101–104, 1904.

Type of the genus: *Metagoniolithon charoides* (Lamx.) Weber-van Bosse, Siboga Exp., Monogr. 61, p. 102, 1904.

Type locality: "Australasie."

c. Genicula unizonal,
  aa. Intergenicular medulla unizonal,

3. *Lithothrix* Gray, Jour. Bot. 5, p. 33, 1867.

Type of the genus: *Lithothrix Aspergillum* Gray, Jour. Bot. 5, p. 33, figs. a, b, 1867.

Type locality: "Vancouver's Island."

bb. Intergenicular medulla multizonal,
  1. Medullary filaments straight, with cells in transverse zones of uniform length,
    1*a.* Segments cylindrical,

4. *Pachyarthron* gen. nov.

Frondes fragiles, dichotomae aut irregulari-dichotomae; segmentis cylindricis aut lente compressis; geniculis unizonalibus; filamentis medullaribus intergeniculorum rectis, cellulis in zonis transversis longe equalibus positis; conceptaculis semi-globosis in articulis intergeniculorum sparsis.

Type of the genus: *Pachyarthron cretaceum* (P. et R.) comb. nov. *Corallina cretacea* P. et R., Ill. 40, p. 20, fig. 104, 1840.

Type locality: "ad Insulam Unalaschka."

1*b*. Segments compressed,

5. *Bossea* gen. nov.

Frondes fragiles, dichotomae, pinnatae aut pinnato-dichotomae; segmentis in parte inferiore compressis aut cylindricis, in parte superiore compressis; geniculis unizonalibus; filamentis medullaribus intergeniculorum rectis, cellulis in zonis transversis longe equalibus positis; conceptaculis semi-globosis usque ad conicis in superficiebus planis articulorum intergeniculorum sparsis.

Type of the genus: *Bossea plumosa* sp. nov.

Frondibus erectis, laete purpureis, 3–6 cm. longis, oppositis plumoso-pinnatis usque ad bi-tripinnatis, infero ramellis curtissimis, supero ramis longis uni-bipinnatis, iisdem infero ramellis curtissimis et supero ramulis, vestitis; conceptaculis conicis 2–4 in intergeniculo quoque, vulgo in superficie quaque 2, singulo aut binis (in seriebus longitudinalibus per axes), et singulis et centralibus in superficiebus planis intergeniculorum ramellorum, poris mediis et tetrasporangiis basalibus.

Species type: tetrasporic, Moss Beach, Coast of Central California, North America (Herb. Univ. Calif. No. 545710).

2. Medullary filaments flexuous and interlacing,

6. *Calliarthron* gen. nov.

Frondes fragilissimae, dichotomae, pinnatae, aut dichotomo-pinnatae; segmentis cylindricis aut compressis; geniculis unizonalibus; filamentis medullaribus intergeniculorum flexuosis intertextisque; conceptaculis semi-globosis aut conicis in superficiebus intergeniculorum, aut in marginibus lateralibus aut etiam in superficiebus planis positis.

Type of the genus: *Calliarthron cheilosporioides* sp. nov.

Frondibus 10–29 cm. altis, opposite et laxe pinnatis aut subalterne ramosis; conceptaculis in lobis superis et marginibus lateralibus primo 1–3 in margine quaque oriendis, ultimo quoque in superficiebus planis intergeniculorum congestis, conicis, in plantis tetrasporangiiferis apicibus obtusis, in plantis antheridiiferis apicibus acutis.

Species type: tetrasporic, Pacific Grove, Coast of Central California (Herb. Univ. Calif. No. 545724); antheridial, Pebble Beach, Carmel Bay, Coast of Central California, North America (Herb. Univ. Calif. No. 545721).

II. Conceptacles on the upper lobes of the intergenicula,

7. *Cheilosporum* Areschoug, in J. G. Agardh, Species Algarum, 2, sect. 2: pp. 543–547, 1852.

Type of the genus: *Cheilosporum sagittatum* (Lamx.) Areschoug, in J. G. Agardh Species Algarum, 2, sect. 2: p. 545, 1852.

Type locality: "Ile-de France."

B. Fronds with terminal conceptacles,

I. Fronds with both terminal and lateral conceptacles,

8. *Joculator* gen. nov.

Frondes fragiles, pinnatae usque ad pinnato-decompositae; segmentis infero compressis aut cylindricis, supero compressis; geniculis unizonalibus; filamentis medullaribus intergeniculorum rectis, cellulis in zonis transversis equalibus positis; conceptaculis terminalibus in ramulorum apicibus et etiam in superficiebus planis intergeniculorum lateralibus.

Type of the genus: *Joculator pinnatifolius* sp. nov.

Frondibus erectis, gracilibus, atropurpureis, 4–7 cm. longis, oppositis et plumoso-pinnatis, aliquando tripinnatis; conceptaculis in apicibus ramulorum aliquando antenniferis, aliquando non-antenniferis et etiam superficiebus intergeniculorum in utraque superficie 2, quaque singula prope lobam superiorem positis.

Species type: tetrasporic, Orange County, Coast of Central California, North America (Herb. Univ. Calif. No. 545769).

II. Fronds with conceptacles all terminal,

a. Branching strictly dichotomous,

9. *Jania* Lamouroux, Nouv. Bull. des Sci. par la Soc. Philomat. 3, p. 186, 1812; Hist. Polyp. Flex., pp. 266–274, 1816.

Type of the genus: *Jania rubens* (L.) Lamouroux, Nouv. Bull. des Sci. par la Soc. Philomat., 3, p. 186, 1812; Hist. Polyp. Flex., pp. 271–273, 1816.

Type locality: "O. Europaeo."

b. Branching wholly or partially pinnate,

aa. Conceptacles non-antenniferous,

10. *Corallina* L. (emend. Lamx.), Linnaeus, Syst. Nat. ed. 12, 1: part 2, pp. 1304–1306, 1767; Lamouroux, Nouv. Bull. des Sci. par la Soc. Philomat. 3, pp. 185–186, 1812; Hist. Polyp. Flex., pp. 275–292, 1816.

Type of the genus: *Corallina officinalis* Linnaeus, Syst. Nat., ed. 12, 1: part 2, p. 1304, 1767.

Type locality: "O. Europaeo, Mediterraneo."

bb. Conceptacles antenniferous,

11. *Corallina* (*Cornicularia*) subgen. nov.

Frondes fragiles, in toto aut ex parte pinnatae; segmentis cylindricis aut compressis; geniculis unizonalibus; filamentis medullaribus intergeniculorum rectis, in zonis transversis equalibus positis; conceptaculis terminalibus, omnino aut plerumque antenniferis.

Type of the subgenus: *Corallina* (*Cornicularia*) *gracilis* Lamouroux, Hist. Polyp. Flex., p. 288, pl. 10, fig. 1 (a and b), 1816.

Type locality: "Australasie."

c. Branching pinnate-cymoid,

aa. Conceptacular pores apical,

12. *Arthrocardia* Areschoug, in J. G. Agardh Species Algarum. 2, sect. 2: pp. 547–553, 1852.

Type of the genus: *Arthrocardia corymbosa* (Lamk.) Areschoug, in J. G. Agardh Species Algarum, 2, sect. 2: pp. 550–551, 1852.

Type locality: "ad littora Americae," *fide* Lamarck; "ad oram Capensem praesertim in sinu Tabulari nec non Algoensi non infrequenter," *fide* Areschoug.

bb. Conceptacular pores slightly lateral (slightly below the apices),

13. *Duthiea* gen. nov.

Frondes fragiles, pinnato-cymoideae; segmentis basi compressis aut cylindricis, supero compressis; geniculis unizonalibus; filamentis medullaribus intergeniculorum rectis, cellulis in zonis transversis equalibus positis; conceptaculis in ordine cymoideo-terminalibus, poris oblique-lateralibus.

Type of the genus: *Duthiea Setchellii* sp. nov.

Frondibus erectis, 4–6 cm. altis, parte vegetabili opposite pinnatis aut tripinnatis, fructifera cymoideo-ramosis; conceptaculis apicalibus in intergeniculis terminalibus, intergeniculis conceptaculiferis e marginibus superioribus intergeniculorum fertilium in ordine, more cymarum oriendis, poris lente oblique-lateralibus, tetrasporangiis in fundo et lateribus cavernarum conceptaculorum positis.

Species type: tetrasporic, Blauwklip, near the mouth of Grote River, South Africa (Herb. Univ. Calif. No. 545765; Duthie No. 8012).

AN EOCENE TITANOTHERE FROM SAN DIEGO COUNTY, CALIFORNIA, WITH REMARKS ON THE AGE OF THE POWAY CONGLOMERATE

BY CHESTER STOCK

BALCH GRADUATE SCHOOL GEOLOGICAL SCIENCES, CALIFORNIA INSTITUTE TECHNOLOGY

Communicated January 16, 1937

Introduction.—The occurrence of Eocene vertebrates in the Poway Conglomerate of San Diego County, California, was first brought to my attention several years ago when, in the course of excavations north of La Mesa and approximately 10 miles east and slightly north of the city of San Diego, fragmentary remains of vertebrates were encountered at a depth of 40 feet. Examination of this material, permitted through courtesy of Director Clinton G. Abbott of the San Diego Museum of Natural History, elucidated the information that several mammals found

at this locality are either closely related to or identical with forms recognized in the upper Eocene fauna from the Sespe deposits, north of the Simi Valley, Ventura County.

Further field investigations conducted in the area have uncovered additional fossil vertebrate localities and at one of these, during the past summer, was found the titanothere to be described in this paper. The specimen is noteworthy because it permits a comparison with related types from the North American Eocene, so comprehensively discussed by Osborn[1] in his monograph on the Titanotheres. In addition, the presence of this material in the Poway Conglomerate, a deposit containing marine lenses from which Hanna[2] obtained an invertebrate fauna tentatively correlated with the Tejon Eocene, offers excellent opportunity to compare the age determination of the Poway based on a study of the titanothere with that derived from a study of the marine mollusks.

DESCRIPTION OF MATERIAL

SUBFAMILY DOLICHORHINAE

Metarhinus(?) pater, n. sp.

Type Specimen.—The right half of the muzzle of a skull from the anterior part of the orbit to the anterior end of the maxillary with the canine and $P\underline{1}$–$M\underline{3}$; No. 2037 Calif. Inst. Tech. Coll. Vert. Pale.; Plate 1. Specimen collected by Jack Dougherty.

Locality.—Sandstones of the Poway formation, exposed in west bank of the San Diego River, approximately one-quarter mile north and east of the Mission San Diego; Calif. Inst. Tech. Vert. Pale. Loc. 249.

Specific Characters.—Muzzle elongate; naso-maxillary recess deep and reaching back of antorbital foramen; antorbital foramen large and situated above anterior border of $M\underline{2}$. $P\underline{1}$ and $P\underline{2}$ small; $P\underline{4}$ relatively long in comparison to its width. Size larger than *Metarhinus fluviatilis* and *M. riparius*, similar to that of *M. earlei* and smaller than *Mesatirhinus superior*.

Comparison with Metarhinus.—The principal point of difference between No. 2037 and skulls of *Metarhinus* is presented in the great backward extent of the naso-maxillary notch as seen in side view. The ascent of the lower border of this notch in its posterior course is more gradual than in skulls of *Metarhinus* with which comparison has been made and, moreover, extends farther behind the level of the antorbital foramen than in these specimens. Above and to the inner side of the foramen is a broad platform of bone which is grooved longitudinally. This forms the posterior part of the floor of the recessed area, the roof of which was formed by the nasal bones, unfortunately not preserved in the Poway specimen. A similar platform is seen in the skull of *Metarhinus fluviatilis*, but the lateral

recess extends back to a point above and in front of the antorbital foramen. The lateral wall of the maxillary in front of the antorbital foramen shows no indentation or groove. The medial dorsal contact of the premaxillaries is long in fore and aft direction.

A deep naso-maxillary recess occurs in the skull of *M. riparius*, the recess reaching nearly to the level of the inner anterior border of the orbit. No. 2037 from the Poway differs principally in greater elongation of snout as expressed by greater length in front of orbit and by a longer

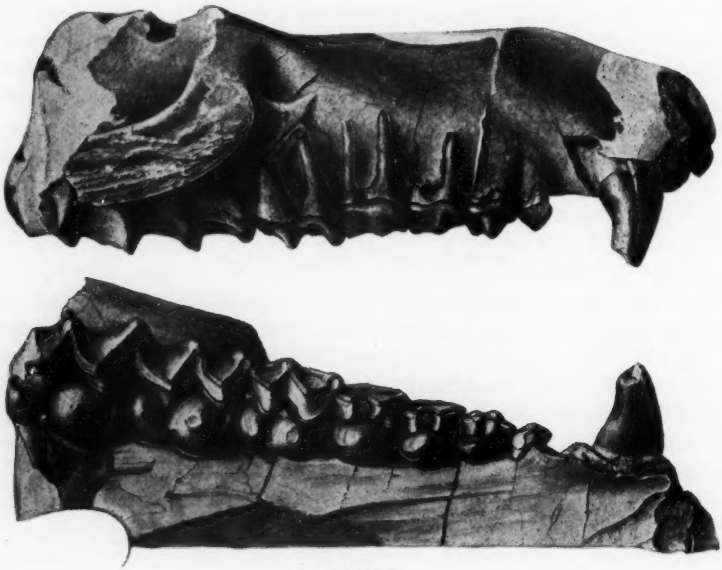

PLATE 1

Metarhinus (?) *pater*, n. sp.

Type specimen, No. 2037, Calif. Inst. Tech. Coll. Vert. Pale. Ventral and lateral views, × 1/2.

Poway Conglomerate, San Diego Co., California. Upper Eocene.

diastema between P1 and canine. In *M. riparius* the lateral face of the snout curves inward more gradually in its upward course and a small platform extends forward from the antorbital foramen.

The surface of the maxillary below the orbit in No. 2037 shows that the jugal has been broken away along the plane of the suture. Examination of the specimen leads to the impression that the infra-orbital shelf was fully as well developed as in *Metarhinus* and thus differed from that in *Rhadinorhinus*.

No. 2037 resembles species of *Metarhinus* in the close approach made by the antorbital foramen to the orbital border, in the position of the postnarial notch opposite or slightly in advance of the posterior level of $M\underline{2}$, and in the small size of $P\underline{1}$. The San Diego specimen differs in presence of a deeper naso-maxillary recess, longer snout, longer postcanine diastema, greater anteroposterior diameter of $P\underline{4}$ in relation to its transverse diameter, and in a more posterior position of the antorbital foramen since the posterior rim of this opening is situated above the anterior end of $M\underline{2}$. A well developed hypocone is present in $M\underline{3}$.

Comparison with Mesatirhinus.—The tooth-row in No. 2037 resembles in length that in the type of *Mesatirhinus petersoni* and in the type of *M. superior*, but the premolar series is shorter. The canine is larger than the comparable tooth in *M. superior* but may be similar in size to that in *M. petersoni*. $P\underline{1}$ is smaller in the San Diego specimen than in *Mesatirhinus*, but $P\underline{2}$ has the subtriangular shape seen in this genus.

In $P\underline{3}$ and in $P\underline{4}$ the internal cingulum swings around from the anterior and posterior sides of the tooth, but does not extend entirely along the inner side of the base of the principal internal cusp. $M\underline{2}$ in No. 2037 is narrower relative to its length than is the comparable tooth in *Mesatirhinus*. The postnarial notch reaches slightly farther forward than in *M. superior*, but not quite so far as in *M. petersoni*. The antorbital foramen is large, relatively more so than in *Mesatirhinus*. The distance between the lateral border of this opening and the anterior border of the orbit is shorter than in *Mesatirhinus*. The narial opening is much more deeply recessed as seen from the side than in the latter genus.

Comparison with Dolichorhinus.—No. 2037 is distinctly smaller than typical members of the genus *Dolichorhinus* and differs markedly from these in the much more deeply recessed narial opening, absence of a secondary palate, more posterior position of the antorbital foramen, decidedly shorter distance between this foramen and the orbital border, shorter postcanine diastema and in the subtriangular rather than subquadrate shape of $P\underline{2}$. In specimens of *Dolichorhinus* the cingulum is complete along the inner sides of the posterior premolars, not interrupted as in No. 2037.

Comparison with Rhadinorhinus.—The tooth-row in No. 2037 resembles in length that in the type of *R. diploconus*, but lacks the upward curvature in a vertical plane of the anterior cheek-teeth. $P\underline{2}$ is not subquadrate as in *Rhadinorhinus;* the postcanine diastema is longer; the postnarial notch is farther back; the infra-orbital shelf is better developed in the San Diego specimen. While the lateral recess of the nose is deep in *Rhadinorhinus*, the notch does not extend backward so far as in No. 2037 and the lower posterior rim of the notch is sharper. The antorbital foramen is large as in *Rhadinorhinus* and, as in this genus, is closely situated to the border of the orbit, but has a position farther back with reference to $M\underline{1}$.

MEASUREMENTS (IN MILLIMETERS) OF NO. 2037

Length from anterior end of *C* to posterior end of $M\underline{3}$	200
Length of premolar-molar series through middle	166.4
Length of molar series through middle	100.7
Length of postcanine diastema	14.4
C, anteroposterior diameter	20
C, transverse diameter	17.5
$P\underline{1}$, anteroposterior diameter	12.4
$P\underline{1}$, transverse diameter	7.2
$P\underline{2}$, anteroposterior diameter	18.6
$P\underline{2}$, transverse diameter	16.4
$P\underline{3}$, anteroposterior diameter through middle	17.4
$P\underline{3}$, transverse diameter	21
$P\underline{4}$, anteroposterior diameter through middle	20.7
$P\underline{4}$, transverse diameter	25.4
$M\underline{1}$, anteroposterior diameter through middle	27
$M\underline{1}$, transverse diameter	30
$M\underline{2}$, anteroposterior diameter through middle	33
$M\underline{2}$, transverse diameter	32.8
$M\underline{3}$, anteroposterior diameter through middle (approximate)	39
$M\underline{3}$, transverse diameter	39

Summary of Comparisons.—Among North American Eocene titanotheres, the type, No. 2037, resembles most closely the genera *Metarhinus*, *Mesatirhinus*, *Dolichorhinus* and *Rhadinorhinus*. In its most striking character the Poway specimen resembles more closely the first and last genera than it does *Mesatirhinus*. Resemblance to *Dolichorhinus* is even more remote. No. 2037 represents a skull with elongated muzzle and with very deeply recessed naso-maxillary opening. In latter character the San Diego species is distinctly more modified than any known member of the Dolichorhinae. Nearest approach in the character of deep recess is to *Metarhinus*. In *Rhadinorhinus* the opening is also deeply recessed, but in other characters of skull and dentition this genus resembles the San Diego form less closely than does *Metarhinus*. The characters which distinguish No. 2037 from *Metarhinus* are possibly diagnostic of a new genus, but I hesitate to describe the Poway specimen as such in view of the present fragmentary material. No. 2037 may represent an offshoot of the metarhine group, later and more specialized than *Metarhinus*, in which an advance is shown particularly by the elongation and further modification of the snout and likewise perhaps by the well developed hypocone in $M\underline{3}$.

REMARKS ON THE AGE OF THE POWAY CONGLOMERATE

Hanna[3] in 1926 published the results of his geologic study of the La Jolla Quadrangle. Rocks of Eocene age exposed in this area were recognized by Hanna as comprising, in ascending order, the following: (1) Delmar Sand, (2) Torrey Sand, (3) Rose Canyon Shale and (4) Poway

Conglomerate. The three lowermost beds were grouped together as the La Jolla formation and were considered as intermediate in age between the Meganos and Tejon formations of the Pacific Coast marine Eocene. The La Jolla formation was regarded as an apparent correlative of the Domengine Eocene of the Simi Valley section, California.

The locality of occurrence of *Metarhinus*(?) *pater* is in an area mapped by Hanna as the Poway Conglomerate. The specimen was found in a sandstone stratum between conglomerate layers. In reaching an age determination of this portion of the Poway it is worthy of note that the titanotheres with which the Poway species is compared, include types that range upward stratigraphically from the Metarhinus beds of the Bridger upper middle Eocene to and into the Dolichorhinus beds representing the Uinta *B* stage of the upper Eocene, as these horizons are now recognized in the Tertiary basins of the Cordilleran Province. Relationship of the San Diego species appears to be with the metarhine titanotheres, but the former is more specialized and advanced than typical *Metarhinus*. *M.*(?) *pater* differs widely from the genera *Diplacodon*, *Eotitanotherium* and *Protitanotherium* recorded from the horizon Uinta *C* of the Uinta basin. It is distinctly less advanced and clearly an earlier type of titanothere than *Teleodus californicus*[4] from the uppermost Eocene Sespe of Ventura County, California. Thus the relationships of the San Diego titanothere suggest an age determination of the land-laid Poway as not older than the Bridger upper middle Eocene and not as late as the Uinta *C* stage of the Upper Eocene. On the other hand, the advance in structural characters which *M.*(?) *pater* exhibits in a comparison to the typical *Metarhinus* may indicate a stage of development later in time than that represented by the related forms from Uinta *B*. Thus it is possible that *M.*(?) *pater* occurred at a time when *Diplacodon* and *Protitanotherium* were present during the accumulation of the later Uinta. In either case, the San Diego titanothere points to an upper rather than middle Eocene age for the land-laid Poway.

[1] Osborn, H. F., *U. S. Geol. Surv. Mon.*, **55**, 1, 383–434 (1930).

[2] Hanna, M. A., *Univ. Calif. Publ., Bull. Dept. Geol. Sci.*, **16**, 256–263 (1927).

[3] Hanna, M. A., *Univ. Calif. Publ., Bull. Dept. Geol. Sci.*, **16**, 187–246, pls. 17–23, map (1926).

[4] Stock, C., *Proc. Nat. Acad. Sci.*, **21**, 456–462 (1935).

RELATIONS BETWEEN CHROMOSOME SIZE AND EFFECTS OF INVERSIONS ON CROSSING-OVER IN DROSOPHILA MELANOGASTER

BY ARTHUR G. STEINBERG

DEPARTMENT OF GENETICS, COLUMBIA UNIVERSITY

Communicated January 15, 1937

Schultz and Redfield[1,2] have shown that inversions in chromosomes I and II cause an increase in crossing-over in chromosome III and that inversions in chromosomes I and III have similar effect on crossing-over in chromosome II. Bridges[3] showed that inversions in chromosomes I, II and III when present simultaneously have no effect on crossing-over in chromosome IV. Steinberg[5] showed that inversions in chromosomes II and III cause an increase in crossing-over in chromosome I. It was found both by Schultz and Redfield and by Steinberg that different inversions caused different amounts of increase in crossing-over in a given chromosome.

Table 1, which is a combination of data of Schultz and Redfield (unpublished) for chromosomes II and III and Steinberg[5] for chromosome I, shows that a given inversion causes a different average increment in crossing-over per unit map length in different chromosomes. For example, the C1B inversion causes a thirty-eight per cent increase in crossing-over per unit map length in chromosome II while in chromosome III it causes an increase of forty-six per cent per unit map length (table 1). The question arises as to what causes this differential quantitative effect of inversions on crossing-over in non-homologous chromosomes. While no complete answer to this question can be given at the present time, reference to tables 2 and 3 will show a partial answer.

TABLE 1

SHOWING A SUMMARY OF THE INCREASES IN CROSSING-OVER CAUSED IN NON-HOMOLOGOUS CHROMOSOMES BY INVERSIONS (VALUES EXPRESSED AS DECIMAL FRACTIONS)

INVERSIONS	CHROMOSOME I	CHROMOSOME II	CHROMOSOME III	TOTALS
C1B	....	0.38	0.46	0.84
Curly	0.22	....	0.49	0.71
Payne	0.33	0.55	....	0.88

Table 2 shows a comparison of the ratios of the relative lengths of metaphase chromosomes[4] with the ratios of the interchromosomal effects of an inversion or pair of inversions on crossing-over in these chromosomes. Thus chromosome I is sixty-nine per cent as long as chromosome II and the effect of the Payne inversions on I is sixty per cent of the effect of the same inversions on II, likewise chromosome I is fifty-seven per cent as

long as III while the effect of the Curly inversions on the former is forty-five per cent of that on the latter; and finally chromosome II is eighty-three per cent of III and the effect of the C1B inversion on chromosome II is also eighty-three per cent of that on III. Within the limits of error which are probably large because:

(1) of the difficulties involved in measuring *Drosophila* chromosomes,

(2) the interchromosomal effects of the inversions were measured in three different experiments, and

(3) the first chromosome was not completely marked,

these pairs of ratios may be considered very similar.

TABLE 2

SHOWING THE RATIOS OF THE RELATIVE METAPHASE LENGTHS OF THE GONIAL CHROMOSOMES AND THE CORRESPONDING RATIOS OF THE INTERCHROMOSOMAL EFFECT OF INVERSIONS

CHROMOSOMES	I/II	I/III	II/III
Ratio of sizes	100/145 = 0.69	100/175 = 0.57	145/175 = 0.83
Ratio of effects	0.33/0.55 = 0.60	0.22/0.49 = 0.45	0.38/0.46 = 0.83

TABLE 3

SHOWING THE PERCENTAGE OF THE TOTAL CHROMATIN LENGTH CONTAINED IN EACH OF THE CHROMOSOMES AND THE CORRESPONDING PERCENTAGE OF THE TOTAL INTERCHROMOSOMAL EFFECT OF INVERSIONS SHOWN BY EACH CHROMOSOME

CHROMOSOMES	I	II	III	IV
Percentage of total chromatin	23.3	33.7	40.7	2.3
Percentage of total effect	22.6	38.3	39.1	0.0

Table 3 shows a comparison of the percentage length of a given chromosome (i.e., the length of the chromosome divided by the sum of the lengths of all four chromosomes and multiplied by 100) with the per cent of the total increase in crossing-over shown in this chromosome. For example, the increases in crossing-over in chromosome I are .22 + .33 = .55 (table 1), the total increase in crossing-over is .84 + .71 + .88 = 2.43 (table 1); the percentage of the total effect which is shown by chromosome I is $.55/2.43 \times 100 = 22.6$. These figures (table 3) show even more clearly than those in table 2 that the effect of an inversion on crossing-over in a non-homologous chromosome is directly proportional to the length of the chromosome affected. In addition table 3 shows that the proportion of the total effect which goes to a given chromosome is approximately equal to that proportion of the total length of all the chromosomes which the affected chromosome constitutes. Therefore, the effect of an inversion on crossing-over in a non-homologous chromosome is a function of both the inversion itself and of the length of the chromosome affected. This fact explains Bridges'[3] observation that inversions do not affect crossing-over in chromosome IV. Chromosome IV, according to the above, would be ex-

pected to show about two per cent of the total increase in crossing-over (table 3), i.e., crossing-over in chromosome IV should be increased by approximately five per cent. Such an increase in crossing-over in chromosome IV is so small as to be detectable only in extremely large test populations.

The author wishes to acknowledge his indebtedness to Professors L. C. Dunn and D. E. Lancefield for their helpful suggestions, and to Dr. J. Schultz and Miss H. Redfield for kindly permitting him to use their unpublished data.

[1] Morgan, T. H., Bridges, C. B., and Schultz, J., *Yearb. Carnegie Instn.*, **31**, 303 (1932).

[2] Morgan, T. H., Bridges, C. B., and Schultz, J., *Yearb. Carnegie Instn.*, **32**, 298 (1933).

[3] Morgan, T. H., Bridges, C. B., and Schultz, J., *Yearb. Carnegie Instn.*, **33**, 274 (1934).

[4] Morgan, T. H., Bridges, C. B., and Sturtevant, A. H., *Bibliog. Genet.*, **1** (1925).

[5] Steinberg, A. G., *Genetics*, **21**, 615 (1936).

LINKAGE STUDIES OF THE RAT (RATTUS NORVEGICUS). II[1]

BY HELEN DEAN KING AND W. E. CASTLE

WISTAR INSTITUTE AND UNIVERSITY OF CALIFORNIA

Communicated January 13, 1937

King[2] has recently described the occurrence and inheritance of waltzing in an inbred race of rats reared at the Wistar Institute. Concerning the mode of inheritance this statement was made: "Available evidence seems to indicate that waltzing is due to a single gene, but that the extent to which this gene expresses itself depends upon modifying factors which favor or inhibit its action." Selection of the most pronounced waltzers through a series of generations increased the incidence of waltzing. In the F_6 generation the percentage of waltzers produced by waltzing parents had risen to 93 per cent.

The waltzing mutation made its first appearance in albino individuals and though it has since been introduced into colored individuals, it consistently occurs in a higher percentage of the albino than of the colored individuals in litters containing both sorts. This indicates that it is linked with albinism and that its gene is borne in the same chromosome as the albino gene. The evidence for this conclusion is as follows:

Crosses were made between albino waltzers and colored non-waltzers of the varieties known as hairless, kinky and blue. All F_1 individuals were, as expected, colored non-waltzers. The F_2 population obtained from each

cross is classified in table 1 as regards the occurrence of albinism. No indication was found of linkage between waltzing and the other mutant characters involved in these crosses, hairless, kinky and blue.

TABLE 1

F_2 POPULATIONS IN WHICH IS SHOWN THE COMPARATIVE INCIDENCE OF WALTZING AMONG ALBINO AND NON-ALBINO INDIVIDUALS, RESPECTIVELY

	ALBINO NON-WALTZERS	ALBINO WALTZERS	PER CENT WALTZERS	COLORED NON-WALTZERS	COLORED WALTZERS	PER CENT WALTZERS
Cross 1. Albino waltzer × hairless	82	7	7.8	202	3	1.5
Cross 2. Albino waltzer × kinky	36	8	19.0	154	10	6.1
Cross 3. Albino waltzer × blue	88	13	14.7	316	22	6.5

It will be observed that the incidence of waltzing was in all three of the F_2 populations higher among albinos than among their colored sibs.

The same relation was, with a single exception, found to hold in certain back-cross populations produced by mating F_1 colored non-waltzers with albino waltzers, as shown in table 2.

TABLE 2

COMPARATIVE INCIDENCE OF WALTZING IN ALBINO AND COLORED INDIVIDUALS IN BACK-CROSS POPULATIONS

	ALBINO NON-WALTZERS	ALBINO WALTZERS	PER CENT WALTZERS	COLORED NON-WALTZERS	COLORED WALTZERS	PER CENT WALTZERS
Cross 4A. Albino waltzer × Curly	104	21	16.8	117	21	15.2
Cross 4B. Albino waltzer × Curly	24	18	42.8	35	9	20.4
Cross 5A. Albino waltzer × Black	44	16	26.6	64	16	20.0
Cross 5B. Albino waltzer × Black	58	10	14.7	63	12	16.0
Cross 7. Albino waltzer × $Curly_2$	52	38	42.2	47	24	33.8
Totals	282	103	26.7	326	82	20.1

In the Cross 5B population alone was the percentage of waltzers as high among the colored as among the albino individuals. For all the populations of table 2 combined, 26.7 per cent of the albinos were waltzers, but of the colored individuals only 20.1 per cent.

One further point of interest should be noted in connection with Cross 3, table 1. The blue parent to this cross was heterozygous for yellow, a recessive gene borne in the same chromosome as the albino gene. If waltzing is linked with albinism, it should show linkage also with yellow.

The F_2 population derived from Cross 3 may be separated into three groups as shown in table 3.

TABLE 3

A FURTHER CLASSIFICATION OF THE F_2 POPULATION OF 426 INDIVIDUALS DERIVED FROM CROSS 3, TABLE 1

	NON-WALTZERS	WALTZERS	PER CENT WALTZERS
Gray, black or blue (i.e., non-yellow colored)	259	16	5.8
Yellow or cream (dilute yellow)	57	6	9.5
Albino	75	13	14.7
Totals	391	35	8.2

As expected, the percentage of waltzers in the yellow group is higher than that in the non-yellow group, suggesting linkage of waltzing with yellow as well as with albinism.

The data presented in tables 1–3 had been obtained prior to March 17, 1936. Subsequent experiments support the tentative conclusion reached at that time, that linkage exists between waltzing and albinism. See table 4.

TABLE 4

FURTHER DATA ON THE COMPARATIVE INCIDENCE OF WALTZING AMONG COLORED AND ALBINO SIBS IN BACK-CROSS POPULATIONS

	ALBINO NON-WALTZERS	ALBINO WALTZERS	PER CENT WALTZERS	COLORED NON-WALTZERS	COLORED WALTZERS	PER CENT WALTZERS
Cross 7A. Albino waltzer × Curly$_2$	171	116	40.4	176	92	34.3
Cross 5C. F_1 (Albino waltzer × black) × black waltzer	30	9	23.1	167	43	20.5
Cross 5D. Albino waltzer × black	146	38	20.6	159	38	19.3
Cross 2A. Albino waltzer × kinky	56	21	27.3	68	16	19.0
Totals	403	184	31.3	570	189	24.9

In each of the four back-cross populations of table 4, the percentage of waltzers is higher among albinos than among their colored sibs, the totals being 31.3 per cent among the albinos to 24.9 per cent among the colored.

Further experiments to test for linkage between waltzing and yellow are as yet incomplete and inconclusive. The total back-cross population obtained by summarizing the various experiments described in tables 2 and 4 consists of 2139 individuals, which fall into the following classes:

	ALBINO NON-WALTZERS	ALBINO WALTZERS	COLORED NON-WALTZERS	COLORED WALTZERS
Observed numbers	685	287	896	271
Corrected for overlapping	463	550	606	519

When we attempt to calculate the crossover percentage between albinism and waltzing, we are confronted with this difficulty, that the observed number of waltzers (558) is less than the observed number of non-waltzers (1581), with which it should be theoretically equal. This, as already explained, we may assume to be due to the occurrence of normal overlaps among the non-waltzers, i.e., of individuals genetically waltzers but actually not manifesting the waltzing behavior. Nevertheless, we observe that the non-crossover class, colored non-waltzers, is larger than the crossover class, albino non-waltzers, and also that the other non-crossover class, albino waltzers, is larger than the other crossover class, colored waltzers, these being the relations which we should expect if linkage exits between albinism and waltzing.

If we assume that overlapping to normality occurs equally among the albino and the colored waltzers, we may use the observed frequencies in calculating a crossover percentage.

The observed number of crossovers will accordingly be the sum of the albino non-waltzers (685) plus the colored waltzers (271), or 956, which is 44.7 ± 0.7 of the total population, 2139. This is a very loose indicated linkage but one of undoubted significance in view of the small probable error and the consistency of the occurrence of a larger percentage of waltzers among albino than among colored individuals in eight out of nine of the back-cross populations.

This calculation of the crossover percentage may be checked by actually deducting from the classes of non-waltzers, and adding to the classes of waltzers, enough individuals (considered as normal overlaps) to make the total in each of the two groups equal to the half population, 1019. Such a "correction for overlapping" has been made in the foregoing summary of the backcross populations. If we base a calculation of the crossover percentage on these corrected numbers, we get $463 + 519 = 982$ as the total of the crossover classes, which is 45.8 ± 0.7 per cent of the entire population, again a statistically significant indication of linkage.

It has been known for some time that the albino chromosome of the rat contains genetic loci for two other mutant characters, red-eyed yellow (*r*) and pink-eyed yellow (*p*).[3] We are now warranted in assuming the existence in this same chromosome of a fourth gene which in its mutant form may produce waltzing. The order of the four genes and their approximate map-distances are as follows:

C	*R*	*P*	*W*
0	0.3	20	45

The experiments described in this paper have been made by King at the

Wistar Institute in consultation with Castle, who has formulated this report.

[1] See also *Proc. Nat. Acad. Sci.*, **21**, 390–399 (1935).
[2] King, H. D., *Jour. Mammology*, **17**, 157–163 (1936).
[3] Castle, W. E., *Genetics and Eugenics*, 4th Ed., 234 (1930).

THE COEFFICIENT OF PREDICTION-ACCURACY

Computation of the Portion of Individual Cases Common to Both the Particular Prediction-Distribution and to the Subsequently Determined Actual-Distribution of the Same Measured and Counted Phenomena

By Harry H. Laughlin

Eugenics Record Office, Carnegie Institution of Washington, Cold Spring Harbor, Long Island, N. Y.

Communicated January 4, 1937

Consider first the specifications for a sound formula for the coefficient of prediction-accuracy. Regardless of how, where or why we got it, if we have in hand a prediction in terms of a probability-distribution, and if the subsequently determined actual-distribution corresponds exactly with the prediction-distribution, it is evident that the particular prediction is perfect, and that consequently the coefficient of prediction-accuracy should equal 1.000. If, in another case, there be no overlapping of the two probability-distributions (that is, if the subsequently determined actual-distribution does not overlap to any degree with the given prediction-distribution which is being tested), then the coefficient of prediction-accuracy should work out in the value 0.000. If, in still another case, 95 per cent of the individual values actually found were as predicted, then the coefficient of prediction-accuracy should register 0.9500. And so on, if three-fourths or if one-half of the case values are common between the prediction-distribution and the actual-distribution, then the nature of the coefficient of prediction-accuracy should be such that its formula would produce measured coefficients respectively of 0.7500 and of 0.5000. Thus the *CPA* is properly measured by that portion of cases common to both areas "p" and "a."

Also both the particular prediction-basis and the subsequent actual check-up by first-hand survey, must be plotted in the same coördinate frame, in which $K = f(R)$, in which R equals the measure of subject-quality and K equals the probability-value. Also each distribution-area (that is, "p" the prediction-area and "a" the actual area) must equal 1.000.

Whenever any two normal probability-curves, each of which bounds an area which equals 1.000, are plotted within the same coördinate frame (as

are the cases herewith) there will always be *some* overlapping. If the prediction-area be an "absolute guess or a chance bet" such set-up should cause the *CPA* to "move away from 1.000 or perfection toward but, of course, never reaching zero" in value.

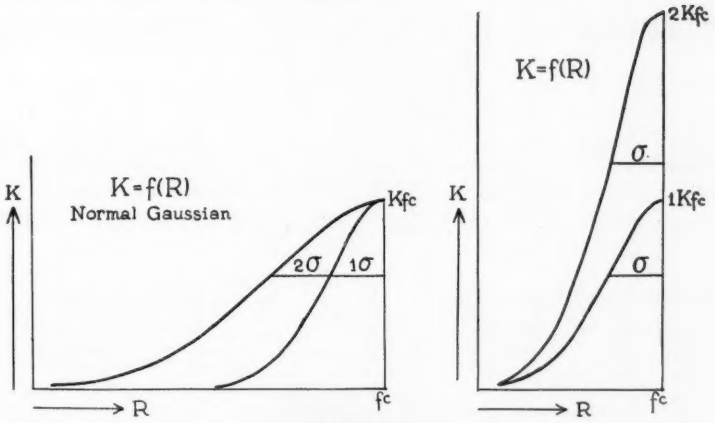

FIGURE 1

K_{fc} being constant, the area varies directly with σ, the Standard Deviation.

The Standard Deviation σ being constant, the area varies directly with the K_{fc}.

When two distribution-areas are plotted within the same frame of coordinates they produce four points on the *R*-or-subject-scale which are of basic importance in the determination of the coefficient of prediction-accuracy. These four points indicate respectively the positions of

(*a*) *fc* or the fluctuation-center of *R*-values in "*p*" the prediction-distribution,

(*b*) *fc* or the fluctuation-center of *R*-values in "*a*" the actual-distribution,

(*c*) the base of the left-most common probability-value caused by the intersection of the boundary curves of the two areas "*p*" and "*a*," and

(*d*) the base of the right-most common probability-value caused by the intersection of the boundary curves of the same two areas "*p*" and "*a*."

Given the foregoing specifications of a coefficient of prediction-accuracy, we find that the possible situations fall into three cases depending upon the relative positions of the four above-listed points on the same *R*-scale, and upon the relative K_{fc} values in "*p*" and "*a*"—that is, in the prediction and actual areas.

With the two "*fc*'s" and their respective area-formulae given, it is evi-

THE COEFFICIENT OF PREDICTION-ACCURACY (C.P.A)

THE PORTION OF CASES COMMON TO BOTH THE PARTICULAR PREDICTION-DISTRIBUTION AND ITS SUBSEQUENT ACTUAL-DISTRIBUTION OF MEASURED AND COUNTED PHENOMENA.

CASE I.

with Example.

PROPERTIES (a) *The total Prediction-area and the total Actual-area each = 1.000. Each is plotted within the same coördinate frame, - the same K, that is the same Frequency or Probability-scale, and the same R-class measure of the common subject.*
1 R-class-range = 1 R-unit. 1 Area-unit = .01 K by 1 R.

(b) *Type of each area-bounding curve,* $K = K_{fc}\, e^{-\frac{fc^2}{2\sigma^2}}$ *Each curve with constant* K_{fc}, *and with its two σ's either equal to or different from each other, but always* $(\sigma_f + \sigma_f) \div 2 = \sigma$ *symmetrical.*

(c) *Two Common Probability-values, due to overlapping of curves "p" and "a", one* cK *to the left of both* fc_p *and* fc_a, *the other* cK *to the right of both* fc_p *and* fc_a.

(d) *Under the particular probability-curve, whether symmetrical or skewed,*
Area to left fc : Area to right $fc = \sigma_f : \sigma_t$ *when Total Area = 1.0000.*
Area to the left of $fc = \frac{\sigma_f}{\sigma_f + \sigma_t}$ *Area to the right of* $fc = \frac{\sigma_t}{\sigma_f + \sigma_t}$

(e) C.P.A = Σ *Four constituent Integral-blocks. Two for Area with greater* K_{fc}, *one in each of its lower extremities,* ① $\int_{cK_f}^{\infty}$ *and* ② $\int_{cK_a}^{\infty}$ *and two for Area with lesser* K_{fc}, *in its central region,* ③ $\int_{cK_a}^{fc}$ *and* ④ $\int_{cK_a}^{fc}$.

GIVEN Prediction-Area = 1.0000

fc_p at point 18.79 on R-scale
K_{fc_p} = 0.1125 on K-scale
σ_{2p} = 3.3245 R-units
σ_{1p} = 3.6342 R-units
σ_{xp} = 2.9948 R-units

GIVEN Actual Area = 1.0000

fc_a at point 20.00 on R-scale
K_{fc_a} = 0.0750 on K-scale
σ_{2a} = 4.9868 R-units
σ_{1a} = 6.6400 R-units
σ_{xa} = 3.3245 R-units

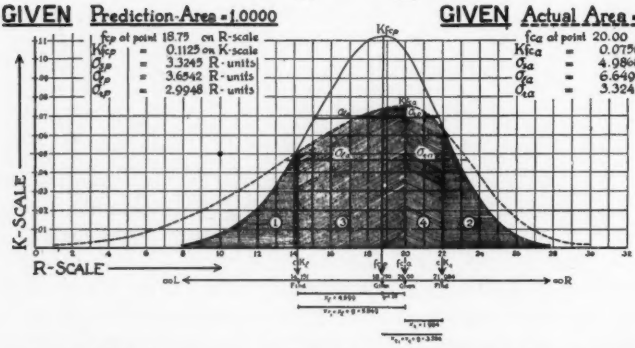

LEGEND: K = Probability; R = Measured Subject-quality; p = a property of Prediction-area; a = a property of Actual-area; fc = fluctuation-center; ℓ = left of particular fc; r = right of particular fc; K_{fc} = probability value at particular fc; σ_f = standard deviation symmetrical - i.e. when probability-curve is bi-symmetrical, - i.e. not skewed; $\sigma_f + \sigma_t = 2\,\sigma_f$, when both portions are equal and K_{fc} are constant; cK_f = the left-most probability-value common to both p and a; cK_a = the corresponding right-most common probability; g = (fcp − fca) in R-units.

FIND

1. fc predicted − fc actual = g = 1.250
2. (a) R-locus of cK_f When $(fc_p - cK_{(op)}) = X_f$, and $(fc_a - cK_{(oa)}) = X_{f_1}$, solve for the positive value of X_f by means of the two simultaneous equations
   ① $K_{fc_p} \cdot e^{-\frac{(cK_f)^2}{2(\sigma_{2p})^2}} = K_{fc_a} \cdot e^{-\frac{(cK_f)^2}{2(\sigma_{1a})^2}}$ *The two formulas for the Common Probability at* cK_f, *and*
   ② $X_f = X_{f_1} - g$ *Locus* cK_f *on R-scale = locus fc predicted −* X_f. X_f = 4.90 R-units, X_{f_1} = 5.84 R-units.
   ∴ *The locus* cK_f = 18.790 − 4.599 = 14.191 *on the R-scale.*
   (b) R-locus of cK_a When $(fc_a - cK_{(oa)}) = X_{f_1}$, and $(fc_p - cK_{(op)}) = X_{f_2}$, solve for the positive value of X_a by means of the two simultaneous equations
   ① $K_{fc_p} \cdot e^{-\frac{(cK_a)^2}{2(\sigma_{2p})^2}} = K_{fc_a} \cdot e^{-\frac{(cK_a)^2}{2(\sigma_{1a})^2}}$ *The two formulas for the Common Probability at* cK_a, *and*
   ② $X_{f_1} = X_a - g$ *Locus* cK_a *on R-scale = locus fc actual +* X_{f_1}. X_a = 1.98 R-units, X_{f_1} = 3.23 R-units.
   ∴ *The locus* cK_a = 20.000 + 1.984 = 21.984 *on the R-scale.*
3. *When the total area under the particular probability-curve = 1.0000*
   (a) *Prediction-area to left of* $fc_p = 2\,\sigma_f \div (\sigma_f + \sigma_t) = 1.0992 \div 2 = .5496$
   (b) *Prediction-area to right of* $fc_p = 2\,\sigma_t \div (\sigma_f + \sigma_t) = .9008 \div 2 = .4504$
   } = 1.0000
   (c) *Actual — area to left of* $fc_a = 2\,\sigma_f \div (\sigma_f + \sigma_t) = 1.3333 \div 2 = .6666$
   (d) *Actual — area to right of* $fc_a = 2\,\sigma_t \div (\sigma_f + \sigma_t) = .6667 \div 2 = .3334$
   } = 1.0000
4. *The Value of Constituent Integral-blocks ① and ② from the overlapping distribution-areas with the greater* K_{fc}, *and of Constituent Integral-blocks ③ and ④ from the overlapping distribution-areas with the lesser* K_{fc}.

		* I	II	III	IV	
(a) When *Prediction-area* = 1.0000	① $fc_p - cK_f = 4.60$ R-units = 1.2989 · σ_{2p}	.5496 − .3494	.1002	= .1144 = *Constituent Integral-block*	①
	③ $fc_p - cK_a = 3.23$ R-units = 1.0799 · σ_{1p}	.4504 − .3159	.0908	= .1262 = *Constituent Integral-block*	②
(b) When *Actual - area* = 1.0000	② $fc_a - cK_f = 5.85$ R-units = .8796 · σ_{2a}	.3106	.3333	= .4140 = *Constituent Integral-block*	③
	④ $fc_a - cK_a = 1.98$ R-units = .9968 · σ_{1a}	.2247	.6667	= .1498 = *Constituent Integral-block*	④

Σ 4 *Constituent Integral-blocks* → .2044 = COEFFICIENT OF PREDICTION ACCURACY (C.P.A)

* I = *Given equivalent number of Standard Deviations* II = *Numerical equivalent of Area to the left or right, as the case may be, of the given fc.*
III = *Portion of total symmetrical area subtending given number of Standard Deviations (from Tables).*
IV = *Total Area, if symmetrical, on basis of particular given σ.*

dent that the first main step toward solution consists in locating the position, on the R-scale, of the foot of each common probability-value.

The analytic geometry of the problem is developed by the three accompanying plates, one for each of the three cases. In each case the final solution is reached by determining the area covered by the overlapping of the prediction-probability-distribution-area and the actual-probability-distribution-area.

As above stated, the two areas being "compared-for-overlapping" must be plotted in the same frame of coördinates, and in each case the total area under each of the two area-bounding curves must be equal to unity. Regardless of the number of cases upon which the particular distribution is based, said distribution must be reduced to percentages by R-classes so that the total area under the particular bounding-curve is always equal to

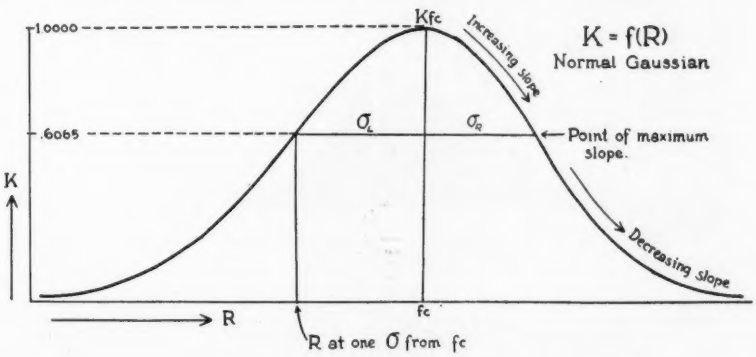

FIGURE 2

The development of 0.6065 K_{fc} as the K-point at which the Standard Deviation σ always crosses the K-scale.

1.000. This rule holds true for both the prediction-distribution and the actual-distribution—each must always equal 1.000. Beyond this specification for unity in extent the two areas and their bounding-curves may be very different. Each curve may have its own fluctuation-center (fc), its own highest probability-value (K_{fc}) and it may be skewed to any degree to either the right or the left.

The three cases, into which the possible types of the present problem fall, run as follows:

Case I is characterized by the set-up in which there are two common probability-values. On the R-scale one common probability-value (cKl) lies below the two fluctuation-centers (fcp and fca), and the second common probability-value (cKr) lies above these two fluctuation-centers.

CASE II.
with Example.

PROPERTIES

(a) *The total Prediction-area and the total Actual-area each* =1.0000. *Each is plotted within the same coördinate frame,- the same K, that is the same Frequency or probability-scale, and the same R-class measure of the common subject.*
1 R-class-range = 1 R-unit. 1 Area-unit = .01 K by 1 R.

(b) *Type of each area-bounding curve,* $K = Kfc \cdot \epsilon^{-\frac{R^2}{2\sigma^2}}$ *Each curve with constant Kfc, and with its two σ's either equal to or different from each other, but always* $(\sigma_l + \sigma_r) \div 2 = \sigma$ *symmetrical.*

(c) *Two Common Probability-values, due to overlapping of curves "p" and "a", either one* cK_l *to the left and the other* cK_s *between the two fC's p and a, or* cK_r *between the two fC's, and the other* cK_m *to the right of both fc's.*

(d) *Under the particular Probability-curve, whether symmetrical or skewed,*
Area to left $fC : Area\ to\ right\ fC = \sigma_l : \sigma_r$ *when Total Area* = 1.0000.
Area to left $fC = \frac{\sigma_l}{\sigma_l + \sigma_r}$ *and Area to right of* $fC = \frac{\sigma_r}{\sigma_l + \sigma_r}$

(e) C.P.A. = Σ *Three Constituent Integral-blocks. Two for Area with greater Kfc, in its lower extremities,* ① $= \int_{\infty\,left}^{cK_s}$ *and* ② $= \int_{\infty\,right}^{cK_m}$, *and one for Area with lesser Kfc* ③ $= \int_{cK_s}^{cK_m}$

GIVEN Prediction-Area = 1.0000

fcp at point 15.00 on R-scale
Kfcp = 0.1125 on K-scale
σ_{lp} = 3.3845 R-units
σ_{rp} = 2.7448 R-units
σ_{xp} = 3.0042 R-units

GIVEN Actual-Area = 1.0000

fca at point 20.00 on R-scale
Kfca = 0.0750 on K-scale
σ_{la} = 4.9868 R-units
σ_{ra} = 6.6490 R-units
σ_{xa} = 3.3245 R-units

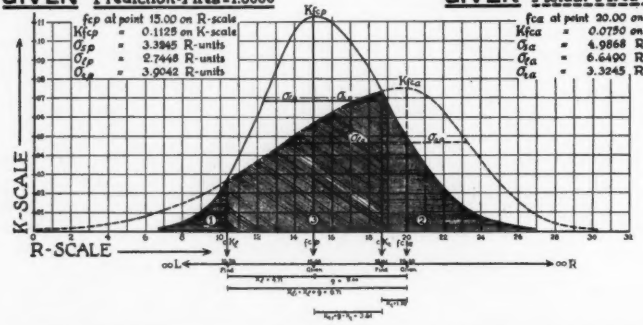

LEGEND:
K = Probability
R = Measured Subject-quality
p = a property of Prediction area
a = a property of Actual-area
fc = fluctuation-center
l = left of particular fc
r = right of particular fc
Kfc = probability value at particular fc.
σ_x = standard deviation symmetrical -i.e. when probability-curve is bi-symmetrical, -i.e. not skewed.
$\sigma_l + \sigma_r = 2\sigma_x$, when both particular ones and Kfc are constant.
cK_l = the left-most probability-value common to both p and a.
cK_s = the corresponding right-most common probability.
q = (fcp − fca) in R-units.

FIND

1. fc predicted − fc actual = q = 5.00 units on the R-scale.
2. (a) R-locus of cK_l when $(fcp - cK_{(left)}) = X_l$, $(fca - cK_{(left)}) = X_l$, solve for the positive value of X_l by means of the simultaneous equations
   ① $Kfcp \cdot \epsilon^{-\frac{(cx_l)^2}{2\sigma_{xp}^2}} = Kfca \cdot \epsilon^{-\frac{(cx_l)^2}{2\sigma_{xa}^2}}$. *The two formulas for the Common Probability at* cK_l, *and*
   ② $X_l = X_a - q$. *Locus* cK_l *on R-scale = locus fc predicted* $- X_l$. $X_l = 4.71$ *R-units,* $X_a = 9.71$ *R-units.*
   ∴ *The locus* $cK_l = 15.00 - 4.71 = 10.29$ *on the R-scale.*
   (b) R-locus of cK_s when $(fcp - cK_{(right)}) = X_{xp}$ and $(fca - cK_{(right)}) = X_{xa}$, solve for the positive value of X_x by means of the simultaneous equations:
   ① $Kfcp \cdot \epsilon^{-\frac{(cx_s)^2}{2\sigma_{xp}^2}} = Kfca \cdot \epsilon^{-\frac{(cx_s)^2}{2\sigma_{xa}^2}}$. *The two formulas for the Common Probability at* cK_s *and*
   ② $X_x = q - X_{xa}$. *Locus* cK_s *on R-scale = locus fc actual* $- X_{xa}$. $X_{xa} = 1.39$ *R-units,* $X_x = 3.61$ *R-units.*
   ∴ *The locus* $cK_s = 20.00 - 1.39 = 18.61$ *on the R-scale.*
3. *When the total area under the particular probability-curve* = 1.0000
   (a) *Prediction-area to left of* $fcp = 2\sigma_l \div (\sigma_l + \sigma_r) = .82563 \div 2 = .4128$
   (b) *Prediction-area to right of* $fcp = 2\sigma_r \div (\sigma_l + \sigma_r) = 1.17437 \div 2 = .5872$ } 1.0000
   (c) *Actual — area to left of* $fca = 2\sigma_l \div (\sigma_l + \sigma_r) = 1.33333 \div 2 = .6667$
   (d) *Actual — area to right of* $fca = 2\sigma_r \div (\sigma_l + \sigma_r) = .66667 \div 2 = .3333$ } 1.0000
4. *The Value, i.e. the Area, of Constituent Integral-blocks ① and ③ from the overlapping distribution-area with the greater Kfc, and of Constituent Integral-block ② from the overlapping distribution-area with the lesser Kfc.*

		I	II	III	IV	
(a) When *Prediction-area* = 1.0000	① $fcp - cK_l = 4.71$ R-units = 1.7151 · σ_{xp} →		(.4128 − (.4560	.8256)]		= .0356 = *Constituent Integral-block* ①
	② $fcp - cK_s = 3.61$ R-units = .9246 · σ_{xp} →		[.5872 − (.3724	1.1744]		= .2086 = *Constituent Integral-block* ②
(b) When *Actual — area* = 1.0000	③ $fca - cK_s = 9.71$ R-units = 1.4600 · σ_{la} →		(.4279	1.3333) = .9705	}	= .4601 = *Constituent Integral-block* ③
	$fca - cK_m = 1.39$ R-units = .2091 · σ_{la} →		(.0828	1.3333) = .1104		

Σ 3 *Constituent Integral-blocks* → .7043 = COEFFICIENT OF PREDICTION-ACCURACY (C.P.A.)

I = *Given equivalent number of Standard Deviations.* II. *Numerical equivalent of area to left —right, as the case may be, of the given fc.*
III = *Portion of total symmetrical area subtending given number of Standard Deviations. (From Table)*
IV = *Total Area, if symmetrical, on basis of particular given σ.*

In this case the coefficient of prediction-accuracy is equal to the summation of four constituent integral-blocks as follows:

From that distribution-area with the greater K_{fc}.
Block 1 = area between $\propto$ left and cKl.
Block 2 = area between CKr and $\propto$ right.
From that distribution-area with the lesser K_{fc}.
Block 3 = area between cKl and fc.
Block 4 = area between fc and cKr.

Case II is characterized by the set-up in which there are two common probability-values (cKl and cKr). On the R-scale one such value lies either above or below and the second lies between the two fluctuation-centers (fcp and fca).

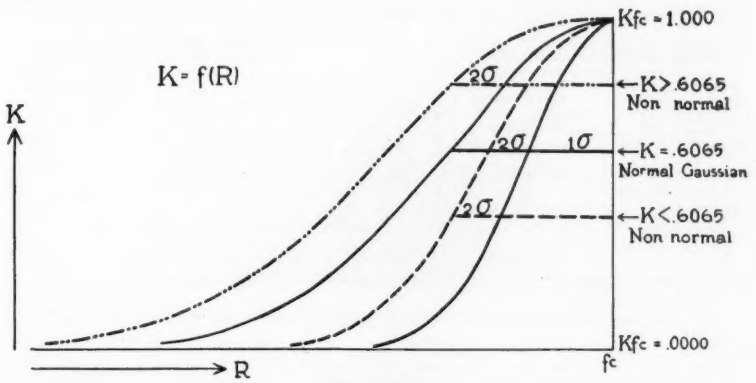

FIGURE 3

The effect, on "normality" and area, of making $R = 2\sigma$, but in causing such R to cross the K-scale at any point other than at 0.6065 K_{fc}.

In this case the coefficient of prediction-accuracy is equal to the summation of three integral-blocks as follows:

From that distribution-area with the greater K_{fc}.
Block 1 = area between cKl and $\propto$ left.
Block 2 = area between cKr and $\propto$ right.
From that distribution-area with the lesser K_{fc}.
Block 3 = area between cKl and cKr.

Case III is characterized by the set-up in which both the predicted and the actual areas possess the same-valued K_{fc}, and each area is either bi-symmetrical or skewed, but if skewed the relationship between areas "p" and "a" is a right-and-left-mirrored skewness, that is, the right-hand standard-deviation of one distribution-area is equal to the left-hand standard

CASE III.
with Example.

PROPERTIES

(a) *The total Prediction-area and the total Actual-area each = 1.0000. Each is plotted within the same coordinate frame – the same K, that is, the same Frequency or Probability-scale, and the same R-class measure of the common subject.*
1 R-class-range = 1 R-unit. 1 Area-unit = .01 K by 1 R.

(b) *Type of each area-bounding curve,* $K = Kfc\,\epsilon^{-\frac{R^2}{2\sigma^2}}$ *Each curve with constant Kfc equal to the Kfc of the other curve, and with two σ's either equal to or different from each other, but always* $(\sigma_l + \sigma_r) \div 2 = \sigma$ *symmetrical. If skewed, the two areas must be skewed in mirror-relation to each other, as in case of the given example.*

(c) *One common Probability-value, due to overlapping of curves "p" and "a". This one cK is always located midway between the two fc's i.e. between fcp and fca.*

(d) *Under the particular probability-curve, whether symmetrical or skewed,* Area to left fc : Area to right fc = $\sigma_l : \sigma_r$. *When total area = 1.0000,* Area to left fc = $\frac{\sigma_l}{\sigma_l + \sigma_r}$ Area to right fc = $\frac{\sigma_r}{\sigma_l + \sigma_r}$

(e) C.P.A. = Σ *Two constituent Integral-blocks, one for each probability-distribution-area.*
① $\int_{-\infty \text{ left}}^{cK_p \text{ and } a}$ *for area with fc to right and* ② $\int_{\infty \text{ right}}^{cK_p \text{ and } a}$ *for area with fc to left.*

GIVEN Prediction-Area = 1.0000

fcp at point 15.00 on R-scale
Kfcp = 0.0875 on K-scale
σ_{rp} = 4.5593 R-units
σ_{lp} = 4.2746 R-units
σ_{ap} = 4.8441 R-units

GIVEN Actual-Area = 1.0000

fca at point 20.00 on R-scale
Kfca = 0.0875 on K-scale
σ_{ra} = 4.5593 R-units
σ_{la} = 4.2746 R-units
σ_{aa} = 4.8441 R-units

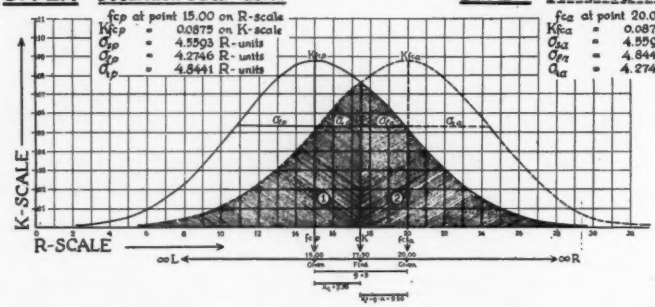

LEGEND: K = Probability; R = Measured Subject-quality; p = a property of Prediction-area; a = a property of Actual-area; fc = fluctuation center; ℓ = left of particular fc; r = right of particular fc; Kfc = probability value at particular fc; σ_l = standard deviation symmetrical – i.e. when probability-curve is in – symmetrical – i.e. not skewed. $\sigma_l + \sigma_r = 2\sigma$, when both particular ones and Kfc are constant; cK = the left-most probability value common to both p and a; cK_1 = the corresponding right-most common probability. g = (fcp – fca) in R-units.

FIND

1. fc *predicted* – fc *actual* = g = 5.00
2. R-locus of cK *when* $(fca - cK) = X_a$, *and* $(fcp - cK) = X_4$, *solve for the positive value of* X_a *by means of the simultaneous equations:*
   ① $Kfcp \cdot \epsilon^{-\frac{(X_4)^2}{2\sigma_{lp}^2}} = Kfca \cdot \epsilon^{-\frac{(X_a)^2}{2\sigma_{ra}^2}}$ *The two formulas for the Common Probability at cK, and*
   ② $X_4 = g - X_a$ *Locus cK on R-scale = locus fc predicted +* X_a. $X_a = 2.50$ R-units $X_4 = 2.50$ R-units.
   ∴ *The locus cK = 15.00 + 2.50 = 17.50*
3. *When the total area under the particular probability-curve = 1.0000*
   (a) *Prediction-area to left of* fcp = $2\sigma_{lp} \div (\sigma_l + \sigma_r)$ = .93754 ÷ 2 = .4688
   (b) *Prediction-area to right of* fcp = $2\sigma_{rp} \div (\sigma_l + \sigma_r)$ = 1.06246 ÷ 2 = .5312 } 1.0000
   (c) *Actual — area to left of* fca = $2\sigma_{la} \div (\sigma_l + \sigma_r)$ = 1.06246 ÷ 2 = .5312
   (d) *Actual — area to right of* fca = $2\sigma_{ra} \div (\sigma_l + \sigma_r)$ = .93754 ÷ 2 = .4688 } 1.0000
4. *The Value of the equal Constituent Integral-blocks ① and ② from the overlapping areas of "p" and "a",*

	* I	II	III	IV	
(a) *When Prediction-area* = 1.0000	② fcp – cK = 2.50 R-units = .9161 σ_{lp} →	[.5312 – (.1971 · 1.0625)]	= .3218 = *Constituent Integral-block* ②		
(b) *When Actual — area* = 1.0000	① fca – cK = 2.50 R-units = .9161 · σ_{la} →	[.5312 – (.1971 · 1.0625)]	= .3218 = *Constituent Integral-block* ①		

Σ 2 *Constituent Integral-blocks* ⟶ .6436 = COEFFICIENT OF PREDICTION-ACCURACY (C.P.A.)

* I. = *Given equivalent number of Standard Deviations.*
II. = *Numerical equivalent of Area to the left or right, as the case may be, of the given* fc.
III. = *Portion of total symmetrical area subtending given number of Standard Deviations (from Table).*
IV = *Total Area, if symmetrical, on basis of particular given σ*

deviation of the second, and vice versa. In this case there is only one common probability-value and this is always midway between the two fluctuation-centers (*fcp* and *fca*).

In this case the coefficient of prediction-accuracy is equal to the summation of two integral blocks—one from each of the two basic distribution-areas.

Block 1, from the distribution-area with the K_{fc} to the right, equals area between cK and $\propto$ left.

Block 2, from the distribution-area with the K_{fc} to the left, equals area between cK and $\propto$ right.

The solution of these problems is made possible by use of the following properties of the probability-distribution area, that is, of the area under the Gaussian or normal curve of error:

(1) The first basic probability-formula for the symmetrical probability-area, in which K = class probability and R = class-range in subject-value, is

$$K = f(R) = K_{fc} \cdot \epsilon^{-\frac{R^2}{2\sigma^2}}.$$

The value of the probability K may be continuous, but R, the measured quality under consideration, must always be broken into a series of classes or grades.

σ = the standard deviation, $\epsilon = 2.7182$ which is the base of the system of natural logarithms. *fc* is the fluctuation-center of R-values.

(2) The second basic formula for the symmetrical probability-distribution area represents the value of the maximum ordinate as

$$K_{fc} = \frac{N}{\sigma \cdot \sqrt{2\pi}}.$$

When distribution-data are given it is always possible to reduce the absolute number within each R-class to the percentage basis, and thus N, or the total area, is made to equal 1.000.

$\sqrt{2\pi} = 2.5066$ is a constant, and when N is constant, K_{fc} and σ are interchangeable and are inversely proportional to each other. If K_{fc} be constant N or total area varies directly with σ, or if σ be constant N varies directly with K_{fc}. (See Fig. 1.)

(3) Regardless of the skewness of the particular distribution, graphically the standard deviation crosses the K_{fc} at a K-point always equal to 0.6065 times K_{fc}. This value is deduced as follows:

Given $K = K_{fc} \cdot \epsilon^{-\frac{R^2}{2\sigma^2}}$

Let $K_{fc} = 1.000$ and let $R = \sigma$.

Then $K = 1 \cdot \epsilon^{-\frac{R^2}{2\sigma^2}} = \frac{1}{\epsilon^{\frac{1}{2}}} = \frac{1}{\sqrt{\epsilon}} = 0.6065$ which is a constant. (See Fig. 2.)

(4) Further significance of the point $0.6065K$ on the maximum ordinate. This point $0.6065K_{fc}$ is the only point on the maximum ordinate at which, if the K_{fc} remain constant, the doubling of the R-value (in this case the σ) will result in the exact doubling of the newly plotted distribution-area. Thus, if R equal two original standard deviations, and if the point of maximum slope on the boundary curve be above 0.6065, the resulting "non-normal" area will be more than doubled; if such point be below 0.6065 the resulting area will be less than doubled—compared with the original normal Gaussian area for which the standard deviation equals 1.000. (See Fig. 3.)

Again, if the R-value of the original normal area be selected at less than one standard deviation (graphically above $0.6065K_{fc}$), and such R-value be doubled but kept at the same K-point (above $0.6065K_{fc}$), the change causes a new "non-normal" slope in the new boundary-curve-of-distribution, and the new area will always be less than the original normal area in which the standard deviation equals 1.000.

Or if the new R-value be greater than one standard deviation (graphically below $0.6065K_{fc}$) and such R-value be doubled, and the new "non-normal" area be plotted in the same manner as when the new standard deviation is less than one, such new area will always be greater than the original normal area in which the standard deviation equals 1.000. (See Fig. 4.)

Thus when the R-value $= 1\sigma$, and the K value $= 0.6065$, all other factors remaining constant, such R-value is the only R-value, the doubling or other increase of which will cause a proportional increase in the normal distribution-area.

Next to the rectangle, the "normal-probability-distribution-area" is probably the simplest flat geometric figure the area of which varies directly with the change (that is, with the first power) of either one of its two coördinate factors, while the second remains constant. But there is this difference: Plot any rectangle and any normal-probability-distribution-area each within an x-y frame of coördinates, the area of the rectangle varies directly with the value of x selected at *any* y-point, or with the value of y selected at *any* x-point; while the area of the normal-probability-distribution-figure varies directly with x *only* when x equals the standard deviation (which always crosses the y-coördinate at the point equal to 0.6065 of the maximum ordinate), and directly with y *only* when y is the maximum ordinate, which always crosses the x-coördinate at the fluctuation-center of x-values.

(5) Relative areas. If the total normal distribution-area be 1.000, and the K_{fc} be constant at $1K$, then that portion of the area to the right of the particular K_{fc} is to that portion of the area to the left of said K_{fc} as

the particular standard deviation right is to the particular standard deviation left.

Area right : area left = $\sigma_{rt} : \sigma_{lft}$.

(6) Skewness. Using the second basic formula above given, we find that, if the K_{fc} be constant the area varies directly with the standard deviation in a symmetrical or non-skewed area. Now, if the area be skewed, a hypothetical area must be postulated temporarily. Let, for example, the "standard deviation symmetrical" (σ_s) equal 0.50, then shift the "standard deviation left" (σ_l) to the value of 0.55. Now if the K_{fc} be constant at $1K$, and the area be made symmetrical with the new $\sigma = 0.55$, the new total postulated-area equals X in the ratio $1:0.50 = X:0.55$, in which case $X = 1.10$, i.e., the σ_{left} would belong to a total area equal to 1.10 with its σ symmetrical at 0.55 and its K_{fc} constant at $1K$—the original value.

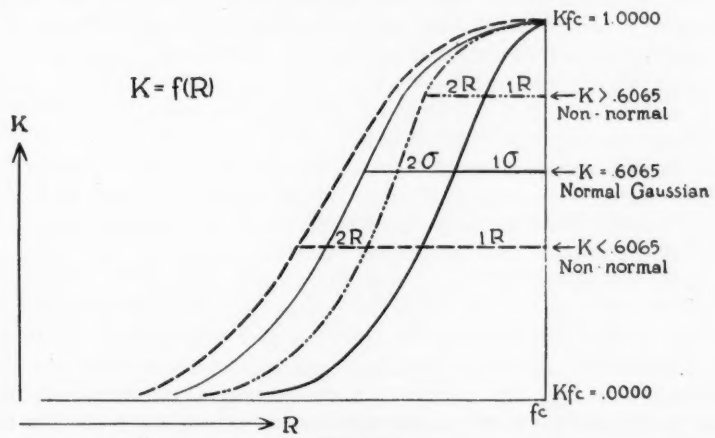

FIGURE 4

The effect, on "normality" and area, of doubling the normal R-value at any point on the K-scale other than at 0.6065 K_{fc}.

But actually the total area must remain constant at 1.000, and K_{fc} must remain constant at $1K$. Then since the actual-skewed-area to the left has already consumed 0.55 of the total-actual-area, this leaves 0.45 for the area to the right of K_{fc}. Similarly computed the σ_{right} would belong to a newly postulated symmetrical distribution represented by a total area equal not to 1.000 but to 0.90, and with K_{fc} constant at the same $1K$ value.

Therefore $2\sigma_{symmetrical} = \sigma_{left} + \sigma_{right}$.

(7) Down the long S-curve (one of which bounds the top side of the probability-distribution to the left and another to the right of the particular

K_{fc}), beginning at the top, where the slope equals zero, and descending the slope increases continuously until the descent-point, located at the height of K at 1σ removed from the particular fluctuation-center, is reached, i.e., until the descent-value $0.6065K_{fc}$ is reached. This descent-point locates also the maximum slope of the long S-bounding-curve. (The greatness of this maximum slope is a function of its adjacent standard deviation σ.) Therebelow the rapidity of descent decreases continuously, and for the latter reason never reaches the level whereat $K = 0$, but theoretically extends indefinitely, continuously approaching but never attaining parallelism with the particular R-scale at $K = 0$.

(8) The total area under each curve (the prediction-area "p" and the actual-area "a") independently is equal to 1.000. The total area, including the overlap covered by both curves, equals ($2 - CPA$ or overlap).

The prediction-basis with the specifications listed in the earlier paragraphs is the one actually used. The selection of the particular prediction-basis must, of course, be justified by the logic of the particular case under analysis, but how the particular prediction-basis was derived or why used are matters which do not concern the basic theory of the coefficient of prediction-accuracy nor the technique of its use. The prediction-basis may thus be a guess or an intuition; it may be based upon a single probability-distribution composed of a few individual cases carelessly measured, or it may be based upon the probability-resultant of many constituent probability-factors, each based upon many individual cases, and each accurately and confidently measured. An example of the latter type of prediction-basis is one produced by the probability-resultant* made by the proper synthesis of one cross-section from each of a number of selected manerkons each of which individually pictures mathematically the relationship $K = f(M, R)$, in which M is the particular prediction-basis, R is the thing-predicted and K is the probability. The point is that, in this particular study, the prediction-basis is being tested for its accuracy, not for its source.

But in interpreting the meaning of a computed value for the coefficient of prediction-accuracy, the situation is such that one can criticize usefully the soundness of construction of the particular prediction-basis. It is evident that if for many quantitative distribution-data on the same trait or quality, within the same population, the prediction-accuracy in many tests runs consistently high, there must be something besides luck or chance which favors the particular prediction-set-up. If the high running coefficient of prediction-accuracy be based upon many independent factors, and each, in turn, is composed of many carefully measured individual cases, then confidence is justified that the essential major factors are in hand and are properly weighted and coördinated in the given prediction-basis.

But if the coefficient of prediction-accuracy run consistently low then,

regardless of how carefully the particular prediction-basis is computed, it indicates that some major factor or factors are omitted, or are improperly weighted or coördinated, in the particular prediction-basis being tested for accuracy.

In comparing two different prediction-bases against the same subsequently determined set of actual distribution-values, the coefficient of prediction-accuracy tests the relative merit of these two prediction-bases as to their relative correctness in the inclusion of their own postulated constituent factors, and in the relative weights and coördinations given such factors.

In any case in which one has in hand a prediction-basis in terms of a probability-distribution, and has also in hand the actual subsequent or other independently secured measuring and counting of the same quality in the same population, the coefficient of prediction-accuracy (*CPA*) presents a sound formula for judging the given probability-distribution-production-basis as to its degree of success—no excuses taken.

The next step in good research is, of course, to find out why the particular prediction-basis which was actually used was not more successful.

* H. H. Laughlin, "The Probability-resultant," *Proc. Nat. Acad. Sci.*, **21**, 11, 601–610 (1935).

STRENGTH-DURATION CURVES AND THE THEORY OF ELECTRICAL EXCITATION

By W. J. Crozier

Biological Laboratories, Harvard University

Communicated December 22, 1936

I. An instructive parallel exists between measurements of electrical excitability, particularly for repetitive condenser discharges or constant current pulses, and the data of visual flicker. The comparison derives from probability considerations, and provides a means of analysis independent of any specific assumptions as to the physico-chemical character of the excitation process.

Numerous observations describe the general relationship between magnitude of stimulating potential or current and the time for threshold excitation, particularly in nerve. It is well known that for a chosen degree of excitation the required current (or voltage) declines to an asymptotic level as the exposure time is increased.[1] No fully satisfactory theory of the form of the strength-duration curve has been provided. From a rational conception of the effects connected with electrical excitation Hill[2] derived equations describing rather closely the relation between current or potential (C) and its duration (t) for constant response. It is not clear that this

equation is an unequivocal fit for all series of observations. Its test involves visual adjustment of a curve on a log-log grid, since the equation cannot be conveniently rectified. There is some indication that the deviations apparent in various sets of measurements, though slight, may be systematic.

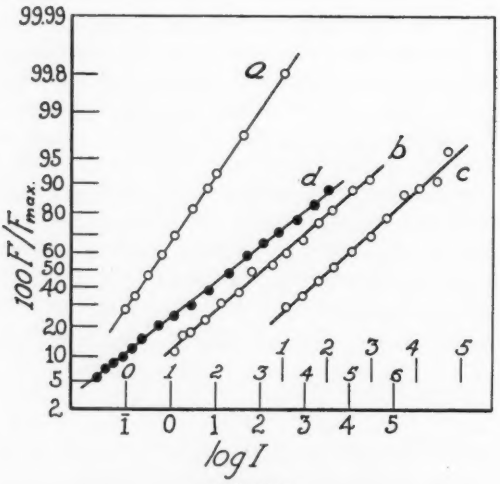

FIGURE 1

The relation of critical illumination for extinction of visual flicker (f) or for threshold response to flicker (F) is adequately described by a logarithmic probability integral. Only illustrative measurements involving cone excitation are here considered; for rod excitation a similar graph obtains.[2,3] Ordinate, $100\ F/F_{max.}$; abscissa for A, log I (millilamberts), for B, log P (photons). Beyond $I_{max.}$, F tends to fall, but the reasons for this[6] do not interfere with the present discussion.

A. Data on the fish Xiphophorus;[4] $F_{max.} = 43.1/sec.$; 21.5°C.; averages of 30 measurements.

B. Three sets of measurements on the human eye (S. H.) from Hecht, Shlaer and Smith:[3]

a—0.3° spot, white, on fovea ($f_{max.} = 54.4$)

b—19° spot, 490 mμ ($f_{max.} = 64.7$).

c—19° spot, 670mμ ($f_{max.} = 67.5$).

Regardless of the descriptive adequacy of Hill's equations, however, the data may be viewed from another standpoint. The general form of the relation between *log C* and *log t* is like that obtained in studies of visual excitation.[3] Here intensity (I) is the variable corresponding to t, and some measure of effect E corresponds to C. For threshold recognition of visual

flicker the critical flash frequency F is a proportionate measure of the intensity of the relevant total photosensory effect obtained.[4] Time is then involved only in the sense that the differential effect producing the response must be achieved (at any fixed flicker-frequency) within the interval set by the flicker cycle. In a voltage duration experiment a fixed level of effect is selected (threshold response, or half-maximum of action current, for example), and the stimulating current C (of fixed frequency) requires a certain measured time t to produce this effect. The two kinds of measurements are therefore alike in that of the three factors involved—time of action, intensity and level of total effect—one is in each case essentially fixed by the procedure.

The stimulation effect achieved is in each case due to the cumulative action of a number of excited elements—in a nerve or muscle either a number of different fibres or a number of "excitable spots" on each fibre or both; and in the reaction visually excited, a number of retinally connected units must be excited. These dynamical units or *elements* are not to be identified with the crudely obvious structural units, nor are they to be conceived as morphologically fixed. The excitability of each element is not stationary but fluctuates as a function of intensity and of time. When E is arbitrarily chosen, the time required for its production will depend upon the time-summation of contributions from a number of elements forming part of a frequency distribution of *time* $\times$ *intensity* thresholds. In such situations one expects the law for E as a function of I (or t) to be dependent upon a logarithmic probability distribution of excitability thresholds, the latter given by $(t)(dE/dt)$. This is quite without reference to the intimate physical basis of the exciting process in any given element.[5]

The curve for critical illumination as a function of flicker-frequency[6] is admirably described as a log-probability integral (Fig. 1). Equations of the photostationary state type,[7] with certain limitations, do so equally well because they are identical with the logarithmic logistic, which except at the extreme ends of the curve gives a fit scarcely distinguishable[8] from that of the log-probability integral; however, the proportionality constant in the "photostationary state" equation has properties which forbid assigning this particular significance to the equation.[9] The log-logistic equation also describes the measurements of cochlear effect as a function of intensity of sound (pressure).[10]

II. Strength-duration curves for repetitive electrical excitation are very efficiently described by a log-probability integral. Several examples are given in figure 2. Series of measurements have been selected from the most recent work which seem to be intrinsically the best determined and which cover the largest range of values of C and t. Numerous less extensive sets of data[11,12] are equally well described by this equation. The test is easily made on a log-probability grid (Fig. 2). This requires that the

acting current (or voltage) be computed as a percentage of the asymptotic minimum C_0. That is, 100 C_0/C represents the percentage of available

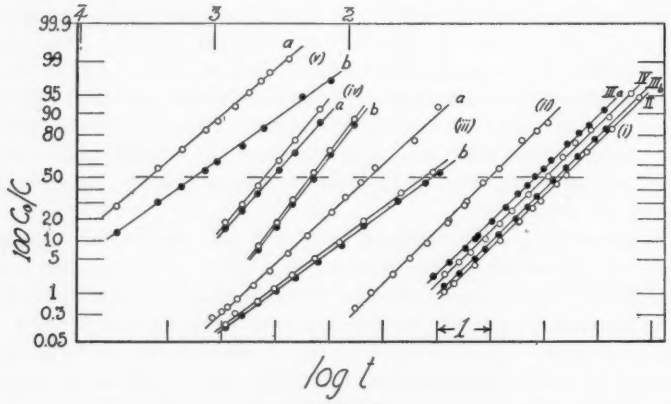

FIGURE 2

Log probability grid: ordinate, 100 C_0/C; abscissa, log RC, the condenser time constant. Repetitive condenser discharges.

(i) Data from: 4 experiments in Hill, 1936*b*;[2] sciatic of frog; II, 5 shocks/*sec.*, 4°C. (C_0 = 0.248). Log t' = $\bar{3}$.35. III*a*, 31.4 shocks/*sec.*, 22.5°C. (C_0 = 0.708). Log t' = $\bar{4}$.84. III*b*, 17.2 shocks/*sec.*, 6.2°C. (C_0 = 0.347). Log t' = $\bar{3}$.245. IV, 31 shocks/*sec.*, 20°C. (C_0 = 0.233). Log t' = $\bar{3}$.04. The slope is the same for each line.

(ii) Data in: Scott, D., 1934, *Jour. Physiol.*, lxxxii, 321; frog sciatic, condenser discharges 9.6/*sec.* (C_0 = 0.52). Log t' = 2.79. [Data read from curve.]

(iii) Data from: Rosenberg, H., 1935, *Jour. Physiol.*, lxxxiv, 50. *a*—cat, sciatic, 21.2° (C_0 = 0.2296). Log t' = 2.74. *b*—crab (*Maia*), leg nerve, 3 *mm.* electrode separation, (C_0 = 0.378) and 15.5 *mm.* (C_0 = 0.320). Log t' = 5.25, 5.40.

(iv) Data from: Bugnard, L., and Hill, A. V., 1935, *Jour. Physiol.*, lxxxiii, 425, fin nerve of *Sepia*.
a—I, 1′ electrode separation 1.7 *mm.* (C_0 = 5.76). Log t' = $\bar{3}$.285.
I, 1″ electrode separation 16 ± 3 *mm.* (C_0 = 5.22). Log t' = $\bar{3}$.44.
b—I, 2′ electrode separation 1.7 *mm.* (C_0 = 3.17). Log t' = $\bar{2}$.86.
I, 2″ electrode separation 13–19 *mm.* (C_0 = 2.7). Log t' = $\bar{2}$.93.

(v) Data from: Jinnaka, S., and Azuma, R., 1922, *Proc. Roy. Soc.* (*London*) *B*, xc, 49; frog sartorius muscle; scale of log t at the top.
a—Single fibre, pore electrode (C_0 = 1.063). Log t' = $\bar{4}$.519.
b—Pelvic end of sartorius, with 0.05 *per cent* curare (C_0 = 0.730). Log t' = $\bar{4}$.82.

"elements," in terms of the intensity × time relationship, stimulated by C at the moment when threshold response occurs. Put in another way, for *very* short times $1/C$ measures directly the excitability of any element of ex-

citation, and should give a normal frequency distribution of excitabilities. At the lower limit of $1/C$ this gives the "constant quantity" rule. C_0 is, of course, not to be confused with the observed rheobase, but is a little below it and must usually be found by trial. The graph is quite sensitive.

This treatment discloses that the voltage duration data in experiments of one type with one kind of nerve often may be compared in terms of a single parameter, namely, the value of log t for which $C_0/C = 50$ *per cent* (cf. Fig. 2). For example, in four series of measurements from Hill's recent paper[13] the values of $RC \equiv t$ have been multiplied by a constant for each series; the four sets are seen (Fig. 3) to be identical as regards the shape of the curve. The value of t for $C_0/C = 50$ *per cent* is a function of temperature, of interelectrode distance, of fibre diameter and of the individual preparation. With fall of temperature $C_0/C = 0.50$ moves to a higher value of t, as is expected on the basis of a frequency distribution of excitabilities. The effect of electrode separation,[2] although probably more complex, is also of this general character; C_0 falls, t for $C = 2C_0$ rises and $\sigma_{\log t}$ is increased, as it should be if a larger population of excitable elements is made available. The parallels with the properties of flicker data are precise. For different types of nerve and muscle and for other differing experimental conditions, the standard deviation of the underlying frequency distribution of excitabilities is not the same, so that an additional parameter ($\sigma_{\log t}$) is needed. Its properties should repay systematic investigation. Graphs with different slopes might be compared by finding that adjustment of the log t scale units which will give them the same slope, after rotation about the 50 *per cent* point, by employing log t^n instead of log t and having n proportional to the slope on the probability grid.

III. The value of t for 100 $C_0/C = 50$, the inflection point of the curve, has a special significance. It gives the time for excitation by a current $= 2C_0$, under given conditions, and consequently corresponds in meaning to the chronaxie of Lapicque[14]—although computed on the basis of the asymptotic level of C_0 and not from the observed apparent rheobase. The curves show that this "true" chronaxie, which may be called τ', is a valid parameter of the excitability function. It is independent of C_0. It is not dependent upon the position of the curve at one point, but (cf. Fig. 2) is weighted by all the observations. The physical meaning of τ' is the time required for excitation by that current which under the conditions imposed stimulates up to the median (mode) of the frequency distribution of excitability thresholds. This relationship between τ' and the classical chronaxie or excitation time is curious because it was largely a matter of accident that twice the rheobase voltage should have been chosen originally for the measurement of the excitability time factor.[15]

It is obvious that τ' alone is not adequate for the efficient description of

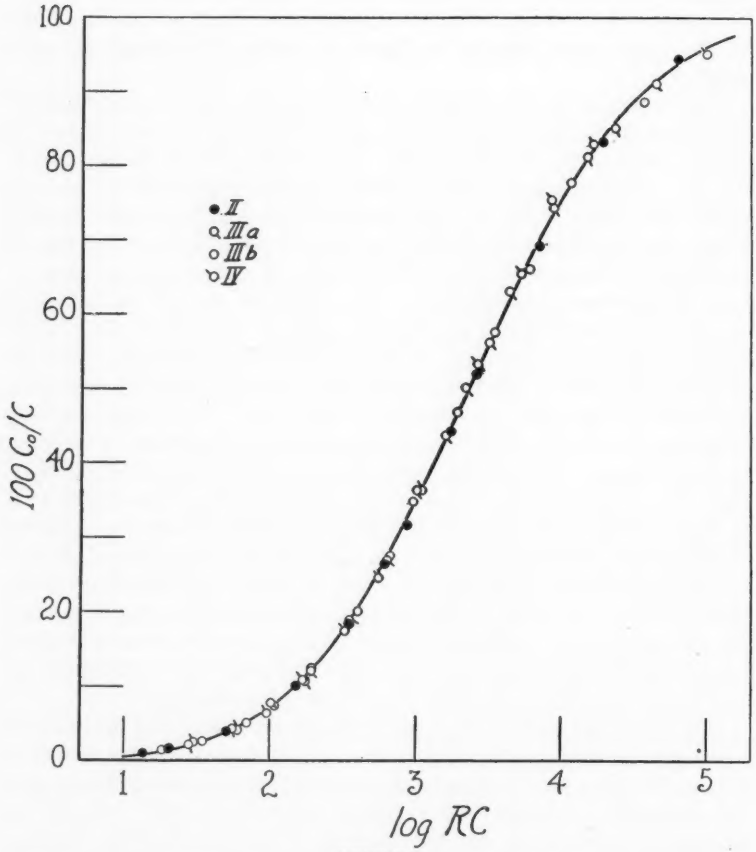

FIGURE 3

The four curves of (i) in Fig. 2 are shown brought together at $C_0/C = 50$ *per cent*, RC being multiplied by the factors 1, 3.273, 1.35 and 2.19, respectively, for II, III*a*, III*b* and IV. The curve is that for the probability integral

$$100C_0/C = K\int_{-\infty}^{x} e^{-\frac{(x-x_0)^2}{2\sigma^2}}de,$$

where $C = 1/V$; $x = \log t$; $x_0 =$ the value of x at the inflection point; and $\sigma = \sigma_{\log t}$.

the strength-duration curve.[16] The slope factor (i.e., $\sigma_{\log t}$) is also required if different kinds of preparations are to be compared.

With these two parameters it is not difficult to compare different forms of *excitability*, for example, photic excitability (Fig. 1) and electrical (Figs. 2, 4) in diverse irritable structures. In a similar way the data of visual excitation may be investigated as a function of wave-length with the expectation of evidence as to the existence of different kinds of receptor excitability distributions. The formulation proposed is in terms of the frequency distribution of excitabilities among a population of excitable elements and is independent of assumptions as to the nature and the interrelationships of the physico-chemical changes which produce excitation in any one kind of sensory element. The result is thus consistent with that arising in the analysis of the sensory discrimination of intensities.[17]

IV. *Summary.*—Measurements of the interrelations of current strength and time for a fixed magnitude of effect due to repetitive electrical excitation in nerve and muscle are found to be described with excellent fidelity by a logarithmic probability integral. The same kind of relationship, in which magnitude of sensory effect is expressed as a function of intensity, appears in phenomena of stimulation by light and by sound. The value of time for which $100\ C_0/C = 50$ *per cent*, where C_0 is the asymptotic lower exciting current, is essentially the chronaxie. This parameter is not by itself sufficient for the description of the strength-duration curve; the standard deviation of the underlying frequency distribution is an independent parameter, being different in various kinds of nerves and according to conditions of excitation. The log-probability integral gives a readily applied means of comparing different forms and manifestations of excitability. It is pointed out that, when an exciting energy is applied to a tissue, it is to be expected that the thresholds for excitation of the elements open to stimulation, in terms of the resultant chosen, will form a logarithmic frequency distribution provided the excitability of each element intrinsically fluctuates.

[1] Rushton, W. A. H., *Biol. Rev.*, **10**, 1 (1935); Lapicque, L., *Ibid.*, **10**, 483 (1935).

[2] Hill, A. V., *Proc. Roy. Soc.* (London) (*B*), **119**, 305, 440 (1936 *a*, *b*).

[3] Hecht, S., and Shlaer, S., *Jour. Gen. Physiol.*, **19**, 965 (1935–36); Hecht, S., and Smith, E. L., *Ibid.*, 979 (1935–36); Crozier, W. J., Wolf, E., and Zerrahn-Wolf, G., *Jour. Gen. Physiol.*, **20** (*in press*) (1936–37 *c*).

[4] Crozier, W. J., Wolf, E., and Zerrahn-Wolf, G., *Jour. Gen. Physiol.*, **21** (*in press*) (1937–38).

[5] Similar reasoning may be applied to measurements of photosynthesis. The form of the frequency distribution of contributions to the total amount of photosynthesis by the individual cellular or other elements is presumably a function of the luminous intensity and of the partial pressure of CO_2. The cumulative result in a fixed period of time will then follow a different law from that expected for an "average" cell. The data, as far as they go, are quite well described by a log probability integral.

In the iron wire model used by Lillie (*Jour. Gen. Physiol.*, **19**, 109 (1935–36)) the "ex-

citation" of a number of "irritable spots" on the wire, resulting in the activation of a propagated wave, will scarcely be influenced by fluctuations in catalytic activity at each spot. With constant current, the voltage duration data for activation are well described by a simple probability integral.

[6] Crozier, W. J., Wolf, E., and Zerrahn-Wolf, G., *Jour. Gen. Physiol.*, **20** (*in press*) (1936–37 *b*, *d*).

[7] Hecht, S., Shlaer, S., and Smith, E. L., *Cold Spring Harbor Symposia Quant. Biol.* **3**, 237 (1935).

[8] Cf. Wilson, E. B., *Proc. Nat. Acad. Sci.*, **11** (1925); Winsor, C. P., *Jour. Wash. Acad. Sci.*, **22**, 73 (1932).

[9] Crozier, W. J., Wolf, E., and Zerrahn-Wolf, G., *Jour. Gen. Physiol.*, **20** (*in press*) (1936–37 *a*, *b*).

[10] Cf. Crozier, W. J., and Holway, A. H. (*in preparation*) (1937).

[11] Cf. [1, 2] and Davis, H., and Forbes, A., *Physiol. Rev.*, **16**, 407 (1936) for citations.

[12] In many instances (e.g., nerve-muscle preparations and others) two intersecting strength-duration curves are obtained due to the presence of two groups of excitabilities. In some cases the separation may not be clear cut. The analogy with the rod and cone situation in the excitation of the vertebrate retina is obvious.

[13] Hill, A. V., *Proc. Roy. Soc.* (*London*) *B*, **119**, 440 (1936 *b*).

[14] Lapicque, L., *L'Excitabilité en Fonction du Temps*, Paris, Presses Universit., 371 pp. (1926).

[15] Lucas, K., *Jour. Physiol.*, **35**, 326 (1906); Lapicque, L., *C. R. Soc. Biol.*, Paris, **67**, 280 (1909).

[16] Cf. Davis, H., and Forbes, A., *Physiol. Rev.*, **16**, 407 (1936).

[17] Crozier, W. J., *Jour. Gen. Physiol*, **19**, 503 (1935–36); *Proc. Nat. Acad. Sci.*, **22**, 412 (1936); Upton, M., and Crozier, W. J., *Ibid.*, 417 (1936); Crozier, W. J., and Holway, A. H., *Ibid.* (*in press*) (1937).

A CONVERGENT SERIES FOR THE PARTITION FUNCTION $p(n)$

By Hans Rademacher

Department of Mathematics, University of Pennsylvania

Communicated January 9, 1937

I. For a discussion of the number $p(n)$ of unrestricted partitions of n there has been used since Euler[1] the generating function

$$f(x) = 1 + \sum_{n=1}^{\infty} p(n)x^n = \frac{1}{(1-x)(1-x^2)(1-x^3)\ldots}. \quad (1)$$

A purely formal treatment of (1) leads to classical formulae of recurrence. In 1917 Hardy and Ramanujan[2] applied on (1) the theory of functions of complex variables and developed a method (Cauchy integral, "Farey-dissection," approximation functions) which yields an asymptotic formula for $p(n)$. Their result is the following:

$$p(n) = \frac{1}{2\pi\sqrt{2}} \sum_{k \leqq \alpha\sqrt{n}} A_k(n) \sqrt{k} \frac{d}{dn} \left(\frac{e^{\frac{C\sqrt{n - 1/24}}{k}}}{\sqrt{n - 1/24}} \right) + O(n^{-1/4}) \quad (2)$$

with α as an arbitrary constant, and

$$A_k(n) = \sum_{\substack{h \bmod k \\ (h,k)=1}} \omega_{h,k} e^{-\frac{2\pi i h n}{k}}, \quad C = \pi\sqrt{2/3}. \quad (3)$$

The symbol $\omega_{h,k}$ designates certain $24k$th roots of unity which have their origin in the theory of the transformation of modular functions.[3] The formula (2) is noteworthy for the fact that its error term tends to zero with increasing n. Tests for $n = 100$ and $n = 200$ showed indeed that $p(n)$ can be obtained as the nearest integer to the sum expression in (2) for a small number of summands.

The following revision and modification of the Hardy-Ramanujan method permits us to replace the asymptotic formula (2) by the equality

$$p(n) = \frac{1}{\pi\sqrt{2}} \sum_{k=1}^{\infty} A_k(n) \sqrt{k} \frac{d}{dn} \left(\frac{\sinh \frac{C\sqrt{n - 1/24}}{k}}{\sqrt{n - 1/24}} \right), \quad (4)$$

in which the series is absolutely convergent. The asymptotic formula (2) is then an immediate consequence of (4).

By Cauchy's theorem we deduce from (1)

$$p(n) = \frac{1}{2\pi i} \int_C \frac{f(x)}{x^{n+1}} dx, \quad (5)$$

where C is a certain circle enclosing the origin and interior to the unit circle. The approach to a treatment of (5) is given by the formula

$$f\left(e^{\frac{2\pi i h}{k} - \frac{2\pi z}{k}}\right) = \omega_{h,k} \sqrt{z} \exp\left(\frac{\pi}{12kz} - \frac{\pi z}{12k}\right) f\left(e^{\frac{2\pi i h'}{k} - \frac{2\pi}{kz}}\right) \quad (6)$$

with $\Re(z) > 0$, $\sqrt{z}$ denoting the principal branch of the square root and h' determined as a solution of the congruence $hh' \equiv -1 (\bmod k)$. The formula (6) itself is a consequence of a transformation formula for $\eta(\tau)$, a modular function introduced by Dedekind,[4] which is essentially the 24th root of the "discriminant."

In (5) we choose C as the circle of radius $e^{-2\pi N^{-1}}$ and divide it by the Farey-dissection of order N. The Farey arc $\xi_{h,k}$ may be described by

$$x = e^{\frac{2\pi i h}{k} - 2\pi N^{-1} + 2\pi i \varphi}, \quad -\vartheta'_{h,k} \leqq \varphi \leqq \vartheta''_{h,k}.$$

Introducing (6) into the integrand we get

$$p(n) = \frac{1}{2\pi i} \sum_{\substack{(h,k)=1 \\ 0 \leqq h < k \leqq N}} \int_{\xi_{h,k}} \frac{f(x)}{x^{n+1}} dx$$

$$= e^{2\pi n N^{-2}} \sum_{\substack{(h,k)=1 \\ 0 \leqq h < k \leqq N}} \omega_{h,k}\, e^{\frac{-2\pi i h n}{k}} \int_{-\vartheta'_{h,k}}^{\vartheta''_{h,k}} \Psi(k(N^{-2} - i\varphi)) f(e^{\frac{2\pi i h'}{k} - \frac{1}{k^2(N^{-2}+i\varphi)}}) e^{-2\pi i \varphi n}\, d\varphi,$$

where we have used the abbreviation

$$\Psi(z) = \sqrt{z} \exp\left(\frac{\pi}{12kz} - \frac{\pi z}{12k}\right). \tag{7}$$

Instead of introducing a special auxiliary function in order to approximate the integral, as Hardy and Ramanujan do, we use $\Psi(z)$ itself, since $f(x')$ approaches 1 very rapidly when x' tends to zero. If we carry out the proper estimates we obtain

$$p(n) = e^{2\pi n N^{-2}} \sum_{\substack{h,k=1 \\ 0 \leqq h < k \leqq N}} \omega_{h,k}\, e^{-\frac{2\pi i h n}{k}} \int_{-\vartheta'_{h,k}}^{\vartheta''_{h,k}} \Psi(k(N^{-2} - i\varphi))\, e^{-2\pi i n \varphi}\, d\varphi + \Theta_1,$$

$$|\Theta_1| < B_1\, e^{2\pi n N^{-2}}\, N^{-1/2}. \tag{8}$$

It may be noticed that in our reasonings the order N of the Farey-dissection is independent of the represented number n.

In (8) we substitute $w = N^{-2} - i\varphi$ and consider the integral in the complex w-plane. In order to get a unique determination of $\Psi(kw)$ we cut the w-plane along the negative real axis. The integral in (8) is then replaced by a loop-integral extended over a path surrounding the cut and connecting the following points by straight segments:

$$-\infty,\ -\epsilon,\ -\epsilon - i\vartheta''_{h,k},\ N^{-2} - i\vartheta''_{h,k},\ N^{-2} + i\vartheta'_{h,k},\ -\epsilon + i\vartheta'_{h,k},\ -\epsilon,\ -\infty.$$

The estimate of the errors is based on the fact that the essential singularity of $\Psi(kw)$ in $w = 0$ arising from a factor $e^{\frac{a}{w}}$ with positive a has bounded values for $\Re(w) \leqq 0$ and that more precisely for $w = u + iv$ we have

$$\left| e^{\frac{1}{w}} \right| = e^{\frac{u}{u^2+v^2}} \leqq e^b$$

for $u \leqq b(u^2 + v^2)$, which, for $b > 0$, is fulfilled *a fortiori* if $u \leqq bv^2$. This, by the way, is the reason for choosing the radius $e^{-2\pi N^{-2}}$ together with the order N of the Farey-dissection.

The calculation leads to

$$p(n) = \sum_{k=1}^{N} A_k(n)\varphi_k(n) + \Theta_2, \tag{9}$$

$$|\Theta_2| < B_2\, e^{2\pi\pi N^{-1}} N^{-1/2},$$

where $A_k(n)$ is the quantity defined in (3) and

$$\varphi_k(n) = \frac{\sqrt{k}}{i}\int_{-\infty}^{(0+)} \sqrt{w}\, e^{\frac{\pi}{12k^2 w}} e^{2\pi(n-1/24)w}\, dw$$

$$+ 2\sqrt{k}\int_{0}^{\infty} \sqrt{u}\, e^{-\frac{\pi}{12k^2 u}} e^{-2\pi(n-1/24)u}\, du. \tag{10}$$

The remainder term in (9) tends to zero for $N \longrightarrow \infty$ and fixed n. Hence we have

$$p(n) = \sum_{k=1}^{\infty} A_k(n)\varphi_k(n). \tag{11}$$

The integrals in (10) are well known, and we get in this way the proof of (4).

From (4) it is possible to derive a definite expression for the O-term in (2). We obtain

$$p(n) = \frac{1}{2\pi\sqrt{2}} \sum_{k=1}^{N} A_k(n)\sqrt{k}\frac{d}{dn}\left(\frac{e^{\frac{C\sqrt{n-1/24}}{k}}}{\sqrt{n-1/24}}\right) \tag{12}$$

$$+ \Theta\cdot\left\{\frac{44\pi^2}{225\sqrt{3}} N^{-1/2} + \frac{\pi\sqrt{2}}{75}\left(\frac{N}{n-1}\right)^{1/2} \sinh\frac{C\sqrt{n}}{N}\right.$$

$$\left. + \frac{1}{2\sqrt{3}}\frac{(N+1)^{3/2}}{n-1}\, e^{-\frac{C\sqrt{n-1}}{N}}\left(\frac{1}{3} + \frac{\sqrt{3}}{5\pi\sqrt{2}}\frac{N+1}{(n-1)^{1/2}}\right)\right\}, \quad |\Theta| < 1,$$

a formula which proves to be useful for numerical computation of $p(n)$.

A detailed account of the outlined proofs will soon be published in the "Proceedings of the London Mathematical Society."

II. The result (4) can in turn be used for a treatment of $f(x)$, which because of its close relation to modular functions deserves some attention for itself. We get from (1), (4) and (3)

$$f(x) = 1 + \frac{1}{\pi\sqrt{2}} \sum_{\substack{(h,k)=1 \\ h \bmod k}} \omega_{h,k}\sqrt{k}\,\Phi_k\left(xe^{-\frac{2\pi i h}{k}}\right), \quad |x| < 1, \tag{13}$$

with

$$\Phi_k(z) = \sum_{n=1}^{\infty} \frac{d}{dn}\left(\frac{\sinh \frac{C\sqrt{n-1/24}}{k}}{\sqrt{n-1/24}}\right) \cdot z^n. \qquad (14)$$

But here

$$g_k(n) = \frac{d}{dn}\left(\frac{\sinh \frac{C\sqrt{n-1/24}}{k}}{\sqrt{n-1/24}}\right) = \sum_{\nu=1}^{\infty} \frac{\left(\frac{C}{k}\right)^{2\nu+1}}{(2\nu+1)!} \nu (n-1/24)^{\nu-1} \qquad (15)$$

is an entire transcendental function in n of order $1/2$. Hence by a theorem of Wigert[5] the function

$$\Phi_k(z) = \sum_{n=1}^{\infty} g_k(n) z^n,$$

originally defined only in the interior of the unit circle, can be continued over the whole z-plane, is regular at $z = \infty$ and has only one isolated essential singularity at $z = 1$.

The expansion (13) can therefore be taken as a generalized Mittag-Leffler decomposition into "partial fractions," each term giving rise to an essential singularity at a root of unity $x = e^{\frac{2\pi i h}{k}}$. The particularity of (13) lies in the fact that all singularities together build up the natural boundary $|x| = 1$ for the function $f(x)$.

The $\Phi_k(z)$ have, by Wigert's theorem, also a meaning outside the unit circle, and a simple consideration shows that the right-hand side of (13) is again convergent for $|x| > 1$. This defines there an analytic function:

$$f^*(x) = 1 + \frac{1}{\pi\sqrt{2}} \sum_{\substack{(h,k)=1 \\ h \bmod k}} \omega_{h,k} \sqrt{k} \Phi_k\left(x e^{-\frac{2\pi i h}{k}}\right), \quad |x| > 1. \qquad (13a)$$

The functions $f(x)$ and $f^*(x)$ are determined by the same expansion (13), (13a), in spite of the fact that they are separated by the unit circle as natural boundary of $f(x)$.

We can establish a power series for $f^*(x)$ around $x = \infty$. From (14) and (15) we get

$$\Phi_k(z) = \sum_{\nu=1}^{\infty} \frac{\left(\frac{C}{k}\right)^{2\nu+1}}{(2\nu+1)!} \nu \sum_{n=1}^{\infty} (n-1/24)^{\nu-1} z^n = \sum_{\nu=1}^{\infty} \frac{\left(\frac{C}{k}\right)^{2\nu+1}}{(2\nu+1)!} \nu \varphi_\nu(z),$$

say. We have

$$\varphi_1(z) = \sum_{n=1}^{\infty} z^n = \frac{z}{1-z} = -\frac{1}{1-z^{-1}} = -\sum_{m=0}^{\infty} z^{-m}$$

and

$$\varphi_{\nu+1}(z) = \left(z\frac{d}{dz} - {}^1/_{24}\right)\varphi_\nu(z).$$

Consequently around $z = \infty$ the expansions

$$\varphi_\nu(z) = (-1)^\nu \sum_{m=0}^{\infty} (m + {}^1/_{24})^{\nu-1}\, z^{-m}, \quad |z| > 1$$

are valid, and we have

$$\Phi_k(z) = \sum_{\nu=1}^{\infty} \frac{\left(\frac{C}{k}\right)^{2\nu+1} \nu(-1)^\nu}{(2\nu+1)!} \sum_{m=0}^{\infty} (m + {}^1/_{24})^{\nu-1}\, z^{-m}$$

$$= \sum_{m=0}^{\infty} \frac{d}{dm}\left(\frac{\sin\frac{C\sqrt{m+{}^1/_{24}}}{k}}{\sqrt{m+{}^1/_{24}}}\right) \cdot z^{-m}$$

with the trigonometric sine instead of the hyperbolic sine. With this determination (13a) takes the form

$$f^*(x) = 1 + \frac{1}{\pi\sqrt{2}} \sum_{\substack{h,\,k=1 \\ h \bmod k}} \omega_{h,k}\sqrt{k} \sum_{m=0}^{\infty} \frac{d}{dm}\left(\frac{\sin\frac{C\sqrt{m+{}^1/_{24}}}{k}}{\sqrt{m+{}^1/_{24}}}\right)\cdot\left(xe^{-\frac{2\pi ih}{k}}\right)^{-m}$$

$$= 1 + \sum_{m=0}^{\infty} p^*(m)x^{-m}, \tag{16}$$

where

$$p^*(m) = \frac{1}{\pi\sqrt{2}} \sum_{k=1}^{\infty} A_k(-m)\,\sqrt{k}\,\frac{d}{dm}\left(\frac{\sin\frac{C\sqrt{m+1/24}}{k}}{\sqrt{m+1/24}}\right). \tag{17}$$

A formal comparison of (4) and (17) can be condensed in the equation

$$p^*(m) = -p(-m).$$

Whereas $p(n)$ is very rapidly increasing with increasing n, $p^*(m)$ turns out to be rather small. An estimate readily obtained is

$$p^*(m) = O(m^{-1/4}).$$

The function $f^*(x)$ requires a further investigation. It is quite possible that $f^*(x)$ is identically zero for $|x| > 1$. Not only certain function-theoretical considerations, but also some numerical computations pertaining to the first coefficients $p^*(m)$, which Dr. D. H. Lehmer was kind enough to carry out, seem to point in this direction.

The whole theory admits an application to a class of functions related to certain "modular forms" of positive dimensions, e.g., to $f^r(x)$ for $2 \leqq r \leqq 24$. Dr. Zuckerman and I are studying these generalizations in a paper now under preparation.

[1] Introductio in analysin infinitorum (1748), cap. 16, "De partitione numerorum," Opera omnia, ser. 1, **8**; "De partitione numerorum" (1753) Opera omnia, ser. 1, **2**, p. 280.

[2] "Asymptotic formulae in combinatory analysis," *Proc. Lond. Math. Soc.* (2), **17**, 75–115 (1918); also Collected Papers of S. Ramanujan, 276–309.

[3] Explicit expressions for $\omega_{h,k}$ can be found in Hardy-Ramanujan, loc. cit., formulae (1.721) and (1.722); cf. also H. Rademacher, "Bestimmung einer gewissen Einheitswurzel in der Theorie der Modulfunktionen," *Jour. Lond. Math. Soc.*, **7**, 14–19 (1932).

[4] "Erläuterungen, &c.," Riemann's Werke, 438–447 (1876); cf. also H. Weber, *Elliptische Funktionen*, 97–102 (1891), and H. Rademacher, *Jour. reine angewandte Math.*, **167**, 312–336 (1931).

[5] "Sur un théorème concernant les fonctions entières," *Arkiv Mat., Astron. Fysik*, **11**, No. 22 (1916).

NOTE ON THE CURVATURE OF LEVEL CURVES OF GREEN'S FUNCTION

By J. L. Walsh

Department of Mathematics, Harvard University

Communicated December 19, 1936

The primary object of this note is the proof of

THEOREM 1. *Let the function* $w = f(z)$ *with* $f(0) = 0$ *map the closed region* $|z| \leqq 1$ *smoothly onto the closed interior of a convex analytic Jordan curve* C *in the* w*-plane. Let* C_r, $0 < r \leqq 1$, *denote the image in the* w*-plane of the circle* $|z| = r$; *that is to say,* C_r *is the level curve* $G(x, y) = \log r$ *of Green's function* $G(x, y)$ *for the interior of* C *with pole in* $w = 0$. *Then the expression*

$$r \cdot [\text{min. curvature of } C_r] \tag{1}$$

increases monotonically as r *decreases, and approaches the limit* $1/|f'(0)|$ *as* r *approaches zero.*

For the present, the term "increases monotonically" is to be interpreted in the weak sense "increases or remains unchanged."

Let z with $|z| = r$ $(0 < r \leqq 1)$ be arbitrary, and let $\kappa(z)$ denote the curvature of C_r at the point $w = f(z)$. We state for reference the well known and easily proved formula

$$\kappa(z) = \frac{\Re\left[1 + z\dfrac{f''(z)}{f'(z)}\right]}{|z| \cdot |f'(z)|}, \tag{2}$$

where the symbol $\Re$ denotes the real part of the complex quantity which follows it. Equation (2) is to be interpreted algebraically rather than numerically; if z traces the circle $|z| = r$ in the positive sense, then $\kappa(z)$ is positive or negative according as the tangent to C_r at $w = f(z)$ rotates in the positive or negative sense.

Under the hypothesis of Theorem 1 the curvature of C is non-negative and continuous. If the curvature vanishes on C, it cannot vanish at every point of the Jordan curve C, and is positive where it is not zero. Then the harmonic function

$$\Re\left[1 + z\frac{f''(z)}{f'(z)}\right]$$

is actually *positive* at every interior point of $\Gamma: |z| = 1$. The function $f'(z)$ is continuous and different from zero on and within Γ. That is to say, if $\kappa(z)$ vanishes at points of Γ, we have shown for $|z| = r < 1$

$$r \cdot \kappa(z) \geqq \min\,[\kappa(z),\ z \text{ on } \Gamma]. \tag{3}$$

It remains to prove (3) when $\kappa(z)$ does not vanish on Γ.

We shall have occasion to apply the following lemma, whose proof is merely a matter of computation:

LEMMA. *If the function* $u(x, y)$ *is harmonic and positive, then for the function* $U(x, y) = \log u(x, y)$ *we have*

$$\frac{\partial^2 U}{\partial x^2} + \frac{\partial^2 U}{\partial y^2} = -\frac{1}{u^2}\left[\left(\frac{\partial u}{\partial x}\right)^2 + \left(\frac{\partial u}{\partial y}\right)^2\right] \leqq 0.$$

Consequently[1] *the function* $U(x, y)$ *is superharmonic.*

We are now in a position to complete the proof of Theorem 1. Under the present hypothesis the curvature of C is positive, so the numerator in (2) is positive on Γ, and being harmonic is positive also for $|z| < 1$. Let us write (2) in the form

$$\log\,[|z| \cdot \kappa(z)] = \log \Re\left[1 + z\frac{f''(z)}{f'(z)}\right] - \log|f'(z)|. \tag{4}$$

The first term on the right is superharmonic on and within Γ, by the Lemma. The second term on the right is the negative of the logarithm of the modulus of a non-vanishing analytic function, hence harmonic on and within Γ. Then the entire right-hand member of (4) is the sum of two functions superharmonic on and within Γ, hence itself is superharmonic on and within Γ. The function $\log\,[|z| \cdot \kappa(z)]$ is continuous on and within Γ, and being superharmonic can have no proper minimum interior to Γ. Then the minimum of $\log\,[|z| \cdot \kappa(z)]$ or of $|z| \cdot \kappa(z)$ in the closed interior of Γ is assumed on Γ itself, so we have established (3) for $|z| = r < 1$.

The function $w' = f(rz')$ with $O < r < 1$ maps the region $|z'| \leqq 1$ smoothly onto the closed interior of C_r in the w'-plane, so from (3) we may write for $|z'| = r_1/r < 1$ or $|z| = r_1 < r$

$$\frac{r_1}{r}\kappa(z) \geqq \min\,[\kappa(z),\ |z| = r];$$

the monotonic character of (1) is now established. The remaining part of Theorem 1 is obvious by inspection of (2).

Let K_r be the curve obtained from C_r ($r \leqq 1$) by stretching the w-plane away from the origin O in the ratio $r : 1$. Theorem 1 asserts that *the minimum curvature of* K_r *increases monotonically as* r *decreases and approaches the limit* $1/|f'(O)|$ *as* r *approaches zero.* Of course the maximum curvature of K_r also approaches $1/|f(O)|$ as r approaches zero. It is also true whether C is convex or not, and is easily proved by studying the modulus of the function $f(z)/z$, that the greatest distance from O to a point of K_r decreases monotonically as r decreases and approaches $1/|f'(O)|$ as r approaches zero; by a similar study of the modulus of $z/f(z)$ it may be proved that the least distance from O to a point of K_r increases monotonically as r decreases, and approaches $1/|f'(O)|$ as r approaches zero.

We remark that the maximum curvature of K_r does not necessarily decrease monotonically as r decreases. Indeed, let C be the circle of radius unity whose center is the point $w = \alpha$, $O < \alpha < 1$, with

$$w = f(z) \equiv \frac{z - \alpha}{\alpha z - 1} - \alpha;$$

we easily compute for $|z| = r$ the value

$$r\cdot\kappa(z) = \frac{1 - \alpha^2 r^2}{1 - \alpha^2},$$

which depends only on $r = |z|$. Then the curvature of K_r, which is constant on K_r and equal to the maximum curvature of K_r, increases monotonically in the strong sense as r decreases.

We shall show later that for arbitrary convex C the maximum curvature of K_r does not necessarily increase monotonically as r decreases.

If the curvature of C is not actually positive at every point, the strong inequality is valid in (3). Suppose now that the curvature of C is positive at every point; we shall prove that except in a trivial case the strong inequality is also valid in (3).

The function $\log\,[|z|\cdot\kappa(z)]$ is continuous and superharmonic on and within Γ. Let $V(x, y)$ denote the function which coincides with $\log\,[|z|\cdot\kappa(z)]$ on Γ, and is harmonic interior to Γ and continuous in the corresponding closed region; the minimum value of $V(x, y)$ on and within Γ

can be taken on by $V(x, y)$ interior to Γ only if $V(x, y)$ is identically constant. Thus the minimum value of the superharmonic function $\log [|z| \cdot \kappa(z)]$ can be taken on by $\log [|z| \cdot \kappa(z)]$ interior to Γ only if $V(x, y)$ is identically constant. In the latter case $\kappa(z)$ is constant on Γ, so C is a circle; the reader will verify from the actual formulas involved (see above) that the point $w = O$ must lie at the center of C. Then in every case where C is not a circle whose center is $w = O$, the strong inequality is valid in (3), so under the hypothesis of Theorem 1, except in the trivial case that $f(z)/z$ is identically constant, *the expression* (1) *increases in the strong monotonic sense as* r *decreases.*

Under the conditions of Theorem 1, the minimum curvature of C is positive or zero. If C is a circle, each curve C_r $(r < 1)$ is convex. If C is not a circle, the strongly monotonic variation of (1) implies that the curvature of C_r $(r < 1)$ is *positive*, so C_r is also convex. The conclusion that in every case C_r $(r < 1)$ is convex is a well known theorem due to Study,[2] thus contained in Theorem 1.

Another generalization of Study's result is the theorem proved by Peschl,[3] that if the function $w = f(z)$ with $f(O) = O$ maps $|z| \leqq 1$ onto the closed interior of an analytic Jordan curve C whose minimum curvature is k, then the minimum curvature of C_r is greater than or equal to k. Peschl's result is more general than Theorem 1 in admitting either positive or negative curvature of C, but is less general in that Theorem 1 asserts for $k \geqq O$ the monotonic character of (1). From the geometric viewpoint, Peschl's result thus does not involve the monotonic character of the minimum curvature of K_r.

It is a consequence of Theorem 1, together with the additional remark on the strongly monotonic variation of (1), that under the hypothesis of Theorem 1 the minimum curvature of C_r increases in the strong sense as r decreases. It cannot be proved that the maximum curvature of C_r always decreases as r decreases; indeed in the case $f(z) \equiv z$ the maximum curvature of C_r increases as r decreases.

It also cannot be proved that under the conditions of Theorem 1 the maximum curvature of C_r always increases as r decreases.[4] Let $w = F(z)$ map $|z| < 1$ onto the interior of a lens-shaped region D in the w-plane, symmetric in the axis of reals and in the origin, bounded by two equal arcs of circles which intersect in points A and B. Let D_R denote the image in the w-plane of the circle $|z| = R < 1$. The Jordan curves D_R are convex curves whose curvature becomes infinite as w approaches A. Let R_2 be arbitrary, $O < R_2 < 1$, and let the maximum curvature of D_{R_2} be k_1. Let R_1 be chosen, $R_2 < R_1 < 1$, so that the maximum curvature of D_{R_1} is greater than k_1. Then the function $w = F(R_1 z')$ maps $|z'| < 1$ onto a region bounded by the convex analytic Jordan curve D_{R_1}. Under this map the maximum curvature of D_{R_1}, the image of $|z'| = 1$, is greater than the maximum curva-

ture of D_{R_2}, the image of $|z'| = R_2/R_1 < 1$. We can also choose the value of R_1, $R_2 < R_1 < 1$, so that we have

$$R_1 \cdot [\text{max. curvature of } D_{R_1}] > R_2 \cdot [\text{max. curvature of } D_{R_2}],$$

which shows that the maximum curvature of K_r does not necessarily increase monotonically as r decreases.

Theorem 1 is formulated for the case that C is analytic, but obviously applies in more general cases, for instance whenever (2) is valid and $\kappa(z)$ is continuous for $|z| \leqq 1$. Whenever $\kappa(z)$ is positive interior to Γ, that is to say, whenever C is convex, we can replace (3) by the inequality

$$r \cdot \kappa(z) \geqq \varliminf_{z \to \Gamma} \kappa(z),$$

where the right-hand member represents the inferior limit of $\kappa(z)$ for all possible sequences of points z interior to Γ approaching Γ.

If in Theorem 1 we omit the requirement that C shall be convex, and if curvature is interpreted numerically rather than algebraically, it is still true that (1) increases monotonically in the weak sense as r decreases. If C is not convex, expression (1) is then zero for $r = 1$ and remains zero for values of r for which C_r is not convex. If r_1 is the greatest r for which C_r is convex (such a value $r_1 > 0$ exists), expression (1) increases strongly monotonically as $r \leqq r_1$ decreases.

Study of the function $\log [-\kappa(z)/|z|]$, where $\kappa(z)$ is defined by (2), yields

THEOREM 2. *Let the function*

$$w = f(z) \equiv \frac{a}{z} + a_0 + a_1 z + a_2 z^2 + \ldots, a \neq 0,$$

map the closed region $|z| \leqq 1$ *smoothly onto the closed exterior of a convex analytic Jordan curve* C *in the* w*-plane. Let* C_r, $0 < r \leqq 1$, *denote the image in the* w*-plane of the circle* $|z| = r$; *that is to say,* C_r *is the level curve* $G(x, y) = \log r$ *of Green's function* $G(x, y)$ *for the exterior of* C *with pole at infinity. Then the expression*

$$\frac{\text{min. curvature of } C_r}{r} \tag{5}$$

increases monotonically as r *decreases, when curvature is interpreted numerically rather than algebraically;*[5] *the increase is strongly monotonic if* C *is not a circle. Both* (5) *and*

$$\frac{\text{max. curvature of } C_r}{r}$$

approach the limit $1/|a|$ *as* r *approaches zero.*

Let K_r *denote the curve obtained from* C_r *by shrinking the latter toward the point*[6] $w = a_0$ *in the ratio* $1 : r$. *Then the minimum curvature of* K_r *increases monotonically as* r *decreases; both maximum and minimum curvature of* K_r *approach the limit* $1/|a|$ *as* r *approaches zero. Whether* C *is convex or not, the greatest distance from* a_0 *to a point of* K_r *decreases monotonically as* r *decreases, and approaches* $1/|a|$ *as* r *approaches zero; the least distance from* a_0 *to a point of* K_r *increases monotonically as* r *decreases, provided* a_0 *is interior to* K_r, *and approaches* $1/|a|$ *as* r *approaches zero.*

[1] For this and the other elementary properties of superharmonic functions that we use, the reader may refer to Kellogg, *Potential Theory* (Berlin, 1929), p. 361.

[2] *Konforme Abbildung einfach-zusammenhängender Bereiche* (Leipzig, 1913).

[3] Peschl, E., *Math. Annalen*, **106**, 574–594 (1932).

[4] But when r is sufficiently small, whether C is convex or not, the maximum curvature of C_r increases as r decreases.

[5] But the minimum curvature of C_r need not increase monotonically nor decrease monotonically as r decreases.

[6] The point $w = a_0$ is the conformal center of gravity of the curve C, hence lies interior to C. See Frank, P., and Löwner, K., *Math. Zeit.*, **3**, 78–86 (1919).

REPRESENTATIONS INDUCED IN AN INVARIANT SUBGROUP

BY A. H. CLIFFORD

INSTITUTE FOR ADVANCED STUDY

Communicated December 21, 1936

If $h \to A(h)$ is any representation $\mathfrak{A}_H$ of a group H in any field K, $A(h)$ indicating the matrix corresponding to the element h of H, and if $h \to \bar{h}$ is any automorphism of H, then the representation $\mathfrak{B}_H$ of H defined by $h \to B(h) = A(\bar{h})$ will be called an *automorph* of $\mathfrak{A}_H$. If H is contained in a group G, and $\bar{h} = u^{-1}hu$ with u in G (H invariant under u), we shall say that $\mathfrak{B}_H$ is an automorph of $\mathfrak{A}_H$ *relative to* G.

If $g \to A(g)$ is any representation $\mathfrak{A}_G$ of a group G, and if H is any subgroup of G, then $\mathfrak{A}_G$ *induces* the representation $\mathfrak{A}_H$ of H defined by $h \to A(h)$. Regarding the representation $\mathfrak{A}_H$ induced by an *irreducible* representation $\mathfrak{A}_G$ of G in an *invariant* subgroup H of G, we have the following general result:

THEOREM 1. $\mathfrak{A}_H$ *is either itself irreducible or is fully reducible into irreducible components all of the same degree, and all are automorphs relative to* G *of any one of them.*

Let $\mathfrak{A}_H^{(1)}, \mathfrak{A}_H^{(2)}, \ldots, \mathfrak{A}_H^{(r)}$ be a complete list of the inequivalent irreducible components of $\mathfrak{A}_H$. Choose a coördinate system in the representation space $\mathfrak{R}$ of $\mathfrak{A}_G$ which exhibits the full reduction of $\mathfrak{A}_H$, and let $\mathfrak{R}_i$

denote the sum of all the equivalent irreducible invariant subspaces of $\mathfrak{R}$ belonging to $\mathfrak{A}_H^{(i)}$, $(i = 1, 2, \ldots, r)$.

THEOREM 2. *The spaces* $\mathfrak{R}_1, \mathfrak{R}_2, \ldots, \mathfrak{R}_r$ *constitute a system of imprimitivity of* $\mathfrak{A}_G$.

Since $\mathfrak{A}_G$ is irreducible, it is transitive, and all the spaces $\mathfrak{R}_i$ have the same dimension. Since all the irreducible components of $\mathfrak{A}_H$ have the same degree t, each of the inequivalent irreducible components of $\mathfrak{A}_H$ must occur the same number of times s, and the degree of $\mathfrak{A}_G$ is therefore rst. In particular, if $\mathfrak{A}_H$ contains at least two inequivalent irreducible components ($r > 1$), then $\mathfrak{A}_G$ is imprimitive.[1]

In the particular case when the factor-group G/H is a finite cyclic group, and the number field K is algebraically closed, we can give a relatively complete description of the situation.

Let m be the index of H in G, and let us write

$$G = H + uH + u^2H + \ldots + u^{m-1}H, \quad (u^m \text{ in } H).$$

Let ϵ be any mth root of unity in K. If $\mathfrak{A}_G$ is any representation $g \to A(g)$ of G, and we define

$$A^*(u^ih) = \epsilon^i A(u^ih), \quad (i = 0, 1, \ldots, m-1;\ h \text{ in } H),$$

then $g \to A^*(g)$ is a representation $\mathfrak{A}_G^*$ of G. We call $\mathfrak{A}_G^*$ an *associate* of $\mathfrak{A}_G$, and more specifically an associate of *index* k if ϵ is a primitive kth root of unity.

With the aid of this definition, we may describe the situation as follows. All the irreducible components of $\mathfrak{A}_H$ are inequivalent ($s = 1$), and their number r is a divisor of the index m of H in G. $\mathfrak{A}_G$ is equivalent to all of its associates of index r, but to none of higher index (this serves to determine r; in particular, $\mathfrak{A}_H$ remains irreducible if and only if $\mathfrak{A}_G$ is equivalent to none of its associates other than itself). If $\mathfrak{B}_G$ is any other irreducible representation of G, and if one of the irreducible components of $\mathfrak{B}_H$ is equivalent to one of those of $\mathfrak{A}_H$, then $\mathfrak{B}_H$ is equivalent to $\mathfrak{A}_H$, and $\mathfrak{B}_G$ is equivalent to an associate of $\mathfrak{A}_G$; the converse is evident. Finally, any irreducible representation of H can be obtained from an irreducible representation $\mathfrak{A}_G$ of G as one of the irreducible components of $\mathfrak{A}_H$.

These results were known by Brauer for the case when G is the full orthogonal group and H the proper orthogonal group,[2] and by Professor Hermann Weyl—to whom I owe the inspiration for the present development—for the case when H is a subgroup of index two in an arbitrary group G. Proofs will be given in a paper to appear in the *Annals of Mathematics*.

[1] A. Speiser, *Theorie der Gruppen von endlicher Ordnung* (Berlin, 1927), Satz 172 on p. 195.

[2] R. Brauer, *Über die Darstellung der Drehungsgruppe durch Gruppen linearer Substitutionen* (Dissertation, 1925), pp. 20–23.

ON THE MEAN VALUE OF r^s FOR KEPLERIAN SYSTEMS

BY SIMON PASTERNACK

CALIFORNIA INSTITUTE OF TECHNOLOGY

Communicated January 13, 1937

I. Waller[1] has proved, by means of the generating function for the Laguerre polynomial, that

$$\overline{r^s} = \left(\frac{na_0}{2Z}\right)^s \frac{1}{2n} \frac{(n-l-1)!(2l+s+2)!}{(n+l)!} \times \text{the coefficient of } (uv)^{n-l-1} \text{ in } \frac{(1-u)^{s+1}(1-v)^{s+1}}{(1-uv)^{2l+s+3}}, \tag{1}$$

where n is the total quantum number, l is the azimuthal quantum number and a_0 is the Bohr radius unit, $a_0 = h^2/4\pi^2e^2m$.

For $s \geqq -1$, this yields the formula

$$\overline{r^s} = \left(\frac{na_0}{2Z}\right)^s \frac{1}{2n} \sum_{k=0}^{s+1} \binom{s+1}{k}^2 \frac{(n-l-1)!(n+l+s+1-k)!}{(n-l-1-k)!\ \ (n+l)!}. \tag{2}$$

For $s = -q$, $2 \leqq q \leqq 2l+2$, we have

$$\overline{r^{-q}} = \left(\frac{2Z}{na_0}\right)^q \frac{1}{2n} \sum_{k=0}^{n-l-1} \binom{q+k-2}{k}^2 \frac{(n-l-1)!\,(n+l-q+1-k)!}{(n-l-1-k)!\,(n+l)!}. \tag{3}$$

The latter expression is not suitable for computation in general, as the summation is from 0 to $n-l-1$.

J. H. Van Vleck[2] has derived an expression for $\overline{r^{-q}}$, using Dirac's "q-numbers." A simpler expression may, however, be derived from (2) and (3) by use of the identity

$$\frac{(2l-q)!}{(2l+q+1)!} \overline{r^{-q-2}}/\overline{r^{q-1}} = \left(\frac{2Z}{na_0}\right)^{2q+1} \tag{4}$$

where $0 \leqq q \leqq 2l$.

Expression (2) may be put into the form

$$\overline{r^{q-1}} = \left(\frac{na_0}{2Z}\right)^{q-1} \frac{1}{2n} \frac{(n+l+q)!}{(n+l)!} \sum_{k=0}^{q} \frac{\{(-q)(-q+1)\ldots(-q+k-1)\}^2(-n+l+1)\ldots(-n+l+k)}{k!\ k!\ (-n-l-q)(-n-l-q+1)\ldots(-n-l-q+k-1)}$$

$$= \left(\frac{na_0}{2Z}\right)^{q-1} \frac{1}{2n} \frac{(n+l+q)!}{(n+l)!} F\left[\begin{matrix} -q, & -q, & -n+l+1 \\ 1, & & -n-l-q \end{matrix}\right], \tag{5}$$

where $F\begin{bmatrix} a, b, c \\ e, f \end{bmatrix} \equiv F(a, b, c;\ e, f;\ 1)$ is the generalized hypergeometric series with unit argument. Similarly expression (3) may be put into the form[3]

$$\overline{r^{-q-2}} = \left(\frac{na_0}{2Z}\right)^{-q-2} \frac{1}{2n} \frac{(n+l-q-1)!}{(n+l)!} \lim_{\delta \to 0} F\begin{bmatrix} q+1, q+1, -n+l+1 \\ 1, \quad -n-l+q+1+\delta \end{bmatrix}. \tag{6}$$

To prove the identity (4), we use the following identity:[4]

$$F\begin{bmatrix} a, b, c \\ e, f \end{bmatrix} = \frac{\Gamma(e+f-a-b-c)\Gamma(f)}{\Gamma(e+f-b-c)\Gamma(f-a)} \quad F\begin{bmatrix} a, e-b, e-c \\ e, e+f-b-c \end{bmatrix}. \tag{7}$$

Putting $a = -n+l+1, b = c = -q, e = 1, f = -n-l-q+\delta$, and then letting $\delta \longrightarrow 0$, we get

$$F\begin{bmatrix} -q, -q, -n+l+1 \\ 1, \quad -n-l-q \end{bmatrix} = \frac{(n+l-q-1)!(2l+q+1)!}{(n+l+q)!(2l-q)!} \lim_{\delta \to 0} F\begin{bmatrix} q+1, q+1, -n+l+1 \\ 1, -n-l+q+1+\delta \end{bmatrix}. \tag{8}$$

The identity (4) follows at once from (5), (6) and (8).

The computation of these mean values may be further simplified by using the following expressions, in which $q \geqq 0$:

$$\overline{r^{2q-1}} = \left(\frac{na_0}{2Z}\right)^{2q-1} \frac{1}{2n} \frac{(2l+2q+1)!}{(2l+1)!} F\begin{bmatrix} -q, q+\tfrac{1}{2}, l+1+n, l+1-n \\ 1, l+1, l+\tfrac{3}{2} \end{bmatrix}$$

$$= \left(\frac{na_0}{2Z}\right)^{2q-1} \frac{1}{2n} \frac{(2l+2q+1)!}{(2l+1)!} \left\{ 1 + \frac{q(q+\tfrac{1}{2})[n^2-(l+1)^2]}{1!1!(l+1)(l+\tfrac{3}{2})} + \frac{(q-1)q(q+\tfrac{1}{2})(q+\tfrac{3}{2})[n^2-(l+1)^2][n^2-(l+2)^2]}{2!2!(l+1)(l+\tfrac{3}{2})(l+2)(l+\tfrac{5}{2})} + \ldots \right\}, \tag{9}$$

$$\overline{r^{2q}} = \left(\frac{na_0}{2Z}\right)^{2q} \frac{(2l+2q+2)!}{(2l+2)!} F\begin{bmatrix} -q, q+\tfrac{3}{2}, l+1+n, l+1-n \\ 1, l+\tfrac{3}{2}, l+2 \end{bmatrix}$$

$$= \left(\frac{na_0}{2Z}\right)^{2q} \frac{(2l+2q+2)!}{(2l+2)!} \left\{ 1 + \frac{q(q+\tfrac{3}{2})[n^2-(l+1)^2]}{1!1!(l+\tfrac{3}{2})(l+2)} + \frac{(q-1)q(q+\tfrac{3}{2})(q+\tfrac{5}{2})[n^2-(l+1)^2][n^2-(l+2)^2]}{2!2!(l+\tfrac{3}{2})(l+2)(l+\tfrac{5}{2})(l+3)} + \ldots \right\}. \tag{10}$$

The expressions (9) and (10) follow from some properties of the polynomials[5]

$$F_n^m(z) = F\left[\begin{matrix} -n,\ n+1,\ \dfrac{1+z+m}{2} \\ 1,\ m+1 \end{matrix}\right]. \qquad (11)$$

It can be shown by means of the operational equation for these polynomials that

$$F_{2n}^m(z) = F\left[\begin{matrix} -n,\ n+{}^1/_2,\ \dfrac{m+1+z}{2},\ \dfrac{m+1-z}{2} \\ 1,\ \dfrac{m+1}{2},\ \dfrac{m+2}{2} \end{matrix}\right] \qquad (12)$$

and

$$F_{2n+1}^m(z) = -\frac{z}{m+1}\, F\left[\begin{matrix} -n,\ n+{}^3/_2,\ \dfrac{m+1+z}{2},\ \dfrac{m+1-z}{2} \\ 1,\ \dfrac{m+2}{2},\ \dfrac{m+3}{2} \end{matrix}\right]. \qquad (13)$$

There is an identity[6]

$$F\left[\begin{matrix} a, b, c \\ e, f \end{matrix}\right] = \frac{\Gamma(e)\Gamma(f)\Gamma(1-a)\Gamma(1+b-f)\Gamma(1+b-e)}{\Gamma(e-c)\Gamma(f-c)\Gamma(1+b-a)\Gamma(1+b+c-f)\Gamma(1+c-e)}$$
$$F\left[\begin{matrix} b,\ e-a,\ 1+b-f \\ 1+b-a,\ 1+b+c-f \end{matrix}\right]. \qquad (14)$$

Putting $a = -q, b = -q, c = -n+l+1, e = 1-\delta, f = -n-l-q+\delta$, and then letting $\delta \longrightarrow 0$, we get

$$F\left[\begin{matrix} -q,\ -q,\ -n+l+1 \\ 1,\ -n-l-q \end{matrix}\right] = \frac{(-1)^q(2l+q+1)!(n+l)!}{(2l+1)!(n+l+q)!}$$
$$F\left[\begin{matrix} -q,\ 1+q,\ n+l+1 \\ 1,\ 2l+2 \end{matrix}\right]. \qquad (15)$$

A comparison of equation (15) with equations (5) and (11) indicates that

$$\overline{r^{q-1}} = \left(\frac{na_0}{2Z}\right)^{q-1} \frac{(-1)^q}{2n} \frac{(2l+q+1)!}{(2l+1)!}\ F_q^{2l+1}(2n). \qquad (16)$$

Equations (9) and (10) then follow immediately from equations (12) and (13).

It can also be proved, by means of these generalized hypergeometric series, that $\overline{r^q}$ may be written in the form

$$\overline{r^q} = \left(\frac{na_0}{Z}\right)^q \frac{1}{n}\{c_0 + c_1 l(l+1) + c_2(l-1)l(l+1)(l+2) +$$
$$c_3(l-2)(l-1)l(l+1)(l+2)(l+3) + \ldots\ldots\}, \qquad (17)$$

where $c_0, c_1, c_2, \ldots\ldots$ are polynomials in n, and are odd or even functions of n according as q is even or odd.

There is a recurrence relation

$$(n+1)(n+m+1)F^m_{n+1}(z) = -(2n+1)zF^m_n(z) + n(n-m)F^m_{n-1}(z). \tag{18}$$

It follows then from equations (16) and (4) that, if $q \geqq 1$,

$$\overline{r^q} = \left(\frac{2q+1}{q+1}\right)\frac{n^2a_0}{Z}\overline{r^{q-1}} - \frac{q(2l+1+q)(2l+1-q)}{q+1}\frac{n^2a_0^2}{4Z^2}\overline{r^{q-2}} \tag{19}$$

and

$$\overline{r^{-q-\delta}} = \frac{1}{(l+1+q/2)(l-q/2)}\left\{\left(\frac{2q+1}{q+1}\right)\frac{Z}{a_0}\overline{r^{-q-2}} - \frac{q}{q+1}\frac{Z^2}{n^2a_0^2}\overline{r^{-q-1}}\right\}. \tag{20}$$

Formulas (4), (9) and (10) are the most useful for computational purposes.

[1] I. Waller, *Zeit. Physik*, **38**, 644 (1926).

[2] J. H. Van Vleck, *Proc. Roy. Soc. A*, **143**, 679 (1934). There is a slight error in his expression for $\overline{r^{-4}}$ for $l=2$, the coefficients being all 10 times too large.

[3] δ may be equated to zero except in the case $q = 2l$.

[4] W. N. Bailey, *Generalized Hypergeometric Series* (Cambridge Tract No. 32), p. 18.

[5] The polynomial $F^0_n(z)$ is discussed by H. Bateman, *Tôhoku Math. J.*, **37**, 23 (1933). The general case will be treated by the author in a paper to be published soon.

[6] W. N. Bailey, *Generalized Hypergeometric Series*, (Cambridge Tract No. 32), p. 22.

ON THE EQUATION OF DIFFUSION

BY PAUL S. EPSTEIN

NORMAN BRIDGE LABORATORY OF PHYSICS, CALIFORNIA INSTITUTE OF TECHNOLOGY

Communicated December 30, 1936

1. Under the title "The Analytical Theory of Probability," A. Kolmogoroff[1] published a few years ago a mathematically elegant account of what might be called the general theory of diffusion. As the main result of his analysis, he sets up two differential equations for transition probabilities (see below). The first of them contains as its independent variables the initial parameters of the transition probability and has an analytical form resembling the ordinary diffusion equation. Unlike it, the second differential equation (depending on the final parameters) has a different form unfamiliar to the physicist.

The puzzling asymmetry of the two equations, as to whose physical reasons the author gives no hint, was, in our opinion, the main cause why the work of Kolmogoroff did not receive more attention. Unless these reasons are fully understood, an intelligent application of the theory to practical problems is very difficult. We think it, therefore, worth while to present in the following lines a discussion of the mutual connection between the two equations of Kolmogoroff and of their relation to other forms of the diffusion equation used in physics.

2. The concept of the transition probability applies to systems composed of many identical elements. If one of these elements was at the time s in the state x, the probability of its being found at a later time t in the state y is called transition probability and is denoted by $v(x, s; y, t)$. The states x and y are in general defined by several geometrical and dynamical coördinates. Following Kolmogoroff, however, we shall restrict ourselves to the case of states depending on a single parameter, since the generalization for many parameters is obvious. Moreover, we shall take this single coördinate as continuous and deal with intervals between x and $x + \Delta x$, etc.

Kolmogoroff considers only the case of *independent* probabilities when $v(s, x; y, t)$ is not influenced by the presence or absence of other particles in the same or neighboring states. Under this restriction this function must satisfy the two fundamental requirements of the theory of probability

$$\int v(x, s; y, t)dy = 1, \tag{1}$$

$$\int v(x, s; y, t')v(y, t'; z, t)dy = v(x, s; z, t), \tag{2}$$

the integrals being extended over the whole region of variability of the parameter y.

By mere mathematical transformations, these conditions lead directly to the equations of diffusion in Kolmogoroff's form

$$-\frac{\partial v(x, s; y, t)}{\partial s} = a(x, s)\frac{\partial}{\partial x}v(x, s; y, t) + b(x, s)\frac{\partial^2}{\partial x^2}v(x, s; y, t), \tag{3}$$

$$\frac{\partial v(x, s; y, t)}{\partial t} = -\frac{\partial}{\partial y}[a(y, t)v(x, s; y, t)] + \frac{\partial^2}{\partial y^2}[b(y, t)v(x, s; y, t)]. \tag{4}$$

The meaning of the coefficients is the *mean transition velocity* of an element at the time t and in the state y

$$a(y, t) = \lim_{\Delta=0}\frac{1}{\Delta}\int(\eta - y)v(y, t; \eta, t + \Delta)d\eta, \tag{5}$$

and the *mean spread of this velocity*

$$b(y, t) = \lim_{\Delta=0} \frac{1}{2\Delta} \int (\eta - y)^2 v(y, t;\ \eta, t + \Delta) d\eta. \qquad (6)$$

Another type of probability which also has considerable physical interest is the distribution probability or density of distribution $D(s, t;\ y)$ which is defined as the chance of finding an element in the state y at the time t, no matter where it came from. It is clear from the definition of the function $v(x, s;\ y, t)$ that the density of distribution is connected with it in the following way

$$D(s, t;\ y) = \int D(s, s;\ x) v(x, s;\ y, t) dx, \qquad (7)$$

provided $D(s, s;\ x)$ is the known density at the time s. Hence $D(s, t;\ y)$ must also satisfy the equation (4).

$$\frac{\partial D}{\partial t} = -\frac{\partial}{\partial y} [a(y, t) D] + \frac{\partial^2}{\partial y^2} [b(y, t) D]. \qquad (8)$$

3. The most important case is the one in which the coefficients $a(y)$ and $b(y)$ are independent of time. The system is then called "homogeneous in time" and it is apparent from (5) and (6) that the transition probability can be represented as $v(x, y, t-s)$, depending only on the elapsed time $t-s$. It will be sufficient for our purpose to consider this simpler case. In fact when we meet in the applications probabilities that are not homogeneous in time they usually are also not independent and, therefore, outside the pale of Kolmogoroff's theory. As the equation (8) shows, the main physical characteristic of these systems is that in them the density of distribution D tends toward a state of equilibrium with the definite value $D_0(y)$. Supposing that the system has reached its equilibrium state, we can apply thermodynamical reasoning: For any interval of time the number of systems which move from the state x into the state y must be equal to the number of those which move in the opposite direction. This leads to the formula

$$D_0(x) v(x, y, t-s) = D_0(y) v(y, x, t-s), \qquad (9)$$

as a direct expression of the second law of thermodynamics.

For the function $v(y, x, t-s)$, the first equation of diffusion (3) takes the simplified form

$$\frac{\partial v(y, x, t-s)}{\partial t} = a(y) \frac{\partial}{\partial y} v(y, x, t-s) + b(y) \frac{\partial^2}{\partial y^2} v(y, x, t-s). \qquad (10)$$

Substituting from (9) $v(y, x, t-s) = D_0(x) v(x, y, t-s)/D_0(y)$, we find

$$\frac{\partial}{\partial t}\frac{v(x, y, t-s)}{D_0(y)} = a(y)\frac{\partial}{\partial y}\left[\frac{v(x, y, t-s)}{D_0(y)}\right] + b(y)\frac{\partial^2}{\partial y^2}\left[\frac{v(x, y, t-s)}{D_0(y)}\right].$$

As a distribution density, $D_0(y)$ must be an integral (independent of time) of the same equation which is satisfied by $v(x, y, t-s)$. We shall see that this requirement is fulfilled if we put

$$D_0(y) = \frac{C}{b}\exp\int\frac{a}{b}\,dy, \tag{11}$$

where C is a constant. In fact, the equation for the transition probability $v(x, y, t-s)$ becomes then

$$\frac{\partial v}{\partial t} = -\frac{\partial}{\partial y}[a(y)v] + \frac{\partial^2}{\partial y^2}[b(y)v], \tag{12}$$

while that for the equilibrium density can be written in the form

$$0 = -\frac{\partial}{\partial y}[a(y)D_0] + \frac{\partial^2}{\partial y^2}[b(y)D_0]. \tag{13}$$

These equations are of the second Kolmogoroff type which is thus obtained from the first. The asymmetry between the two types is, therefore, shown to be an immediate consequence of the second law of thermodynamics.

4. It is important to understand the physical nature of the coefficients a and b of the diffusion equation. According to the equation (5), $a(y)$ is the mean transition velocity of all elements starting from the state y. At first sight, one should be inclined to think that systems in which this mean velocity vanishes must tend toward an equilibrium with uniform density of distribution. This is, however, not the case: Applying the second law of thermodynamics we found, in the preceding section,[2] that the equilibrium distribution $D_0(y)$ is not given by the general integral of the equation (13) but by the special integral (11). The condition for D_0 being independent of y is, therefore, $\partial\left[\exp\left(\int\frac{a}{b}dy\right)/b\right]/\partial y = 0$ or $a - \frac{db}{dy} = 0$. In other words, the mean transition velocity a contains a part (equal to db/dy) which has no tendency to change an existing uniformity of distribution but the remainder $a - db/dy$ is operative in disturbing it. This fact is in complete harmony with the considerations by which the equation of diffusion (8) is usually derived in physics. The argument starts from calculating the number of elements which move across a plane, y = const, per unit area and unit time. There are two classes of causes for this motion to be considered. Such causes as *external forces or temperature gradients* belong to the first class and produce an effect of the form c_1D simply proportional to the density. (For instance,

in the case of an external force F the coefficient $c_1 = MF$, where M is called the mobility). The causes of the second type are called *forces of diffusion* and produce an effect proportional to the negative gradient of the density $-c_2 \partial D/\partial y$. The accumulation of the elements in any point is, therefore, determined by the (negative) divergence of the total effect. This leads to the equation[3]

$$\frac{\partial D}{\partial t} = -\frac{\partial}{\partial y}(c_1 D) + \frac{\partial}{\partial y}\left(c_2 \frac{\partial D}{\partial y}\right). \tag{14}$$

Comparing this with the form (8) we find

$$b = c_2, \quad a - db/dy = c_1. \tag{15}$$

The expression for c_1 is in agreement with the conclusions arrived at above. It shows that the form (14) of the equation of diffusion is a good guide to the physicist as it brings in evidence the quantities significant from his point of view. On the other hand, Kolmogoroff's equations (3) and (4) are more general since they include the case of transition probabilities which are inhomogeneous in time.

[1] A. Kolmogoroff, *Mathematische Annalen*, **104**, 415 (1931).

[2] The substitution of the general integral of equation (13) for D_0 in (9) and (10) does not lead to the equation (12). Kolmogoroff claims the same results by imposing upon D_0 the condition $\lim D_0 = 0$ for $y = \pm\infty$. That this argument is unconvincing, appears from the fact that it would exclude the uniform density. It is inconvenient to restrict oneself to finite systems.

[3] E.g., P. S. Epstein, *Gerlands Beitr. Geophysik*, **35**, 154 (1932).

ON THE STATISTICAL THEORY OF TURBULENCE

By Th. von Kármán

Guggenheim Aeronautics Laboratory, California Institute of Technology

Communicated January 2, 1937

G. I. Taylor[1] gave an important impetus to the statistical theory of turbulence by introducing the concept of "isotropic" turbulence, defined by the feature that the mean squares and mean products of the velocity components and of their derivatives are invariant with respect to rotation and reflection of the coördinate axes. Taylor found that under the assumption of the isotropy, the squares and double products of the first derivatives of the velocity components can be expressed by one single correlation function $R(y)$. This function is defined by the ratio $\frac{\overline{u_1 u_2}}{\overline{u^2}}$ where u_1 and

u_2 are the simultaneous values of the x-components of the velocity fluctuation at two points at a distance y perpendicular to the x-axis. Taylor defines a characteristic length λ by writing

$$R(y) = 1 - \frac{y^2}{\lambda^2} + \text{higher terms in } y. \tag{1}$$

Obviously $\frac{1}{\lambda^2} = -\frac{1}{2}\left(\frac{d^2R}{dy^2}\right)_{y=0}$ and Taylor shows that

$$\overline{\left(\frac{\partial u}{\partial y}\right)^2} = 2\frac{\overline{u^2}}{\lambda^2}. \tag{2}$$

Taylor shows furthermore that the rate of decrease of the kinetic energy of the unit volume by dissipation is equal to $15\mu\frac{\overline{u^2}}{\lambda^2}$ (μ = viscosity coefficient). He applies this result to the calculation of the decrease of the mean energy of the turbulent fluctuations downstream from a certain turbulence producing device such as a grid or a mesh. Denoting the velocity of the main stream by U, he obtains the equation

$$U\frac{d}{dx}\overline{u^2} = -10\nu\frac{\overline{u^2}}{\lambda^2} \tag{3}$$

where $\overline{u^2}$ and λ^2 are both unknown functions of the distance x from the grid; ν is the coefficient of kinematic viscosity. Taylor introduces a somewhat arbitrary hypothesis connecting $\overline{u^2}$ and λ^2 with the linear dimension of the turbulence producing device, and tries to show that the reciprocal $\frac{1}{\sqrt{\overline{u^2}}}$ of the root mean square of the velocity fluctuation is always proportional to x.

In this paper a second equation is established connecting $\overline{u^2}$ and λ^2, and it is shown that the decay of the turbulence is fully determined without further assumption by the correlation function $R(y)$. Taylor's result appears as a special case corresponding to a certain type of the correlation function.

We write the hydrodynamic equations in the form:

$$\frac{\partial \omega}{\partial t} + q\nabla\omega - \omega.\nabla q = \nu\nabla^2\omega. \tag{4}$$

In this equation q is the velocity vector and ω the vorticity vector. Multiplying the three-component equations by ξ, η, ζ (where ξ, η, ζ are the components of ω), respectively, and adding, the equation

$$\frac{1}{2}\frac{D}{Dt}\omega^2 - \omega(\omega.\nabla)q = \nu\omega.\nabla^2\omega \qquad (5)$$

is readily obtained.

We consider a fluid without mean velocity enclosed in a very large vessel and assume uniform, isotropic turbulence over the whole space considered. It is assumed that the vessel is so large that the influence of the walls can be neglected. Then taking mean values over time and the space considered, $\frac{D\overline{\omega^2}}{Dt}$ will be replaced by $\frac{d}{dt}\overline{\omega^2}$ and $\omega.\nabla^2\omega$ by $\overline{(\nabla \times \omega)^2}$. The second term needs special consideration. Writing out the expression in coördinates

$$\omega.(\omega.\nabla)q = \xi^2\frac{\partial u}{\partial x} + \eta^2\frac{\partial v}{\partial y} + \zeta^2\frac{\partial w}{\partial z} + \xi\eta\left(\frac{\partial u}{\partial y} + \frac{\partial v}{\partial x}\right) + \eta\zeta\left(\frac{\partial v}{\partial z} + \frac{\partial w}{\partial y}\right) + \zeta\xi\left(\frac{\partial w}{\partial x} + \frac{\partial u}{\partial z}\right). \qquad (6)$$

It will be seen that the expression is built up as the sum of the products of the components of the tensor $(\omega\,\omega)$ and of the components of the deformation tensor. Now it can be shown that because of the isotropic feature of the correlations between the velocity components and their derivatives, expression (6) vanishes in mean value. The proof will be given elsewhere. As a matter of fact, any value of the expression (6) different from zero would mean that the vortex filaments had a permanent tendency to be stretched or compressed in the direction of the vorticity axis. With the expression (6) vanishing, equation (5) leads to the simple result:

$$\frac{3}{2}\frac{\partial\overline{\xi^2}}{\partial t} = -3\nu\overline{\left(\frac{\partial\xi}{\partial y} - \frac{\partial\eta}{\partial x}\right)^2} \qquad (7)$$

and two similar equations obtained from (7) by cyclic permutation. Defining a length λ_ω by the relation

$$\overline{\left(\frac{\partial\xi}{\partial y}\right)^2} = 2\frac{\overline{\xi^2}}{\lambda_\omega^2}$$

which is analogous to (2), and computing the relations between squares and products of the derivatives of ξ, η, ζ, we obtain

$$\frac{d}{dt}\overline{\xi^2} = -10\nu\frac{\overline{\xi^2}}{\lambda_\omega^2}. \qquad (8)$$

Because of the isotropic feature of the system considered, $\overline{\xi^2}$ can be expressed by $\overline{u^2}$ and λ^2; namely $\overline{\xi^2} = 5\frac{\overline{u^2}}{\lambda^2}$. Hence, equation (8) together with

Taylor's equation (1) determines $\overline{u^2}$ as a function of the time, provided a relation between λ and λ_ω is known.

We substitute in equation (3) $\frac{d}{dt}$ for $U\frac{d}{dx}$ and write

$$\frac{d}{dt}\overline{u^2} = -10\nu\frac{\overline{u^2}}{\lambda^2}. \tag{9}$$

Then we multiply (8) by $\overline{u^2}$ and (9) by $\overline{\xi^2}$ and subtract. Taking into account that $\lambda^2 = 5\frac{\overline{u^2}}{\overline{\xi^2}}$, we readily obtain

$$\frac{d}{dt}\lambda^2 = 10\nu\left(\frac{\lambda^2}{\lambda_\omega^2} - 1\right). \tag{10}$$

Let us assume for the time being a constant value of the ratio $\frac{\lambda^2}{\lambda_\omega^2}$. The physical significance of this assumption is discussed later. Then it follows that λ^2 is increasing at a constant rate with the time. Denoting $\left(\frac{\lambda^2}{\lambda_\omega^2} - 1\right)$ by β

$$\lambda^2 = \lambda_0^2 + 10\beta\nu t \tag{11}$$

where λ_0^2 is the value of λ^2 at $t = 0$. Then from (9) we obtain

$$\overline{u^2} = \frac{\overline{u_0^2}}{\left(1 + \frac{10\beta\nu}{\lambda_0^2}\,t\right)^{1/\beta}} \tag{12}$$

denoting by $\overline{u_0^2}$ the initial value of $\overline{u^2}$ at $t = 0$.

Applying equation (12) to Taylor's problem, i.e., replacing t by x/U, we obtain

$$\frac{1}{\sqrt{\overline{u^2}}} = \frac{1}{\sqrt{\overline{u_0^2}}}\left(1 + \frac{10\beta\nu x}{\lambda_0^2 U}\right)^{1/2\beta}. \tag{13}$$

The symbols $\sqrt{\overline{u^2}}$, $\sqrt{\overline{u_0^2}}$ denote root mean squares. Taylor's result is

$$\frac{1}{\sqrt{\overline{u^2}}} = \frac{1}{\sqrt{\overline{u_0^2}}} + \text{const.}\ \frac{x}{U}. \tag{14}$$

Our equation (13) gives this result as the first term of a series development. Obviously

$$\frac{1}{\sqrt{\overline{u^2}}} = \frac{1}{\sqrt{\overline{u_0^2}}} + \frac{5\beta_1'}{\lambda_0^2\sqrt{\overline{u_0^2}}}\,\frac{x}{U} + \text{higher terms in } x. \tag{15}$$

If the linear law is correct for arbitrary large values of x, β must be equal to 1/2. Now β can be expressed by the coefficients of the development of the correlation function $R(y)$. We write

$$R(y) = 1 - \frac{y^2}{\lambda^2} + by^4 + \ldots$$

First it can be shown that $\overline{\left(\frac{\partial^2 u}{\partial y^2}\right)^2} = \overline{u^2}\left(\frac{d^4R}{dy^4}\right)_{y=0} = 24b\overline{u^2}$. Then going through an analysis of the correlation between the various products of the second derivatives of u, v, w, similar to that performed by Taylor for the first derivatives,[2] we obtain

$$\frac{\lambda^2}{\lambda_\omega^2} = \frac{28}{45}\frac{\overline{u^2}\overline{\left(\frac{\partial^2 u}{\partial y^2}\right)^2}}{\left[\overline{\left(\frac{\partial u}{y\partial}\right)^2}\right]^2} = \frac{28}{45}\frac{\left(\frac{d^4R}{dy^4}\right)_{y=0}}{\left(\frac{d^2R}{dy^2}\right)^2_{y=0}}.$$

In order to estimate possible values of $\frac{\lambda^2}{\lambda_\omega^2}$, the error function was first assumed as correlation function, substituting $R(y) = e^{-\frac{y^2}{\lambda^2}}$. This leads to $\frac{\lambda^2}{\lambda_\omega^2} = 28/15$ and $\beta = 13/15 = 0.87$. Taylor gives an example of the correlation function (see loc. cit., p. 45). Estimating b from the diagram $\frac{\lambda^2}{\lambda_\omega^2} = 1.63$ and $\beta = 0.63$. Plotting $\frac{1}{\sqrt{\overline{u^2}}}$ as a function of x with values of $\beta > 1/2$, we obtain curves similar to those observed by H. L. Dryden. Unfortunately, no exact comparison between our theory and Dr. Dryden's experimental results is possible because apparently the decay of the inherent turbulence of the wind tunnel and the decay of the turbulence produced by the screens interfere with each other, and this interference modifies the law of decay, especially in the region of small intensity of turbulence in which the deviations from the linear law are significant.

Taylor found that the constant factor in the second term at the right side of (14) is proportional to $1/M$, where M is the linear dimension of the mesh which produces the turbulence. Obviously, we obtain the same result by assuming $\frac{\lambda_0^2\sqrt{\overline{u_0^2}}}{v}$ proportional to M. Taylor made the arbitrary assumption that $\frac{\lambda^2\sqrt{\overline{u^2}}}{\nu}$ remains constant and proportional to M along the whole

stream. In this new theory, it is sufficient to connect the initial values λ_0^2 and $\overline{u^2}$ with the characteristic length of the turbulence producing device, the values of λ^2 and $\overline{u^2}$ downstream are determined by differential equations. It is felt that this represents a progress from the theoretical point of view.

Considering the problem from a general point of view, it seems to the author that in an isotropic field the mean value of the turbulent fluctuations and the correlation function $R(y)$ being given at a certain instant $t = 0$, both $\overline{u^2}$ and R are determined for all positive values of t. In other words we must be able to obtain a partial differential equation for $R(y)$ with t and y as independent variables. As an illustration of such a general theory, let us consider the case which can be described as "one-dimensional turbulence." Let us assume that the fluid has only one degree of freedom corresponding to a motion in the x-direction. We can imagine, for instance, that sheets of fluid extending parallel to the x-z plane are oscillating irregularly in the x-direction. The velocity is a function of y and t; however, it will be assumed that the oscillations of the fluid sheets are so fast and the "wave length" of the oscillations so small that the mean value of $\overline{u^2}$ can be considered as a slowly varying function of y and t. We consider the particular case in which $\overline{u^2}$ is independent of y (homogeneous turbulence) and the correlation between the instantaneous velocities u_1 and u_2 of two sheets at $y = y_1$ and $y = y_2$ is a function of the time t and the relative distance $\eta = y_2 - y_1$. Let us now calculate the derivative of the product with respect to the time. Obviously

$$\frac{\partial}{\partial t}(\overline{u_1 u_2}) = \overline{\frac{\partial u_1}{\partial t} u_2} + \overline{u_1 \frac{\partial u_2}{\partial t}}. \tag{16}$$

Now the hydrodynamic equations applied to the motion considered lead to

$$\frac{\partial u}{\partial t} = \nu \frac{\partial^2 u}{\partial y^2} \tag{17}$$

and consequently

$$\frac{\partial}{\partial t}(\overline{u_1 u_2}) = \nu \left(\overline{\frac{\partial^2 u_1}{\partial y^2} u_2} + \overline{\frac{\partial^2 u_2}{\partial y_2^2} u_1} \right). \tag{18}$$

If the correlation function is denoted by $R(\eta, t)$

$$\overline{u_1 u_2} = \overline{u^2} R$$

and

$$\overline{\frac{\partial^2 u_1}{\partial y_1^2} u_2} = \overline{u_1 \frac{\partial^2 u_2}{\partial y_2^2}} = \overline{u^2} \frac{\partial^2 R}{\partial \eta^2}.$$

Hence equation (18) can be written in the form

$$\frac{\partial}{\partial t}(R\overline{u^2}) = 2\nu\overline{u^2}\frac{\partial^2 R}{\partial \eta^2}. \tag{19}$$

Applying this equation when $\eta = 0$ and taking into account that $R(0) = 1$ and $\left(\frac{\partial R}{\partial t}\right)_{\eta=0} = 0$, we obtain

$$\frac{d}{dt}(\overline{u^2}) = 2\nu\overline{u^2}\left(\frac{\partial^2 R}{\partial \eta^2}\right)_{\eta=0} \tag{20}$$

and eliminating $\overline{u^2}$ from (19) and (20)

$$\frac{\partial R}{\partial t} = 2\nu\left\{\frac{\partial^2 R}{\partial \eta^2} - R\left(\frac{\partial^2 R}{\partial \eta^2}\right)_{\eta=0}\right\}. \tag{21}$$

The partial differential equation (21) is the fundamental equation of the problem considered. If R is given for $t = 0$ as a function of η, equation (21) determines the whole further development of the correlation and the mean value of the velocity fluctuation for all time.

The most interesting case is that in which the shape of the correlation function does not change with time. If the shape of R remains similar, $R(\eta, t)$ must be a function of the one dimensionless variable $\frac{\eta}{\sqrt{\nu t}}$. One of these solutions is, for example, $e^{-\frac{\eta^2}{8\nu t}}$. However, it is evident that in order to obtain such solutions, the initial shape itself must satisfy a certain total differential equation. In general the shape of the correlation curve will vary with the time. The practical consequence of this result is the conclusion that simple rules like Taylor's linear law for the decay of turbulence represent only approximations or special cases.

Using for $R(\eta)$ the development

$$R(\eta) = 1 - \frac{\eta^2}{\lambda^2} + b\eta^4 \tag{22}$$

$$\left(\frac{\partial^2 R}{\partial \eta^2}\right)_{\eta=0} = -\frac{2}{\lambda^2}$$

and equation (20) reads

$$\frac{d}{dt}\overline{u^2} = -4\nu\frac{\overline{u^2}}{\lambda^2} \tag{23}$$

which is analogous to our former equation (8) for the three-dimensional case. Substituting (22) in (21) and comparing the terms in η^2, we easily obtain

$$\frac{d\lambda^2}{dt} = 4\nu(6b\lambda^4 - 1) \tag{24}$$

which corresponds $\left(\text{putting } 6b\lambda^2 = \frac{1}{\lambda_\omega^2}\right)$ to (10). From (23) and (24) it follows that

$$\frac{d}{dt}\left(\frac{\overline{u^2}}{\lambda^2}\right) = -4\nu\frac{\overline{u^2}}{\lambda^2\lambda_\omega^2} \tag{25}$$

and introducing the vorticity fluctuation $\omega = -\frac{\partial u}{\partial y}$, $\overline{\omega^2} = 2\frac{\overline{u^2}}{\lambda^2}$.

$$\frac{\overline{\omega^2}}{dt} = -4\nu\frac{\overline{\omega^2}}{\lambda_\omega^2}. \tag{26}$$

Hence, the equation (23) for the dissipation of energy and the equation (26) for the dissipation of vorticity appear as applications of the general partial differential equation (21), to small values of η, i.e., to the immediate neighborhood of the point considered. In the special case that the correlation function preserves its shape throughout the whole motion, i.e., R is a function of $\frac{\eta^2}{\nu t}$ only, the ratio $\frac{\lambda}{\lambda_\omega}$ remains constant; this was the assumption made earlier in this paper. Then the whole process of the decay of turbulence is determined by the initial values of $\overline{u^2}$, λ and λ_ω, and we obtain equations analogous to (11) and (12).

The equation corresponding to (21) for three-dimensional turbulence is given elsewhere.

The author is indebted to C. B. Millikan and L. Howarth for discussions on the subject and for their assistance in calculations.

[1] *Proc. Roy. Soc. A*, **151**, 421 (1935).

[2] As a matter of fact, the analysis was carried out by means of a more general and more direct method than that used by Taylor. The new method which uses the conception of the "correlation tensor" will be published elsewhere.

INTRINSIC PROPERTIES OF LIGHT AND CORPUSCLES FROM DISTANT SOURCES

BY F. ZWICKY

NORMAN BRIDGE LABORATORY OF PHYSICS, CALIFORNIA INSTITUTE OF TECHNOLOGY

Communicated December 31, 1936

Spectra of distant nebulae, compared with those of neighboring nebulae, are shifted toward the red by amounts which increase with the distance which the light has traveled. This fact indicates that we are confronted with a phenomenon which involves history on a large scale, history either of the universe as a whole, or history of some of its individual parts.

Scientifically speaking, *history means the change in time of dimensionless ratios of significant physical quantities.* Thus, on the relativistic interpretation of the redshift of light from nebulae the dimensionless ratio D/d between two lengths changes (increases) in time. Appropriate choices for these two lengths are Bohr's characteristic length $d = h^2/4\pi^2me^2$ as a supposedly fixed terrestrial measuring stick, and $D = V^{1/3}$ where V is the volume which on the average contains one extragalactic nebula. However, many other interpretations of the redshift are possible. The assumption that history must be operative clearly suggests the necessity of an investigation of *all* dimensionless ratios between significant physical quantities. Only after this investigation has been completed will a final understanding of the redshift and other cosmic phenomena be possible.

The following discussion will be concerned with the behavior of the most trivial dimensionless ratios only. A more general program may be outlined, but so far essential data for its realization are lacking.

A. *Nebular Light and Terrestrial Light.*—We shall designate one and the same property for nebular light and terrestrial light with p_N and p_T, respectively. The first step in our program consists in procuring data which will enable us to decide whether or not for a given property p the dimensionless ratio p_N/p_T is equal to unity or not.

For instance, we may put $p_N = c_N$ and $p_T = c_T$ where c_N and c_T are the velocities of nebular light and terrestrial light, respectively, as measured simultaneously at the time of their arrival. Since no direct measurements are available we are forced to accept the values of c_N obtained from the astronomical aberration as a legitimate substitute. Also, c_T in the actual case refers to light from nearby stars instead of terrestrial light directly.

The aberration of light from nebulae relative to the aberration of light from stars was measured by Strömberg and van Biesbroeck. Strömberg[1] has determined the positions of nebulae in the Ursa Major I cluster relative to the surrounding star field in the course of a year. The distance of the

Ursa Major I cluster is of the order of 72×10^6 light-years. Strömberg found that for light from these nebulae

$$c_N/c_T = 1 \pm 0.002. \tag{1}$$

This result indicates that if the redshift from nebulae is in any way related to a change of the velocity of light in time, this change can become apparent only if c_N is measured relative to some standard other than the velocity of terrestrial light. This suggests that we investigate, as functions of time, ratios of the type c/v where v is any significant prototype of a velocity other than c_T. For instance we might choose $v = 2\pi e^2/h$, where v is the "velocity" of an electron in the first "orbit" of a hydrogen atom. Such a dependence of c/v on time might exist if the physical properties of the universe as a whole were subject to history. Although a few experiments have been carried out with some bearing on the above problem, no direct data are available from which one might deduce the behavior of c/v over long intervals of time. We therefore drop this matter for the present.

Our next step calls for a comparison of the interaction with matter of nebular light and terrestrial light.

We *define* the wave-length λ of a monochromatic beam of light by the angle Θ which the diffracted beam forms with the original beam of normal incidence on a plane grating whose spacing is Δ. The definition equation is

$$\lambda = \Delta \sin \Theta. \tag{2}$$

Assuming that Δ/d is independent of time, wave-lengths, through the observation of diffraction patterns, are measured in terms of the fundamental atomic length $d = h^2/4\pi^2me^2$. The frequency ν is not measured but is introduced by *definition* as $\nu = c/\lambda$. Absorption measurements and the photoelectric effect show that light of the wave-length λ acts in many ways as if it were composed of photons characterized by individual energies $\epsilon = h\nu = hc/\lambda$, where Planck's constant h is presumed to be a universal constant. If this is correct then we should have $h_N/h_T = 1$. Observations to test this point have been made by W. S. Adams and M. L. Humason.[2] These observers have determined the redshift relative to a terrestrial source of light from the extragalactic nebula N. G. C. 4151 both with a grating and a prism spectrograph. The refraction measurements yielded an average apparent velocity of recession $\bar{v}_R = 958$ km./sec., whereas the grating gave $\bar{v}_G = 962$ km./sec. Assuming that only an insignificant part of v is due to the peculiar motion of the nebula it follows from these observations that

$$(hc)_N/(hc)_T = 1 \pm 0.02. \tag{3}$$

In combination with (1) we obtain

$$h_N/h_T = 1 \pm 0.02 \qquad (4)$$

and we may conclude from (1) and (4) that nebular light and terrestrial light possess intrinsically identical physical properties.

In view of the fact that the nebula used in the above observations might accidentally have a peculiar motion with a large component of recession it will be advisable to repeat the observation with some more distant nebula and to use an absorption test (rare earth filter) instead of the refraction test. If this test gives the same result as the one made by Adams and Humason we will have ascertained that nebular light at the time of arrival has intrinsically the same properties as terrestrial light. Assuming this to be correct, the existence of a redshift simply means that certain characteristic features, such as maxima and minima of intensity, or emission and absorption bands in the spectra of distant nebulae appear to be displaced toward the red as compared with what we think to be *comparable features* in the spectrum of a nearby nebula or in the spectra of appropriately chosen stars and terrestrial sources. Continuing our scrutiny of apparently trivial facts, the question then arises as to what we mean by comparable features. The analysis of this question which leads to the investigation of a number of fundamental dimensionless ratios will be given in another paper.

Before abandoning this discussion of the intrinsic properties of light I sketch briefly a related problem which may find its solution through astronomical observations. Certain effects have recently come to our knowledge which suggest that the differential equations governing the propagation of light through empty space are not strictly linear. *Non-linearity* of these equations results in a *dependence* of the *velocity of light on frequency*. One reason for the existence of slight deviations from the superposition principle of light lies in the potential possibility of the formation of pairs of positive and negative electrons by interacting photons. This interaction necessitates a generalization of Maxwell's field equations through the introduction of non-linear terms in the field strengths.[5] As a result, light traveling through space which is free of matter but filled with radiation will have a velocity depending on its frequency. In addition similar effects arise from the gravitational interaction of light with light and matter. Although the effects to be expected are in all probability small the possibility of an experimental test may be kept in mind.

An obvious way of investigating effects of the kind mentioned lies in the observation of light signals of different frequency which have traveled through space for a long time. If we knew of any signals which have started *simultaneously* from a very distant source the dependence of the velocity on frequency could perhaps be demonstrated by checking up on

the times of arrival of these signals. A unique case to perform this test is afforded by the observation of distant nova outbursts. For such an outburst we may safely assume that photons in the various emission lines of, say, hydrogen have started out simultaneously on their long journey. We must therefore attempt to determine whether or not the intervals in which the different hydrogen lines flare up in the spectrum of a distant super-nova are zero or not. With the present telescopic equipment it is probably possible to find super-novae to distances as great as 10^8 light-years. With reasonable luck it should be possible to detect differences in the time of arrival of various emission lines amounting to as little as a few days. Observations of this kind will therefore enable us in the most favorable cases to determine the ratio of the velocity of violet light to that of red light traveling through internebular space with a relative accuracy of 10^{-10}.

There already are available some data which might have a bearing on our problem. These data refer to a difficulty which has arisen with respect to the absolute magnitudes and the shape of the light curves of common novae in the Andromeda nebula (Messier 31). About one hundred novae have been found in this galaxy, a number which would seem sufficiently large to constitute a fair collection and to make possible a statistical comparison with the characteristics of galactic novae. This comparison results in two serious discrepancies.

In the first place no common nova in M31 has been observed whose absolute magnitude is brighter than $M = -6.7$. Galactic novae on the other hand often are as bright as $M = -8$ or even $M = -9$. This discrepancy was pointed out to me by Dr. W. Baade of the Mt. Wilson Observatory.

In the second place the light curves of the novae in M31 are on the average considerably flattened as compared with the light curves of similar galactic novae. In particular, the familiar flash or peak which forms the maximum of the light curves of many galactic novae has apparently never been exhibited by any of the novae in M31.

Both of these discrepancies could readily be understood if the velocity of red light and violet light differed by about 10^{-3} to 10^{-2} km./sec.

I have also tried to check up on the light curves of Cepheid variables in nebulae. Extragalactic variables of a given period should have flatter light curves than galactic variables of the same period if the velocity of light depends on frequency as strongly as conjectured above. The data available at the present unfortunately are not accurate enough to test this point.

Another startling fact was observed by Sinclair Smith[3] of the Mt. Wilson Observatory in the spectrum of the recent super-nova in N. G. C. 4273, a member nebula of the Virgo cluster. The spectrum of this nova, contrary

to all expectations, did not contain any emission lines in the ultra-violet region between $\lambda = 3100$ Å and $\lambda = 3600$ Å. In fact the intensity of light in this region which might be ascribed to the super-nova is indistinguishable from zero. This fact again can be explained on the assumption that the ultra-violet light from the super-nova mentioned did not arrive simultaneously with the visible light and that it hence was missed. Alternative explanations, however, are still possible. It will be of great interest to discover super-novae in as early stages as possible and to carefully analyze their spectra.

Provided that cosmic rays originate in novae[4] the study of fluctuations in the intensity of these rays will be of particular interest in regard to the problems formulated in this paper. So far, however, the available data are insufficient to draw any definite conclusions.

B. *Corpuscular Rays.*—Common novae, super-novae, Wolf-Rayet stars, etc., eject into interstellar space energetic corpuscular rays of all descriptions. On the other hand, investigations of the polar and the non-polar aurora, as well as the cosmic ray phenomena, indicate that corpuscular rays are continually impinging on the earth's atmosphere from extraterrestrial regions. To correlate these phenomena with the happenings on unstable stellar objects is very suggestive. It is also suggestive to extend the inquiry proposed in this paper from photons to corpuscular rays and to ask whether or not extraterrestrial corpuscles exhibit the same intrinsic properties as terrestrial corpuscles. To answer this question one must investigate dimensionless ratios of the type p_N/p_T, where $p = e, m, \mu$, etc., are the charge, mass, characteristic wave-length, magnetic moment of a corpuscle. Little evidence is available at the present which would enable us to determine any of the significant ratios p_N/p_T. It will be well, however, to keep in mind the eventuality of values $p_N/p_T \neq 1$ for the interpretation of cosmic ray phenomena in order to prove or disprove the so far tacitly made assumption of the *uniformity* of all happenings in the observable parts of the universe.

The program submitted in this paper was outlined several years ago and was discussed on various occasions with those astronomers at the Mt. Wilson Observatory who have made the investigation of distant nebulae their specialty. I am particularly indebted to Drs. W. Baade, E. Hubble and M. L. Humason for coöperating in the attempt to test some of the points of this program.

[1] G. Strömberg, *Pub. Astr. Soc. Pac.*, **43**, 266 (1931).

[2] W. S. Adams and M. L. Humason, *Pub. Astr. Soc. Pac.*, **48**, 107 (1936).

[3] I am indebted to Dr. Sinclair Smith for private communication of his data.

[4] See W. Baade and F. Zwicky, these PROCEEDINGS, **20**, 259 (1934).

[5] Euler and Kockel, *Naturwiss.*, **23**, 246 (1935).

SPECTROSCOPIC ABSOLUTE MAGNITUDES OF THREE HUNDRED AND SEVENTY SOUTHERN STARS

By Dorrit Hoffleit

Harvard College Observatory, Cambridge, Massachusetts

Communicated December 29, 1936

The Mount Wilson Observatory has published spectroscopic absolute magnitudes for more than four thousand stars north of declination $-26°$;[1] the Harvard Observatory, in obtaining comparable data for stars south of

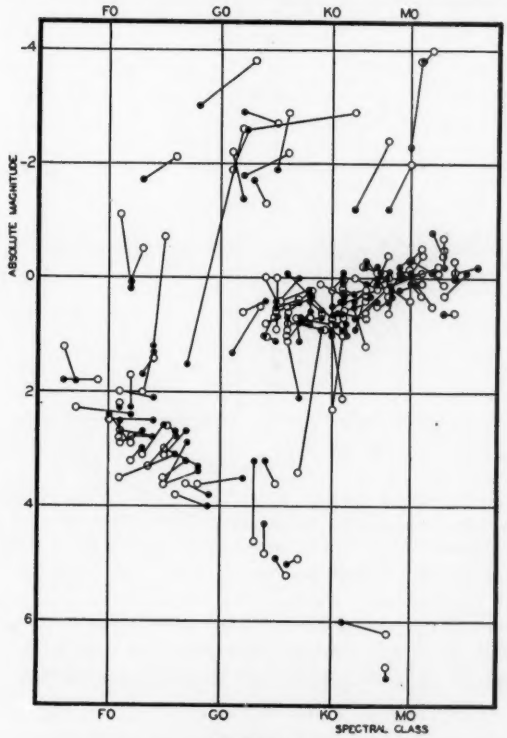

FIGURE 1

A composite Russell diagram. Dots represent Harvard data; open circles, Mount Wilson data. Corresponding points are joined by straight lines. Ordinates are absolute magnitudes, abscissae are spectral classes.

$-20°$, is extending the survey of spectroscopic parallaxes to the South Pole. The spectra were made with the 13-inch Boyden telescope and a

singe objective prism (dispersion = 22 mm. between $H\beta$ and $H\epsilon$). Absolute magnitudes have now been determined for 370 stars with spectral types later than $A5$ and brighter than the fifth apparent visual magnitude. The present note summarizes the principal results; the detailed investigation is to be published later in the *Harvard Annals*.

1. For the determination of absolute magnitudes an accurate classification of the spectra is of importance. On account of the well-known gaps in the Draper system of classification it was necessary to sub-classify the spectra for the 370 stars. For this purpose a few selected spectra were

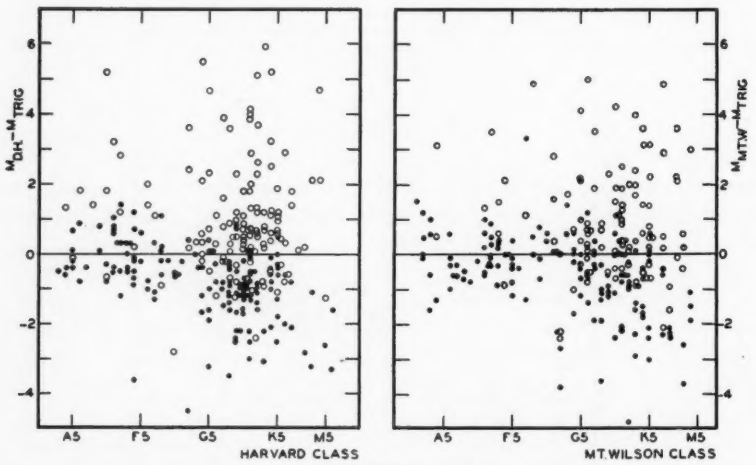

FIGURE 2

Dependence of $M_{sp}-M_t$ on spectral class. Dots represent trigonometric parallaxes $\geq 0''.020$; open circles, trigonometric parallaxes $< 0''.020$. Diagram at left gives Harvard data; at right, Mount Wilson data for bright stars in first 8 hours of Right Ascension and the stars common to the two lists.

used as standards for comparison. The revised Harvard system differs slightly in scale from the system of classification used at Mount Wilson, viz., the Harvard class $F5$ corresponds to the Mount Wilson $F4$, and the Harvard $K5$ to the Mount Wilson $K6$ or MO.

2. Absolute magnitudes were derived from the ratios in intensity of various pairs of lines. The number of pairs available within any one spectral class varied from four to ten. For calibrating the intensity ratios three different methods were used based on (*a*) spectroscopic absolute magnitudes determined at Mount Wilson for the 140 stars common to the Harvard and the Mount Wilson lists, (*b*) trigonometric parallaxes and (*c*) proper motions. The zero points of the mean calibration curves were

corrected to bring the final system of absolute magnitudes into close agreement with the Mount Wilson system.

3. From the agreement between the magnitudes derived from the various pairs of lines, the average probable error of a final mean absolute magnitude is found to be $0^m.15$. The average difference between the magnitudes determined from the two important pairs 4077:4071 and 4216:4250 is $0^m.65$. These two errors are of the same order as the cor-

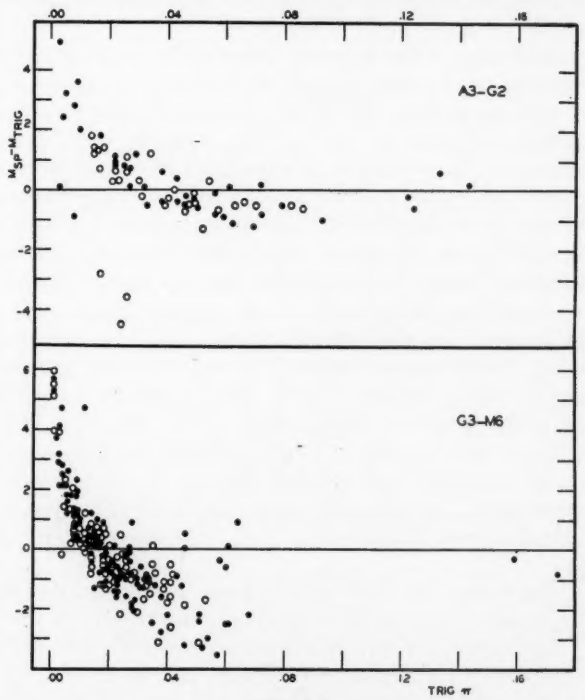

FIGURE 3

Dependence of $M_{sp}-M_t$ on trigonometric parallax. Dots indicate high galactic stars; open circles, stars within 15° of galactic equator. The five discrepant points in the upper diagram all represent c-stars.

responding errors of the northern stars studied at the Dominion Astrophysical Observatory;[2] other available catalogs are not published in sufficient detail for similar comparison.

4. The differences between the recently determined absolute magnitudes for southern stars and the absolute magnitudes for the same stars determined elsewhere are summarized below:

SOURCES OF M	DIFFERENCE AVERAGE	DIFFERENCE SYSTEMATIC	NO. STARS
Mt. Wilson *minus* Hoffleit	$\pm 0^M.40$	$+0^M.04$	137
Rimmer[3] *minus* Hoffleit	± 0.66	$+0.21$	103
H.C. 228, 232 *minus* Hoffleit	± 0.82	-0.72	46
H.C. 243, 246 *minus* Hoffleit	± 0.50	-0.18	162

The values in *Harvard Circulars* 228 and 232 are based on the system of *Mount Wilson Contribution* 199, those in *Circulars* 243 and 246 on proper motion data.

5. A comparison of the Harvard and the Mount Wilson systems of absolute magnitudes is given in the composite Russell-diagram (see Fig. 1). Only the stars common to the lists of both observatories are included. The systematic difference in spectral class, already noted above, is the most conspicuous feature of the comparison. For the supergiants and the few intermediate giant stars the mean differences in absolute magnitude are large because of insufficient calibration material for such stars at Harvard. The mean differences in absolute magnitude between the Harvard and the Mount Wilson systems show no dependence on spectral class.

6. The spectroscopic absolute magnitudes (M_{sp}) have been compared with absolute magnitudes computed from trigonometric parallaxes (M_t) taken from the *Yale Catalogue* (1935). The dispersion in the differences $M_{sp} - M_t$ increases with advancing spectral type (Fig. 2). The average difference $M_{sp} - M_t$ does not vary with spectral class if no trigonometric parallaxes, large or small, are rejected; but if we reject parallaxes with errors greater than half the parallaxes themselves (the open circles in Fig. 2), then the mean difference $M_{sp} - M_t$ increases negatively with the later types.

7. For the stars with small trigonometric parallaxes, the differences $M_{sp} - M_t$ show a pronounced dependence on the size of the parallax (Fig. 3). The correlation may be attributed in part to systematic errors in the trigonometric parallaxes: for example, a constant error of $-0''.005$ in the trigonometric parallaxes would, in the absence of any other sources for systematic errors, account for the run in the observed differences $M_{sp} - M_t$.

[1] *Mt. Wilson Contr.*, No. 511; *Astrophys. J.*, **81**, 57 (1935).
[2] *Pub. D. A. O.*, **3**, No. 1 (1924).
[3] *Mem. R. A. S.*, **62**, 113 (1923); **64**, 1 (1924).

CHANGES OF PERIOD IN VARIABLE STARS OF LONG PERIOD

BY T. E. STERNE AND L. CAMPBELL

THE HARVARD COLLEGE OBSERVATORY

Communicated December 23, 1936

One of us has investigated elsewhere[1] the mathematical theory of the accuracy of periods determined from dates of maximum, or minimum, or mth magnitude increasing or diminishing, of a variable star. The existence of cumulative errors[2] in the periods of long-period variables was shown to provide a simple explanation for the major part of their observed irregularities of period, as revealed for instance by $O-C$ diagrams,[3] and plots of cycles against epoch number. The existence of cumulative errors was shown to be in itself sufficient to cause an erratic behavior in $O-C$ diagrams, so that such diagrams did not by themselves furnish safe evidence for changes of true, or mean, period. Further, it was shown that a value of the mean period, obtained from observations extending over any finite interval of time, would be liable to errors of sampling, so that the mere existence of a scatter among values of the mean period obtained from differing intervals of time was not in itself evidence for a changing true or mean period.

Before the appearance of the previously mentioned investigations, it had been the common practice among workers in the field of variable stars to identify irregularities in $O-C$ diagrams with "changes of period" in the stars. Thus, of the 566 variables with known long periods listed[4] in the *Katalog der Elemente des Lichtwechsels für 1687 veränderliche Sterne*, sine terms were assigned to 85. Many of the reported "changes of period" were possibly of the nature of mere statistical fluctuations among cycles having a natural dispersion. It therefore became eminently desirable that the matter of changes of period should be reëxamined at length, in an impartial and systematic fashion.

The authors have examined systematically, for changes of true (or mean) period, 377 variable stars with periods usually in excess of 100 days. The stars include nearly all of the best-observed long-period variables. Apparent "changes" of period, that can reasonably be ascribed entirely to statistical fluctuations, have been carefully distinguished from systematic changes of period, here called changes of true or mean period. The material examined was obtained from

(1) observations by members of the American and French variable star associations, and

(2) earlier observations, referred to in (*a*) the extensive card catalogue bibliography of variable stars, compiled by Miss A. J. Cannon at Harvard,

and in (*b*) the bibliography contained in the *Geschichte und Literatur des Lichtwechsels*, edited by the Astronomische Gesellschaft.

The method of study employed the χ^2 test of Karl Pearson. More complete details will be published in the *Annals of the Harvard College Observatory*. We have obtained the following results.

1. The SS Cygni type stars, SS Cygni, U Geminorum and SS Aurigae, are found to have sinuously changing true periods.

2. The Z Camelopardalis type stars, RX Andromedae and Z Camelopardalis, show evidence of change in the true periods of the $12^m.0$ increasing phases, but show no good evidence of change in the true periods of the $12^m.0$ decreasing phases. The existence of sinuous changes in the widths of maxima would constitute a possible explanation of the difference between the results obtained from the two phases.

3. Twenty of the 372 remaining variables are "suspected" of having changing true or mean periods, but of these only about five can be stated with any high degree of assurance, on the evidence, to have changing true periods. Although it is not certain which five these are, the most reasonable choices are R Hydrae, R Aquilae, R Cancri, U Boötis and S Serpentis. The first two have probably had diminishing true periods, the remaining three sinuously changing true periods.

4. The small percentage of the stars which can now be stated with assurance to have changing true periods arises probably in part from the insufficient duration and number of observations. However, among 52 of the stars, not of the SS Cygni or Z Camelopardalis types, observed since before J. D. 2,400,000 and therefore longest observed, only about four can be stated with assurance to have changing periods. These 52 stars have been observed, on the average, for over ninety-four years.

5. Most of the previously reported "changes of period" among long-period variables can be reasonably interpreted as mere statistical fluctuations.

6. There is no good evidence for any secular increase or diminution of period, of an evolutionary nature, among the long-period variables as a whole.

7. We have obtained an accurate list of periods.

In closing, the authors wish clearly to point out that no conclusions as to the proportion of variables with changing periods, reached by this or any other investigation, can be regarded as final. An increase in the interval of time covered by the observations, and in their number, must render any tests more sensitive to continuing changes of period. All that we have been able to do has been to find out how many of the 377 variables which we have studied may be said with assurance, on the basis of observational material now available, to have changed their periods in a manner which cannot be entirely attributed to mere statistical fluctuations.

[1] T. E. Sterne, *Harvard Circular* Nos. 386, 387 (1934); *Popular Astronomy*, **42**, 558 (1934).

[2] The existence of cumulative errors in long-period variables had previously been inferred by Eddington and Plakidis, *Monthly Notices*, **90**, 65 (1929). See also Plakidis, *Ibid.*, **92**, 460 (1932); **93**, 373 (1933).

[3] *O–C* diagrams are plots, against epoch number, of the difference, observed date *minus* computed date, of the phase selected for study.

[4] *Geschichte und Literatur des Lichtwechsels*, **3** (1922).

THE SYNTHESIS OF GAMMA-METHYL-5,6-CYCLOPENTENO-RETENE, A COMPOUND STRUCTURALLY RELATED TO "DIELS' HYDROCARBON"[1]

BY DAVID E. ADELSON[2] AND MARSTON TAYLOR BOGERT

ORGANIC LABORATORIES, DEPT. OF CHEMISTRY, COLUMBIA UNIVERSITY

Communicated January 12, 1937

By fusion with selenium, the so-called "Diels' Hydrocarbon" (I) (*gamma*-methyl-1,2-cyclopentenophenanthrene) has been obtained from such interesting biologically and chemically important compounds as cholesterol, ergosterol, lumisterol, isopyrovitamin, pyrocalciferol, cholic acid, strophanthidin, gitogenin, anhydro-uzarigenin, sarsasapogenin and pseudobufotalin.

Retene (II), likewise a phenanthrene derivative, is formed in the destructive distillation of coniferous woods, or of rosin, due to the breakdown of the abietic acid present, and is found in large amount in the higher boiling fraction of the resultant tar. When abietic acid itself is heated with either sulfur or selenium, retene is the chief product. Further, retene carries the methyl and isopropyl groups, two radicals which are frequently found associated in natural products (cymene, terpenes, camphors, etc.), and which seem to have some significant function in nature. The attachment of the isopropyl group in the retene molecule, for example, exhibits the same carbon skeleton as is found in that important natural building unit isoprene, viz.:

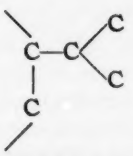

It seemed to us, therefore, desirable to attempt the synthesis from retene of products akin to the Diels' hydrocarbon and related compounds,

in the hope of leading ultimately to the establishment of closer chemical and biological connections between the resin acids and such other noteworthy phenanthrene derivatives as the sterols, bile acids, hormones,

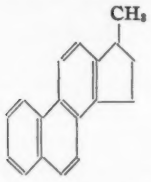

(I) Diels' hydrocarbon

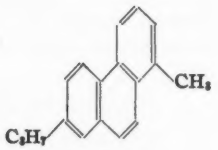

(II) Retene

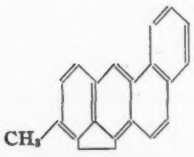

(III) Methylcholanthrene

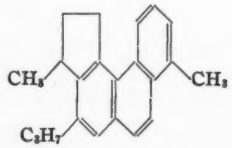

(IV) *gamma*-Methyl-5,6-cyclopentenoretene

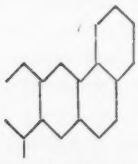

(V) Carbon skeleton common to (III) and (IV)

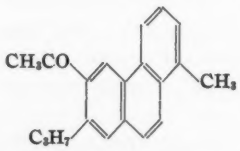

(VI) 6-Acetylretene

cardiotonic drugs, toad poisons, morphine alkaloids and the like; and of throwing additional light upon the relation between chemical constitution and physiological action in these interesting compounds.

This applies also to the cancerigenic and estrogenic properties already recorded for certain phenanthrene derivatives. Of those so far investigated from this standpoint, the most potent cancerigenic hydrocarbon is methylcholanthrene (III).

The new hydrocarbon synthesized by us is a *gamma*-methyl-5,6-cyclopentenoretene (IV) and, as will be seen by a comparison of the structural formulas, differs from the Diels' hydrocarbon (I) (which is neither cancerigenic nor estrogenic) in the location of the methylcyclopenteno ring and in the presence of the additional methyl and isopropyl groups. From the methylcholanthrene (III), it likewise varies in the position of the cyclopenteno cycle, and in lacking the 4th hexacarbocyclic system. The carbon skeleton common to both (III) and (IV) is shown in (V). Some of our good friends in the medical profession are generously coöperating by ex-

amining this new product pharmacologically, to determine whether or not it possesses cancerigenic properties.

The steps included in the synthesis of (IV) from 6-acetylretene (VI) are shown below, in which $C_{18}H_{17}$ signifies the retyl residue:

$$C_{18}H_{17}COCH_3 + BrCH_2COOR + Zn \longrightarrow$$

$$C_{18}H_{17}\overset{\displaystyle OH}{\overset{|}{C}}(CH_3)CH_2COOR + KOH + MeOH \longrightarrow$$

$$C_{18}H_{17}\overset{\displaystyle OH}{\overset{|}{C}}(CH_3)CH_2COOH + (CH_3CO)_2O + CH_3COONa \longrightarrow$$

$$C_{18}H_{17}C(CH_3):CHCOOH + Na\text{-}Hg \longrightarrow$$

$$C_{18}H_{17}CH(CH_3)CH_2COOH + PCl_5 \longrightarrow$$

$$C_{18}H_{17}CH(CH_3)CH_2COCl + AlCl_3 \longrightarrow$$

$$C_{18}H_{16}\begin{cases} CH(CH_3) \\ CH_2 \\ CO \end{cases} + Zn\text{-}Hg + HCl \longrightarrow$$

$C_{18}H_{16}\begin{cases} CH(CH_3) \\ CH_2 \\ CH_2 \end{cases}$; short white needles, m. p. 74.5–75.5° (corr.); soluble in the common organic solvents and in vegetable oils. Absorption spectra, x-ray crystal measurements and other physical data, as well as other details concerning the above products and certain of their derivatives, will appear in full elsewhere.

Similar syntheses leading to benzoretenes are nearing completion and will also be published shortly.

The intense activity in this field at present, both here and abroad, has made it seem wise to issue this preliminary communication without further delay.

[1] Reported to the Symposium on Cancer, *Am. Assoc. Adv. Sci.*, Atlantic City Meeting, Dec. 30 (1936). This is a preliminary communication; full experimental details will appear in one of the chemical journals.

[2] NATIONAL RESEARCH COUNCIL FELLOW.

THE INTERMEDIATE NUCLEUS IN THE DISINTEGRATIVE-SYNTHESIS OF ATOMIC NUCLEI: DISINTEGRATION IN STEPS*

BY WILLIAM D. HARKINS**

GEORGE HERBERT JONES CHEMICAL LABORATORY, UNIVERSITY OF CHICAGO, AND BAKER CHEMISTRY LABORATORY, CORNELL UNIVERSITY

Communicated December 21, 1936

1. *Introduction: Nuclear Reactions.*—This paper deals with the most fundamental problem of nuclear reactions. While much has been written concerning the artificial disintegration of atoms, very little attention has been paid to their synthesis. For a considerable number of years the writer has used the point of view that the primary process is always the synthesis of a new nucleus, which disintegrates only to get rid of the excess of energy, over that of a stable state, which has been given to it by the synthesis. Thus the first nuclear reaction to be studied was that in which a fast helium atom, with a velocity greater than that which corresponds to an energy of more than three million electron volts, collides with the nucleus of a nitrogen atom in a gas. The reaction which occurs is the synthesis of an atom of fluorine:

$$ {}^{0}_{7}N^{14} + {}^{0}_{2}He^{4} \rightarrow {}^{0}_{9}F^{*18} \qquad (1) $$

Here for nitrogen (N) the 7 represents the atomic number or nuclear positive charge, the 14 gives the atomic mass number (A) and the 0 represents the isotopic number I,

$$ I = A - 2Z \qquad (2) $$

which is very important in the classification of atomic nuclei.

The composition of any nucleus is represented by the formula of Harkins[1] (1922) adopted later by Heisenberg[2] which is

$$ (pn)_{z}n_{I} \qquad (3) $$

in which p is a proton, and n a neutron.

The excited fluorine nucleus has a short life and may disintegrate by either of the two methods:

$$ {}^{0}_{9}F^{*18} \rightarrow {}^{1}_{8}O^{17} + {}^{-1}_{1}H^{1} \qquad (4) $$

or

$$ {}^{0}_{9}F^{*18} \rightarrow {}^{-1}_{9}F^{*17} + {}^{1}_{0}n^{1} \qquad (5) $$

followed by

$$ {}^{-1}_{9}F^{*17} \rightarrow {}^{1}_{8}O^{17} + {}^{-2}_{1}e^{0}. \qquad (5') $$

2. *Theories of Nuclear Disintegration.*—There have been two theories of the mechanism of the nuclear disintegration of atomic nuclei, as follows:

(1) Theory of the Intermediate Nucleus.

This type of mechanism, as suggested by the writer and outlined above, was opposed by nuclear theorists prior to February 1936.

(2) Theory of Direct Disintegration, or Non-Existence of the Intermediate Nucleus.

This latter theory was supported by all quantum theorists interested in the nucleus.

The idea that a nuclear reaction occurs in at least two steps (Theory 1) and not as a single step, was expressed by the title of an early paper[3] "The

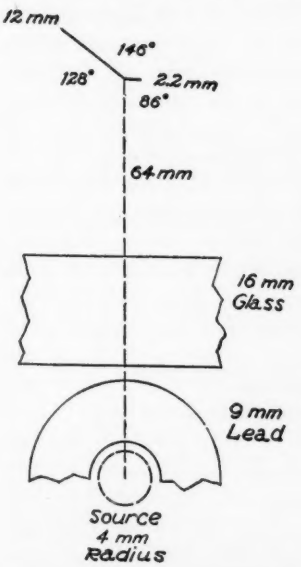

FIGURE 1

This figure gives the actual dimensions for the capture of a neutron (dotted line) by a nitrogen nucleus of mass 14 (upper end of dotted line) to give a nitrogen atom of mass 15, which disintegrated into a boron 11 atom with a track 2.2 mm. long and a helium atom (track 12 mm. long). The neutron had a velocity of 1.89×10^9 cm. per second, and an energy of 3.00 million electron volts, and passed in a straight line through 9 millimeters of lead, 16 mm. of glass and 64 mm. of air. The velocity corresponds to 14700 miles per second. This was the first neutron found in America.

Synthesis and Disintegration of Atoms." This expression was later shortened to "the disintegrative-synthesis of atoms."

An independent type of theory[2] was favored by nuclear quantum theorists. According to this point of view a disintegration is always direct, without an intermediate nucleus, but may occur in two ways:

(*a*) By capture of the projectile,
For example

$$N^{14} + He^4 \rightarrow O^{17} + H^1. \qquad (6)$$

According to this theory the intermediate nucleus has no life and no existence: There is only a trading of parts.

(*b*) Disintegration without capture: "pure disintegration."

That is, a nucleus, P, used as a projectile, strikes a nucleus T, used as a target, and rebounds, while T splits in two (or possibly more) parts:

$$T \rightarrow C + D. \qquad (7)$$

This point of view presented by Gamow, and supported by Chadwick and others, was that generally adopted, as corresponding to one type of disintegration.

That neutrons, at least, can give "non-capture" or pure nuclear disintegrations seemed to be demonstrated by the work of Feather[4] at Cambridge, and may be expressed in his own words:

"About 130 cases of interaction between a neutron and a nitrogen nucleus have been observed; of these about 30 resulted in disintegration, more than half of the latter *without capture of the neutron.* This is very different from the results obtained under α-particle bombardment, where elastic collisions, resulting in measurable spurs in an expansion chamber, outnumber inelastic (disintegration) collisions by a factor of the order of 1000:1. Moreover, although the possibility of non-capture disintegration by α-particles has frequently been considered, unexceptionable evidence for its occurrence has yet to be obtained. The former of these points of difference is certainly to be ascribed to the different extent of the external fields of the two particles, that of the neutron falling off very rapidly to become already inappreciable at a few diameters distance; it is quite possible that further investigation will exhibit the latter difference, also, as a direct result of the same circumstances."

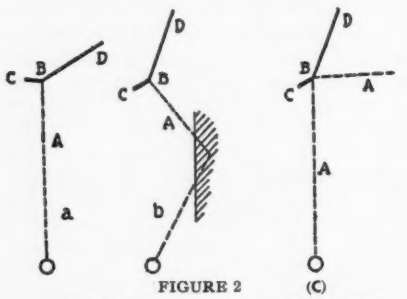

FIGURE 2

Capture. Non-capture.

The disintegration "by capture" is illustrated by figure 1, in which the dotted line indicates the invisible track of the neutron. Figure 2*c* illustrates the disintegration by "non-capture" as assumed by Feather and by Chadwick. Thus the reaction must occur by non-capture if the neutron comes directly from the source. It was assumed, however, by Harkins, Gans and Newson,[5] that an intermediate F^{18} is formed, by the action of a *scattered* neutron (Fig. 2*b*). According to them the reaction is

$$ {}_{7}^{0}N^{14} + {}_{0}^{1}n^{1} \rightarrow {}_{7}^{1}N^{15*}, \qquad (8)$$

$$ {}_{7}^{1}N^{15*} \rightarrow {}_{5}^{1}B^{11} + {}_{2}^{0}He^{4}. \qquad (8')$$

3. *Rapid Shift of Theory.*—In a paper written early in 1933, the writer,[5] who believed that the synthesis of an intermediate nucleus is an essential preliminary to a nuclear disintegration, assumed that all of these disinte-

grations which seem to be obviously by non-capture, occur actually by capture, but that in each case the neutron has been deflected (scattered) by another nucleus. (Fig. 2*b*).

It seemed that an essential step in the advancement of the theory of the formation of the intermediate nucleus, was to secure evidence against the non-capture disintegrations. To obtain this Harkins and Gans,[6] in 1933–34 developed the (relativistic) mechanics for a non-capture disintegration. This had not been done previously, and it was at once obvious that all of the apparently non-capture disintegrations which had been obtained were actually by capture. Thus the velocities for the projectile given by these equations are much higher in general than those necessary if by capture, as is apparent from the equations as given below. The velocities were found to be in general much higher than any possible velocities for the actual projectiles, as may be deduced from the equations given below. The relativity equation for the velocity of the projectile is:

$$V_A = \frac{(k_C m_C v_C + k_D m_D v_D)^2 - c^2(k_C m_C + k_D m_D - m_B)^2 + 2c^2 k_A m_A (k_C m_C + k_D m_D - m_B)}{2k_A m_A (k_C m_C v_C + k_D m_D v_D) \cos \alpha}$$

while the similar equation for not too high velocities is

$$V_A = \frac{M^2 + 2m_A E_C + E_D + c^2(m_C + m_D - m_B)}{2m_A M \cos \alpha}$$

in which M represents momentum, E is kinetic energy, m mass, v velocity, c the velocity of light and A, B, C and D are the nuclei involved. If a γ-ray is emitted the expression between brackets in equation (16) contains in addition a term $E\gamma$.

4. *Theory of the Intermediate Nucleus.* (*Fig. 3*).—As an example of the use of the idea of the intermediate nucleus, Harkins, Gans and Newson[5] consider that in the production of neutrons by bombardment of atomic nuclei by α-particle ($_2^0He^4$) the first step is an increase in the atomic number to a value 2 higher than that of the target atom, and in speaking of the case in which nuclei of isotopic number 1 are used as targets they state: "the kinetic energy of the α-particles, plus the energy of mass of the α-particle, and of the nucleus to which it becomes attached, should, in general be sufficiently great to incite the emission of a neutron."

They predicted, for example, that silicon 29 would react in the following way provided an α particle were captured:

$$_{14}^{1}Si^{29} + {}_{2}^{0}He^{4} \rightarrow {}_{16}^{1}S^{33} \rightarrow {}_{16}^{0}S^{32} + {}_{0}^{1}n^{1} \qquad (9)$$

since a stable atom of sulphur 32 could be formed by the disintegration of the intermediate nucleus sulphur 33.

They also considered that if the intermediate nucleus formed were phos-

phorus 31, which could itself be in a stable state, it would emit a proton since it could thus emit its excess energy and return to a stable state. Thus

$$ {}_{13}^{1}Al^{27} + {}_{2}^{0}\alpha \rightarrow {}_{15}^{1}P^{31} \rightarrow {}_{14}^{2}Si^{30} + {}_{1}^{-1}H^{1}. \qquad (10) $$

Both of the above have been found to be correct. There is, however, another reaction by means of which the excess energy of phosphorus 31 may be released by giving silicon 30 as a product. This is

$$ {}_{15}^{1}P^{31} \rightarrow {}_{15}^{0}P^{30} + {}_{0}^{1}n^{1} \qquad (11) $$

excited state of stable atom — unstable atom

$$ {}_{15}^{0}P^{30} \rightarrow {}_{14}Si^{30} + {}_{1}^{-2}e^{0}. \qquad (12) $$

The use of a star to indicate the energy of activation of the intermediate product was introduced by Harkins and Gans[6] who gave the general reaction as

$$ A + B \rightarrow AB^{*} \rightarrow C + D \qquad (13) $$

which may be written

$$ T + P \rightarrow I^{*} \rightarrow C + D \qquad (14) $$

where a target nucleus (T) struck by a projectile (P) gives an excited intermediate nucleus I^{*}. In the earlier paper it had already been assumed that C or D may be emitted in an excited state, or

$$ T + P \rightarrow I^{*} \rightarrow C^{*} + D \qquad (15) $$

which means either the emission of a γ-ray or a further disintegration of C^{*}.

Our use of the star should not be confused with its later use by others, who have used it to designate merely the possibility of emission of electrons or γ-rays, but not the energy of excitation of the intermediate state.

What has been presented thus far represents the state of the Intermediate Nucleus theory at the end of 1935 except that in 1933 the writer determined experimentally for reaction (9) that the life of this particular intermediate nucleus, with the energies used, is less than 10^{-7} seconds. This was not unexpected as from general considerations it was expected that the life of any intermediate nucleus to be less than 10^{-12} seconds, but in this case more of the order of 10^{-16} or 10^{-17} seconds.

Nuclear quantum theorists assumed the time of interaction to be of the order of R/v, where R is the radius of the nucleus and v is the velocity of the projectile. However, the theory of the intermediate nucleus assumed that the time of disintegration does not depend upon the velocity of the projectile, except in a very much less direct way. The time of disintegration does, however, have a certain indirect dependence upon the energy of the pro-

jectile, as considered later. The theorists also assumed the interaction between the projectile and the particles in the nucleus to be much greater than that with the whole nucleus, while the intermediate theory assumed exactly the opposite.

Thus the writer considered that both the kinetic energy of the projectile, and also the energy of any excess mass which it and the target nucleus may possess, are very rapidly distributed in the new nucleus by the motion of its component particles, and thus put the nucleus in some excited state, the nature of which, together with the possible modes of disintegration, decides the life of the particle.

A general outline of this theory was presented[7] in an address given January 1, 1936, and the theory was given the support of Bohr[8] in an address presented January 27, 1936.

The purpose of this paper is to outline more definitely the postulates of the theory.

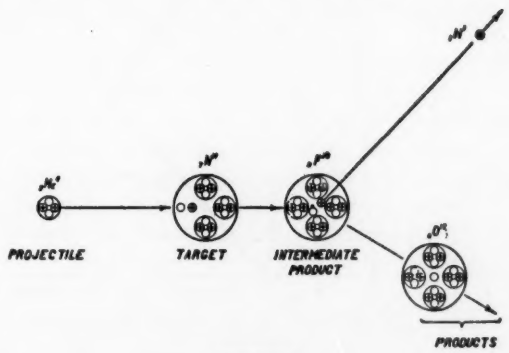

FIGURE 3
Illustrates the Theory of the Intermediate Nucleus.

(1) The fundamental theory is that the intermediate nucleus has an actual life and a separate existence.

(2). The life period of any definite intermediate nucleus is independent of the components from which it has been formed provided it is in a definite excited state, but the state of excitation depends upon both the kinetic and mass energies of these components. For example C^{12*}, whether formed from (1) $B^{10} + H^2$, (2) $B^{11} + H^1$ or from (3) $Li^6 + Li^6$, should have the same half-period provided the sum of the mass energy and the kinetic energy is the same in all three cases.

(3) The life period depends upon the particular excited state of I^*, and on the energy of this state, and upon the nature and the energy states of its possible products.

(4) When any definite intermediate nucleus is formed by the union of

two definite nuclei the life period may in general be expected to decrease as the energy of the projectile increases. From the quantum viewpoint this is due to the general broadening of nuclear levels as the nuclear energy increases. On the classical basis it may be explained by the assumption that the greater the internal energy of the nucleus, the greater is the probability that a single particle [or group of particles such as $(np)_2$], should in any given interval of time, be given enough energy to allow it to escape from the nucleus. On the classical basis this would be considered as energy of vibration, and the case becomes similar to that of a monomolecular reaction as considered in chemical kinetics.

(5) The intermediate nucleus I^* may disintegrate into the components T and P as well as into other particles.

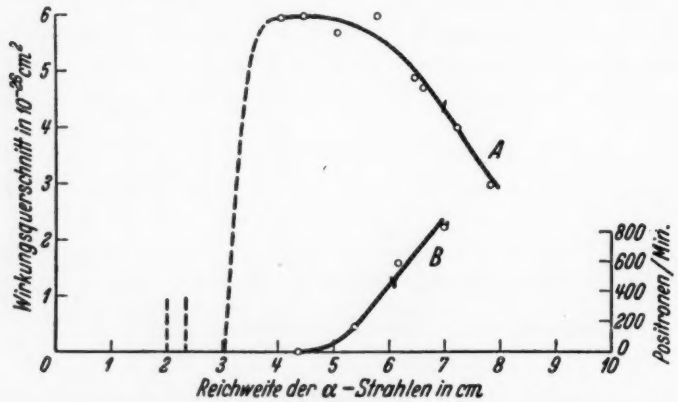

FIGURE 4

Excitation curve for the action of Helium on Nitrogen. (A) Proton Emission. (B) Neutron and Positive Electron Emission (work of Häxel).

(6) On account of the low decimal mass of helium (0.0034 or 3.2 *MEV*) the emission of helium is favored when the energy of excitation of I^* is low, the nuclear charge is low, and also a state of even number is involved (Bose statistics), since the angular momentum of the α-particle is zero. For protons and neutrons the level should be odd (Fermi statistics).

(7) According to the theory the total number of nuclear disintegrations obtained must be equal to the number of syntheses of the excited intermediate nucleus minus the number of these nuclei which return to a stable state by γ-ray emission alone. Here disintegration into either heavy particles, or into negative and positive electrons is considered, but with light nuclei it is well known that heavy particles, such as neutrons, protons, α-particles, etc., are almost always emitted by the first or primary intermediate nucleus.

The only definitely determined case in which an electron is emitted but not a heavy particle is the following:

$$ {}^{0}_{6}C^{12} + {}^{-1}_{1}H^{1} \rightarrow {}^{-1}_{7}N^{13*} \tag{16} $$

$$ {}^{-1}_{7}N^{13*} \rightarrow {}^{-1}_{7}N^{13*} + \gamma \tag{17} $$

$$ {}^{-1}_{7}N^{13*} \rightarrow {}^{1}_{6}C^{13} + {}^{-2}_{1}e^{0*} \tag{18} $$

Here, however, the primary excited intermediate product emits a part of its energy of excitation and changes into an unstable form. This, which has a half-life of 660 seconds, emits a positive electron.

(8) From (5) the total number of disintegrations is thus in a secondary sense dependent upon the nature of the constituents T and P, including their energies, but is independent of the nature of the products, C and D, formed by the disintegration.

(9) The types of disintegration which occur and their corresponding widths of level depend upon the state of the intermediate nucleus, particularly upon its energy, and the angular momentum.

(10) The disintegration of the intermediate nucleus I^* may occur in steps, such that a second intermediate nucleus I'^* is formed.

Consider reactions (4), (5) and (5′) for which Harkins and Shadduck assumed the existence of an intermediate fluorine nucleus. It is known that oxygen 17 is formed by reactions in which (A) hydrogen is formed. and (B) a neutron is formed. Now, if the total number of captures of helium by nitrogen were known (N_C) for any given velocity of the projectile (helium), this would give the number of disintegrations to give hydrogen (N_H) plus those to give neutrons (N_n),

$$ \text{or } N_C = N_H + N_n \text{ at a given energy.} \tag{27} $$

Let it be assumed that N_C is zero for low energies of the projectile, but increases rapidly above a range of 3 cm. (4 *MEV*) for the helium (α). It becomes constant above 4 cm. as the range (or energy) increases. Then reaction (2) does not begin until the range is 4.5 cm. or more (energy > 5.5 *MEV*). The reason for the necessity of this extra energy for (2) is apparent in the reactions, since in (5) and (5′) a positive electron is formed, in addition to the neutron which has a slightly higher mass than the hydrogen of (4). According to (27) as the number of reactions (B) increases, the number of (A) should decrease. Now this is just what has been found by Häxel (Fig. 4). Thus the study of excitation potentials should give evidence for the theory of the intermediate nucleus. Unfortunately the total curve for the number of captures is not in general of this simple form.

Let it be assumed that heavy hydrogen is used to synthesize carbon 12, by the reaction

$$ {}_5B^{10} + {}_1H^2 \rightarrow C^* \qquad (19)$$

$$15.0 + (13.7 + 1) = 3.4 + 26.1^* \; MEV + 0.2 \; MEV.$$

and that the hydrogen of mass 2 (deuterium) has a kinetic energy of 1 million electron volts. The atom itself at rest contains an excess mass (mass above a whole number) equal to 0.0147 which corresponds to 13.7 *MEV*, while boron 10 has an excess of 15 *MEV*. The sum of these is 29.7 *MEV*. Now the excess energy of a carbon 12 atom in its normal nuclear state is 3.4 *MEV*, so the excited level of C^* has an excitation energy of

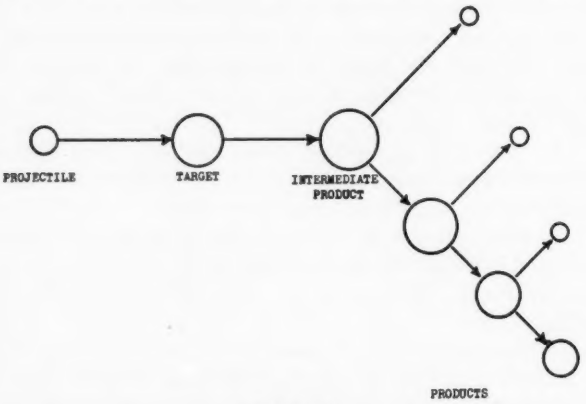

FIGURE 5

The Disintegration, beginning with the First Intermediate Product may occur in Several Steps or a Disintegration Series. This requires that the energy of excitation of the intermediate nucleus be very high. Such a series is entirely analogous to that exhibited in natural radioactivity.

26.1 million volts, or the star indicates 26.1 *MEV*, since about 0.2 *MEV* is carried off by the kinetic energy of the carbon 12.

Now if C^{12} is formed from light hydrogen

$$ {}_5B^{11} + {}_1H^1 \rightarrow C^* \qquad (20)$$

$$11.9 + (7.6 + 10.9) = 3.4 + 26.1^* \; MEV + 1 \; MEV.$$

Here, since about 1 million volts of energy are carried off by the C^* as *kinetic energy*, the hydrogen of mass 1 should be projected with a kinetic energy of 10.9 million volts to give a carbon 12 nucleus (C^*) of the same energy as with a 1 million volt deuteron.

Provided the same excited state is reached the method of disintegration of the excited carbon atom should not be dependent upon its method of formation: Thus

$$C^{12*} \rightarrow B^{11} + H^1 \qquad (21)$$

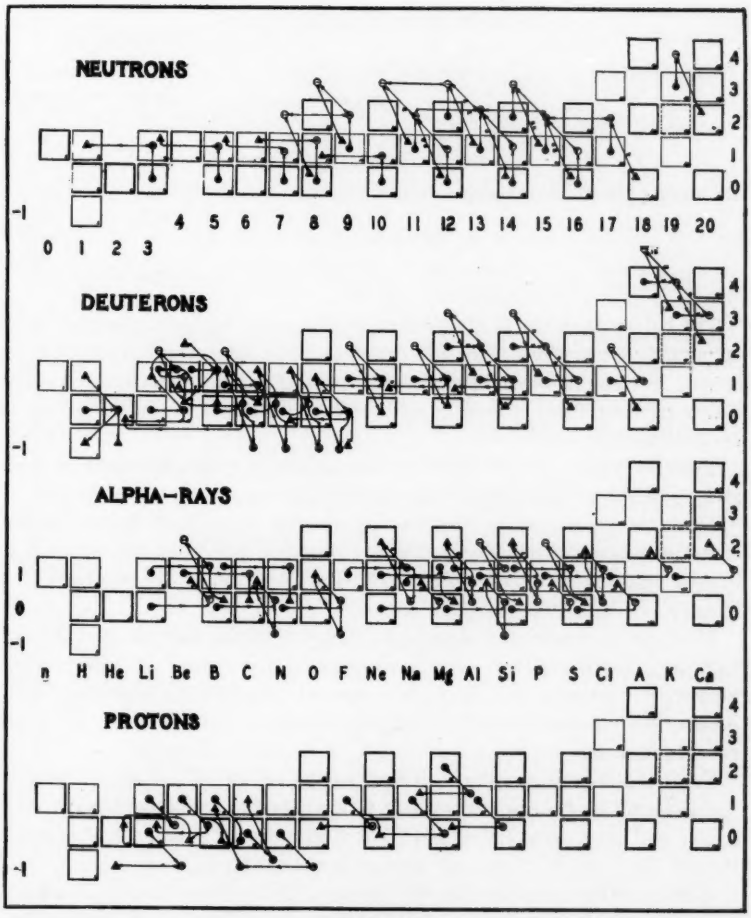

FIGURE 6

Reactions of Light Atoms according to Theory of the Intermediate Nucleus, arranged according to projectiles as named. The target nucleus is represented by a black closed circle, the intermediate nucleii by open circles with a symbol inside. Thus + or − indicates the emission of an electron, p, of a proton, n, of a neutron and α, of an α-particle. A black triangle indicates the heavier of the two end products. The nature of the projectile, as for example for an alpha-particle, is given not only by the words but also by the fact that the intermediate nucleus lies two squares to the right of the target. In the emission of an α-particle the other product lies two squares to the left of the intermediate product. If the intermediate product emits a proton the arrow shows a unit displacement in the direction of slope −1, that is, the isotopic number is increased by 1 but the atomic number changes by −1. Emission of a negative electron lowers n by 2 and increases Z by one, for a positive electron the change is the opposite. In the emission of a neutron, n decreases by 1. For the emission of any particle the change in the plot is just the opposite of that for its addition as a projectile.

$$C^{12*} \rightarrow B^{10} + H^{2} \quad (22)$$

$$C^{12*} \rightarrow Be^{8*} + He^{4} \quad (23)$$

$$C^{12*} \rightarrow C^{11*} + n^{1} \quad (24)$$

are among the reactions which should ensue. In addition

$$C^{11*} \rightarrow B^{11} + \epsilon^{+} \quad (25)$$

$$\text{and } Be^{8*} \rightarrow He + He. \quad (26)$$

The half-lives of the excited states may be a few seconds, minutes, hours or possibly even years if an *electron* is emitted from an intermediate nucleus. For the emission of a neutron, proton, helium nucleus or so-called heavy particle, the life may be predicted in some cases from the energy of excitation of the state.

Thus Be^{8*} has a narrow energy level from which γ-rays alone are emitted, and a superimposed broad level from which helium nuclei are emitted.

From the present value of the energy of this latter level Bethe (private communication) estimates the life of this particular intermediate nucleus in this state as 10^{-13} seconds, which is a long life for the emission of a "heavy" particle from a light nucleus.

With heavy nuclei and neutrons, energy levels as narrow as 1/50 volt have been found in silver. An energy level of this width in an intermediate nucleus would correspond also to the general order of 10^{-13} seconds. With α-particles, for example with aluminum, levels of widths of 0.5 *MEV* are not uncommon.

From this it may be estimated that for the emission of "heavy" particles (particles which are not electrons or γ-rays) the life periods of intermediate nuclei will in general lie between the limits of 10^{-13} and 10^{-18} seconds, though 10^{-20} and 10^{-12} seconds are not improbable in certain cases.

It is of course possible that the life of a nucleus may in some instances become so small that the complete independence of the disintegration from the method of formation may partly vanish.

The theory of the intermediate nucleus is illustrated by figure 5, which shows the course of most of the known nuclear reactions of light atoms, on the basis of this idea. Direct evidence for the theory of the intermediate nucleus would be that which indicates that the assumed intermediate, as C^{12*}, actually disintegrates in two (or more) steps. In this special case in reaction (23) the first helium atom could be emitted with a variety of velocities, but in the disintegration of the second intermediate, as Be^{8*}, the velocities of the two helium nuclei produced (reaction (26)) *must be identical* when referred to the moving center of gravity of the system of the two helium atoms as the origin of the system of coördinates. Dee and Gilbert[9] seem to have shown that this is true.

* Presented by title at the meeting of the National Academy of Sciences, Chicago, November 17, 1936.

** George Fisher Baker Non-Resident Lecturer in Chemistry at Cornell University.

REFERENCES TO THEORY OF THE INTERMEDIATE NUCLEUS

[3] Harkins, W. D., and Shadduck, H. A., *Proc. Nat. Acad. Sci.*, **12**, 707–714 (1926); Harkins, W. D., *Chem. Rev.*, **5**, 374–435 (1928).

[5] Harkins, W. D., Gans, D. M., and Newson, H., *Phys. Rev.*, **44**, 530, 533, 534, 537 (1933).

[6] Harkins, W. D., and Gans, D. M., *Phys. Rev.*, **46**, 397–404 (1934); *Nature*, **133**, 794–795 (May, 1934).

[7] Harkins, W. D., *Science*, **83**, 533–543 (1936). Address presented before Section C of the American Association for the Advancement of Science, and the St. Louis Section of the American Chemical Society, St. Louis, January 1, 1936.

[8] Bohr, N., *Nature*, **137**, 344–348 (1936).

[9] Dee, P. I., and Gilbert, C. W., *Proc. Roy. Soc.*, **149**, 200 (1935).

GENERAL REFERENCES

[1] Harkins, W. D., *Phil. Mag.*, **42**, 305–339 (1921); *Phys. Rev.*, **19**, p. 137, line 15 (1922).

[2] Heisenberg, W., *Zeit. Physik*, **77**, 1–11 (1932).

[4] Feather, N., *Proc. Roy. Soc.*, **A136**, 709–727 (1932).